Novel physiological function of proline and mTOR regulator tuberin

Yoko Obayashi

2018

Contents

Introduction 1

Chapter I

Proline protects liver from D-galactosamine hepatitis by activating the IL-6/STAT3 survival signaling pathway 7

Chapter II

The protection mechanism of proline from D-galactosamine hepatitis involves the early activation of ROS-eliminating pathway in the liver 29

Chapter III

Anti-atherogenic effect of proline in a rat model of high sucrose diet-induced hyperlipidemia 45

Chapter IV

Impaired lipid accumulation in the liver of Tsc2-heterozygous mice during liver regeneration 59

Chapter V

The effect of cisplatin on blood ammonia elevation by alanyl-glutamine supplementation 73

Conclusion 88

Acknowledgements 90

Publications 91

Introduction

The liver is the main organ involved in amino acid metabolism, and it utilizes glucogenic amino acid as an energy source. Under catabolic conditions, glucogenic amino acid is converted to alpha-keto acid and finally generates glucose and adenosine triphosphate (ATP). There are many reports that some of glucogenic amino acids protect liver from liver damage and dysfunction induced by alcohol, hepatotoxin, ischemia-reperfusion, etc.[1-3]. Energy production may be important especially at a recovery phase, but it should not be a primary mechanism for glucogenic amino acids to protect liver from hepatic dysfunction.

Proline is one of glucogenic amino acids and is reported to protect liver from D-galactosamine (GalN)-induced hepatitis, but the mechanism of protection has not been fully elucidated [2]. In a variety of liver injury including toxic damage induced with hepatotoxins, one of the major inflammatory cytokines Tumor necrosis factor-α (TNF-α) and its downstream signaling play an important role to determine the extent of injury. TNF-α induces either proliferation or apoptosis in a variety of cells, and the activation of nuclear factor kappa B (NF-κB) is critical to determine the cell's response, i.e., survival or death. For cell's survival, the upregulation of NF-κB-dependent protective genes is essential. When NF-κB-dependent gene expression is blocked, TNF-α treatment activates apoptotic signaling such as caspase-2, -3 and -8 [4]. Interleukin-6 (IL-6) is one of the targets of NF-κB and activates a variety of regenerative pathways, including mitogen-activated protein kinase (MAPK) pathway and Signal transducers and activator of transcription 3 (STAT3) pathway, whose contribution to cell proliferation have been well documented [5,6]. Thus, regenerative signaling is an essential factor against cell death.

In addition to the activation of regenerative signaling, regulation of reactive oxygen species (ROS) generation is another important factor to suppress severe hepatic damage. ROS are mediator of cellular injury by activated immune cells. Inflammatory cells, such as hepatic macrophage and neutrophils, are activated by inflammatory mediators such as TNF-α and infiltrate into hepatic stroma, causing extensive hepatocellular necrosis [7]. These activated inflammatory cells produce and release large

quantity of ROS, such as superoxide anion, hydrogen peroxide, nitric oxide, and their derivatives, which attack the surrounding tissue and cause oxidative stress intra- or extracelluarly [8-10].

Considering these mechanisms associating with liver injury, I investigated the effect of proline on regenerative signaling and anti-oxidative pathway in the liver using GalN-induced hepatitis rat model to elucidate the protective mechanism of proline.

For further understanding on liver regeneration, it should be noted that liver regeneration is achieved by cell proliferation and cell growth, where the IL-6/STAT3 and phosphatidylinositol-3-kinases / pyruvate dehydrogenase kinase, isoenzyme 1 / protein kinase B (PI3K/PDK1/Akt) pathways play pivotal roles, respectively [11]. TNF-α/ NF-κB signaling activates IL-6/STAT3 pathway which regulates hepatocyte proliferation via cyclin D1/ cyclin dependent kinase inhibitor 1A (p21) and protects against cell death by upregulating FLICE-like inhibitory protein (FLIP), Bcl-2, Bcl-xL, redox effector factor-1 (Ref1), and manganese superoxide dismutase (MnSOD). PI3-K/PDK1/Akt is known to be responsible for regulation of cell size via its downstream molecules such as mammalian target of rapamycin (mTOR) in addition to anti-apoptotic and anti-oxidative properties.

mTOR is regulated not only by Akt but also by various factors such as L-leucine (positive regulator) and tuberin-hamartin complex (negative regulator). Tuberin-hamartin complex works as a critical nutrient sensor, which regulates cell growth and proliferation via mTOR pathway. Tuberin is a GTPase-activating protein and convert mTOR activator, Ras homolog enriched in brain (Rheb), from active form to inactive form. Under energy starvation (e.g., increased AMP:ATP ratio), 5'AMP-activated protein kinase (AMPK) becomes activated and phosphorylates tuberin to enhance its activity to inhibit mTOR signaling, leading to a suppression of cell/growth/ proliferation [12]. On the other hand, the anabolic signaling such as insulin inactivate tuberin via protein kinase Akt [13]. Tuberin is directly phosphorylated by Akt at Thr 1462, followed by an inactivation of tuberin, a disruption of its interaction with hamartin, and activation of mTOR. Thus, tuberin protect cells from energy deprivation-induced apoptosis through inactivation of mTOR pathway and stimulates cell growth through activation of

mTOR when it receives growth-stimulating signals. Although tuberin is well-known to be a negative regulator of mTOR pathway, the role of tuberin on liver regeneration has not been elucidated.

When amino acids are administered to patients for clinical treatment, ammonia should be properly metabolized to prevent hyperammonemia, which causes various systemic disorders especially on nervous system. Among various organs which metabolize ammonia, liver plays pivotal roles in detoxification of ammonia. Ammonia in the circulation is mainly detoxified by periportal hepatocytes through urea cycle [14]. Excess ammonia not used by urea cycle is taken up by perivenous hepatocyte and is detoxified to glutamine by glutamine synthetase (GS) [15]. The significance of the contribution of hepatic ammonia-detoxifying capacity to control blood ammonia level is evident from the fact that 90% of heperammonemia cases in adults is associated with liver disease [16]. In addition to hepatic function, renal function is also important to control blood ammonia level by excreting ammonia and urea through urine. Although there are many drugs which have a possibility to cause hepatic and renal dysfunction, the effect of these drugs on systemic ammonia detoxification capacity have not been studied.

In this thesis, I elucidated the mechanism of the protective effect of proline on GalN-induced hepatitis and the role of tuberin, the negative regulator of mTOR pathway, in liver regeneration. I also investigated the effect of cisplatin (CDDP), widely-used anti-tumor agent, on systemic ammonia detoxification capacity. In chapter I, using GalN-induced hepatitis rat model, I show proline pre-administration activates hepatic regenerative response and alleviates subsequent inflammation. I also demonstrate the activation of IL-6/STAT3 pathway, which is regenerative and anti-inflammatory signaling downstream of TNF-α/NF-κB. In chapter II, I demonstrate that proline pre-administration on GalN-induced hepatitis rat activates haptic major ROS-eliminating system, such as catalase and glutathione redox system within 12 h after GalN treatment. During the study on the mechanism of protective effect of proline on GalN-induced hepatitis rat model, I noticed that in the liver of proline-preadministered rats, the morphology of endothelial cells is relatively well-maintained compared with that of control animals without proline administration during the time when infiltration of inflammatory cells are facilitated. In addition, the cell proliferation of perivascular area in the liver of

proline-preadministered rats was found to be significantly enhanced at very early phase. Based on these observations, I hypothesize that proline has a protective effect on endothelial cells, and this effect contributes to anti-inflammatory effect through suppression of the infiltration of inflammatory cells into parenchyma. In chapter III, I demonstrate the protective effect of proline on endothelial dysfunction and inflammatory reaction, using early atherogenic model, short-term high sucrose diet-fed rat model. This animal model exhibited a triglyceridemia, which is known to cause endothelial dysfunction and inflammatory response, including the elevation of plasma inflammatory cytokines. These inflammatory mediators upregulate the expression of adhesion molecules on neutrophils (β2 integrins) and on endothelial cells (intercellular adhesion molecule 1 (ICAM-1), monocyte chemoattractant protein-1 (MCP-1), E-selectin, etc.) through activation of NF- κB to facilitate neutrophil adhesion to vascular endothelium [17, 18]. In chapter IV, I show a role of tuberin in liver regeneration, including a possibility of new function of tuberin. I also demonstrate impaired accumulation of lipid vesicles in the liver of TSC complex subunit 2 (TSC2)+/- mice after hepatectomy, which serves as a primary energy source during early liver regeneration. In chapter V, I demonstrate CDDP treatment deteriorates systemic ammonia detoxification capacity by showing that CDDP treatment enhances the increase in blood ammonia level by intravenous infusion of alanyl-glutamine.

References

[1] Suzuki H, Tominaga T, Mizuno H, Kouno M, Suzuki M, Kato Y, Sato A, Okabe K, Uchikoshi T, Maezono K, et al: Ethanol and hydrazine sulfate induced chronic hepatic injury in rats: the curative effect of administration of glucogenic amino acids. Alcohol Alcohol Suppl. 1993;1A:111-117.

[2] Ajinomoto Co., Inc.: Japan Patent Kokai 1996-208472.

[3] Hawkins RL, Mori M, Inoue M, Torii K: Proline, ascorbic acid, or thioredoxin affect jaundice and mortality in Long Evans cinnamon rats. Pharmacol Biochem Behav 1995; 52:509-15. doi:10.1016/0091-3057(95)00118-G.

[4] Xu Y, Bialik S, Jones BE, Iimuro Y, Kitsis RN, Srinivasan A, et al: NF-kappaB inactivation converts a hepatocyte cell line TNF-alpha response from proliferation to apoptosis. Am J Physiol 1998; 275(4 Pt 1):C1058-66.

[5] Singh A, Jayaraman A, Hahn J: Modeling regulatory mechanisms in IL-6 signal transduction in hepatocytes. Biotechnol Bioeng 2006; 95(5):850-62. doi: 10.1002/bit.21026

[6] Li W, Liang X, Kellendonk C, Poli V, Taub R: STAT3 contributes to the mitogenic response of hepatocytes during liver regeneration. J Biol Chem 2002; 277:28411-7. doi:10.1074/jbc.M202807200

[7] MacDonald JR, Beckstead JH, Smuckler EA: An ultrastructural and histochemical study of the prominent inflammatory response in D(+)-galactosamine hepatotoxicity. Br J Exp Pathol 1987; 68:189-99.

[8] Bautista AP, Mészáros K, Bojta J, Spitzer JJ: Superoxide anion generation in the liver during the early stage of endotoxemia in rats. J Leukoc Biol 1990; 48(2):123-8.

[9] Sakaguchi S: Metabolic aspects of endotoxin as a model of septic shock--approached from oxidative stress. Yakugaku Zasshi 2004; 124(2):69-87.

[10] Sakaguchi S, Furusawa S: Oxidative stress and septic shock: metabolic aspects of oxygen-derived free radicals generated in the liver during endotoxemia. FEMS Immunol Med Microbiol 2006; 47(2):167-77.

[11] Fujiyoshi M, Ozaki M: Molecular mechanisms of liver regeneration and protection for treatment of liver dysfunction and diseases. J Hepatobiliary Pancreat Sci. 2011;18(1):13-22. doi: 10.1007/s00534-010-0304-2.

[12] Inoki K, Zhu T, Guan KL, TSC2 mediates cellular energy response to control cell growth and survival. Cell 2003; 115(5):577-90.

[13] Inoki K, Li Y, Zhu T, Wu J, Guan KL: TSC2 is phosphorylated and inhibited by Akt and suppresses mTOR signaling. Nat Cell Biol. 2002; 4(9):648-57.

[14] Walker V: Ammonia toxicity and its prevention in inherited defects of the urea cycle. Diabetes Obes Metab 2009; 11(9):823-35.

[15] Hakvoort TB, He Y, Kulik W, Vermeulen JL, Duijst S, Ruijter JM, Runge JH, Deutz NE, Koehler SE, Lamers WH: Pivotal role of glutamine synthetase in ammonia detoxification. Hepatology 2017; 65(1):281-293.

[16] Cichoż-Lach H, Michalak A: Current pathogenetic aspects of hepatic encephalopathy and noncirrhotic hyperammonemic encephalopathy. World J Gastroenterol 2013; 19(1):26-34.

[17] Jaeschke, H: Mechanisms of neutrophil-mediated liver cell injury during ischemia-reperfusion and other acute inflammatory conditions, Am J Physiol Gastrointest Liver Physiol 2006; 290:G1083–1088.

[18] Bevilacqua MP, Pober JS, Mendrick DL, et al: Identification of an inducible endothelial-leukocyte adhesion molecule. Proc Natl Acad Sci U S A 1987; 84:9238-9242.

Chapter I

Proline protects liver from D-galactosamine hepatitis by activating the IL-6/STAT3 survival signaling pathway

Summary

The oral administration of proline, one of the non-essential amino acids, has been shown to effectively protect the liver from D-galactosamine(GalN)-induced liver injury and to improve the survival rate. The aim of this study was to investigate the mechanism of this protective action of proline. I paid particular attention to the effect of proline on inflammatory activation, regenerative response, and the associated signal transduction in the liver.

Male Fischer rats received intraperitoneal injections of GalN(1.4g/kg) with or without the oral administration of proline(2g/kg) 1 h before GalN treatment. Liver pathology, plasma indices of inflammation, and the level of proliferative marker in the liver were monitored. The hepatic activation of interleukin-6 /signal transducer and activator of transcription (IL-6/STAT3) pathway, which is downstream of tumor necrosis factor(TNF)-α/nuclear factor-κB, was also studied.

D-galactosamine induced massive inflammatory expansion in the liver, leading to a high death rate(60%) more than 72 h after the treatment. Proline administration significantly suppressed inflammatory infiltration in the liver after 48 h, which was accompanied by depletion of plasma TNF-α, glutamic oxaloacetic transaminase (GOT) and glutamic pyruvic transaminase (GPT). The mRNA expression of histone H3, a marker of proliferation, was significantly upregulated in the livers of proline-treated animals. Furthermore, IL-6/STAT-3 pathway, an anti-inflammatory and regenerative signaling pathway, was strongly activated prior to these observations, with the upregulated expression of downstream genes.

These results suggest that the tissue-protective mechanism of proline involves the early activation of IL-6/STAT-3 pathway in the liver, with subsequent activation of the regenerative response and suppression of massive inflammatory activation.

Introduction

The administration of a GalNactosamine to rodents results in extensive hepatocellular necrosis, accompanied by prominent infiltration of active macrophages into the hepatic stroma [1]. The symptoms are accompanied by endotoxemia along with the release of TNF-α. Because this liver injury histopathologically resembles human fulminant viral hepatitis, the biology of this animal model is well established. Endotoxin is known to induce the release of inflammatory mediators including TNF-α [2], and endotoxemia contributes significantly to the pathogenesis of GalNa hepatitis [3]. Fulminant hepatitis has similar symptoms, and is also accompanied by endotoxemia along with the release of TNF-α.

The TNF-α signaling induces either proliferation or apoptosis in a variety of cells, and NF-κB activation is the critical intracellular signal that determines the cell's response: survival or death. For cells to survive, the upregulation of NF-κB-dependent protective genes is essential. Xu et al. reported that the inhibition of NF-κB-dependent gene expression by actinomycin D sensitized hepatocytes to TNF-α cytotoxicity. When NF-κB-dependent gene expression is blocked, TNF-α treatment activates caspase-2, caspase-3 and caspase-8 [4].

It is well documented that the NF-κB/IL-6/STAT3 pathway plays a pivotal role in liver protection and regeneration in a variety of liver-injury models, including toxic damage induced with hepatotoxins [5], ischemic liver injury [6], and Fas-mediated injury [7].

Interleukin-6 is known as one of the most important initiators of the regenerative response [8,9]. Interleukin-6-deficient mice exhibit impaired liver regeneration characterized by liver necrosis and failure, a blunted DNA synthesis response in hepatocytes, no STAT3 activation, and reduced gene

induction of the G1 phase. Treatment of IL-6-deficient mice with a single preoperative dose of IL-6 rescued STAT3 binding, gene expression, and hepatocyte proliferation to almost normal levels and prevented liver damage.

Interleukin-6 activates a variety of pathways, including the MAPK pathway and the STAT3 pathway, which are associated with the acute response [10]. Li et al. created liver-specific STAT3 deletion mice and reported that these mice exhibited reduced hepatocyte DNA synthesis at 40 h posthepatectomy, and lower expression level of G1-phase cyclins, such as cyclin D1 and E, in the liver. From these results, they conclude that STAT3 accounts for at least part of cell cycle progression and cell proliferation during liver regeneration [11]. In contrast, Moh et al. conditionally knocked out STAT3 in the liver (L-STAT3(-/-)) and reported significantly higher mortality of L-STAT3(-/-) mice within 24 h after 70% hepatectomy [12]. The level of hepatocyte DNA synthesis in the surviving L-STAT3(-/-) mice was slightly lower than that in STAT3(f/+) mice at 40 h posthepatectomy, whereas the liver mass completely recovered in the L-STAT3(-/-) mice. They also showed deteriorated DNA synthesis along with increased infiltration of neutrophils and monocytes in the liver in a carbon tetrachloride model using L-STAT3(-/-) mice. They concluded that STAT3 is required for survival in the acute stage after hepatectomy and plays an important role in the inflammatory reaction despite the limited role observed in the liver regeneration.

The importance of STAT3 in the inflammatory response is also supported by experiments in macrophage- and neutrophil-specific STAT3-deficient mice [13]. These mutant mice are highly susceptible to endotoxic shock, which involves the increased production of inflammatory cytokines, including TNF-α. It has been suggested that STAT3 plays a critical role in the IL10-mediated anti-inflammatory response by macrophages and neutrophils.

The importance of IL-6/STAT3 pathway for the proliferative signaling was shown by Kirillova et al. [14]. They used LE6 cells, a growth-arrested rat liver epithelial cell line, to show that the NF-κB/IL-6/STAT3 pathway is essential for TNF-α-induced proliferation. They found that the

TNF-α-induced upregulation of IL-6 mRNA expression and STAT3 activation was dependent on NF-κB activation and was essential for DNA replication.

Mori et al. previously found that pre-administration of proline could counteract galactosamine hepatitis by suppressing plasma GOT and GPT elevation and significantly decreasing the mortality rate [15]. They also found that proline administration delayed the onset of jaundice and subsequent death in LEC rats, which spontaneously develop lethal fulminant hepatitis due to excessive copper accumulation in the liver [16].

To investigate the mechanism of the protective effect of proline on GalN-induced hepatitis, I investigated the effect of proline on the activation of inflammation, the proliferative response, and the relevant survival signaling in the liver.

I found that proline administration activated the regenerative response and alleviated subsequent inflammation with the significant activation of survival signaling in the liver during the early phase of the disease.

Material and Methods

Animals and experimental design

Nine-week-old male Fischer 344 rats (Charles River Laboratory, Japan), weighing from 180-200 g, were maintained at 23ºC, given standard laboratory chow and water ad libitum, and kept under a 12 h light (7:00-19:00)/12 h dark schedule. Inbred rat, Fischer 344, was chosen because of the large individual difference of liver damage induced by GalN in case of outbred rats. All animals received humane care in accordance with the Japanese guidelines for animal experimentation (Japanese Association for Laboratory Animal Science). All procedures used in animal experiments were approved by the Animal Ethics Committee of the institution. Before the start of the experiment, food was withdrawn for 15 h, but the rats had free access to a 10% glucose solution. The animals were divided to 2 groups, each of which consisted of 5 animals. Only in the case of TNF-α experiment, each group consisted of 4 animals. The

control group received a single intraperitoneal injection of 30% GalN saline solution between 9:00 and 10:00 am at a dose of 1.4 g/kg body weight, and the proline group received a 10% proline solution orally at a dose of 2 g/kg body weight 1 h before GalN administration. Pre-administration of proline was determined based on the report that it's more effective than administration after GalN treatment [15].

Blood was collected from the inferior vena cava of anesthetized rats at the indicated time points after GalN treatment. After animals were killed by exsanguination at each time point, the livers were harvested and rinsed in ice-cold saline. A part of the liver was immediately frozen in liquid nitrogen for mRNA quantification and Western blot analysis, and the rest of the liver was used for histological analysis.

Survival rate

The survival rate was quantified twice per day between 8:00 and 9:00, and between 17:00 and 18:00 for up to 14 days after GalN injection.

Measurement of GOT, GPT and TNF-α levels

The collected blood samples were centrifuged to obtain plasma. The plasma GOT and GPT levels were measured using a FUJI DRI-CHEM analyzer (Fuji Film Corporation, Japan), and the plasma TNF-α level was measured using a rat TNF-α US UltraSensitive Kit (BIOSOURCE International, CA, USA).

Histology

The liver was fixed in 10% formalin and embedded in paraffin. The blocks were sectioned at 4 μm and stained with hematoxylin-eosin according to the standard protocol. Because several animals in the control group died at 72 h after the GalN injection, the surviving animals were used at this time point.

Isolation of total RNA and cDNA synthesis

Total RNA was isolated from liver tissue with ISOGEN (Nippon Gene Co., Ltd., Tokyo, Japan) according to the manufacturer's instructions. Total RNA was used as the template for cDNA synthesis with Superscript II reverse transcriptase (Invitrogen, CA, USA).

Real-Time PCR

The specificity of the PCR amplification with each primer pair was electrophoretically confirmed with a 4% NuSieve 3:1 agarose gel (Cambrex Corporation, USA). The PCR reactions were carried out in 20-μl reaction volumes using the SYBR Green PCR Master Mix (Applied Biosystems, USA) with 600 nM oligonucleotide primers and cDNA reverse-transcribed from 10 ng or 40 ng total RNA. For signal detection, the ABI Prism 7700 sequence detector (Life Technologies, CA, USA) was programmed to execute an initial step of 2 min at 50ºC and 10 min at 95ºC, followed by 40 thermal cycles of 15 sec at 95ºC and 1 min at 60ºC. The amount of the target gene was determined using a calibration curve that was constructed using serial dilutions of the target gene. The level of mRNA was expressed as the expression level relative to the average for the control group at 0 h, which was set to 1.0.

Western blot analysis

Liver tissue was homogenized in a lysis buffer (20 mM Tris-HCl, pH 8.0, 1% Triton X-100, 150 mM NaCl, 10% Glycerol, 1 mM NaF, and 1 mM EDTA) containing a protease inhibitor and a phosphatase inhibitor and centrifuged at 13,000 rpm for 20 min at 4ºC. The protein concentration of the supernatant was calculated using the BCA protein assay (Pierce, IL, USA). An aliquot of protein was resolved by SDS-polyacrylamide gel electrophoresis, transferred onto a nitrocellulose membrane, and probed with the primary antibody. Membranes were washed and probed with horseradish peroxidase-conjugated secondary antibodies. Protein bands were visualized by enhanced chemiluminescence using the ECL Plus Western Blotting Detection Reagent (GE Healthcare, CT, USA).

Expression of data and statistical analysis

The results are expressed as the mean ± SEM. The Student's *t* test was used for the comparison of data from two groups. The difference between groups was considered significant when P was less than 0.05.

Results

The effect of proline on the inflammatory response in the liver

Hematoxylin-eosin staining of liver sections was performed to observe the infiltration of inflammatory cells and expansion of the necrotic area, and the correlation with the survival rate was determined. First, the survival rate was compared between the control and the proline groups (Fig.1-1a). All of the control animals survived to 48 h after GalN administration, but the survival rate decreased to 60% at 72 h and to 40% at 80 h, after which point all remaining animals survived. In contrast, no animals in the proline group died.

Representative images of the hematoxylin-eosin staining of the liver sections from the 2 groups are presented in Figure 1-1b. In the control animals, a small number of focal necrotic areas started to appear at 6 h. The necrotic areas grew extensively between 24 and 48 h and further expanded at 72 h. The infiltration of inflammatory cells gradually became evident along with expansion of the necrotic areas. In the proline group, a few focal necrotic areas appeared as early as 3 h, at which point no sign of cell death was found in the control group. Although these early necrotic areas had grown to some extent by 24 h, they almost disappeared in association with the disappearance of infiltrated inflammatory cells by 48 h.

These results suggest that proline preadministration protects the liver from GalN-induced hepatotoxicity by suppressing inflammatory activation, and as a result, significantly increased the survival rate.

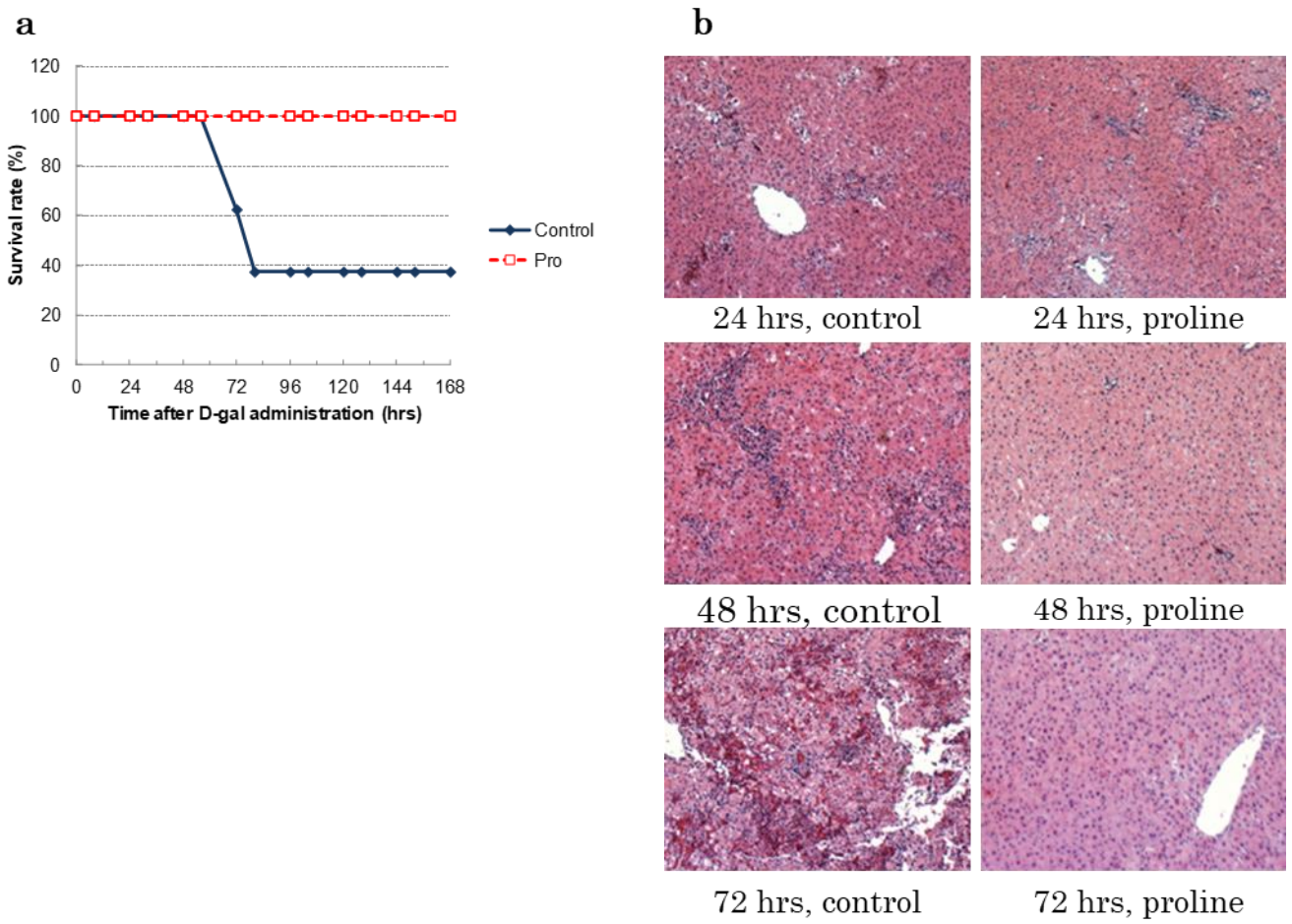

Fig.1-1. Survival rate and histology of the liver sections after GalN administration.
a Time course of the survival rate. All animals were injected with GalN (1.4g/kg body weight) intraperitoneally. The survival rate was quantified twice per day in the morning(8:00-9:00) and in the late afternoon(17:00-18:00). Time course of control and proline groups are denoted by *solid line* and *dotted line*, respectively. b The histology of the rat liver sections at 24, 48, 72 h. Hematoxylin-eosin staining was performed to observe the inflammatory infiltrates. The blue arrows indicate the area which is infiltrated by a lot of inflammatory cells. The black arrows indicate necrotic area which shows the deletion of hepatocytes and the infiltration of red blood cells. (Original magnification, 100x.)

Effects of proline on the plasma GOT, GPT and TNF-α levels

To quantitatively assess the effect of proline on inflammatory activation, I examined the elevation of the plasma levels of GOT, GPT and TNF-α in GalN-treated rats.

In both the control and proline groups, GalN injection caused marked elevations in the plasma GOT and GPT levels as early as 3 to 6 h after GalN injection. The plasma GOT and GPT levels in the proline

group started to increase earlier than in the control group, peaked at 24 h, and then declined at 48 h, in contrast to the continuous elevation in the control group (Fig.1-2a, b) The plasma GOT and GPT levels in the proline group at 48 h was statistically significantly lower than that of control group. ($P<0.05$)

The plasma TNF-α levels in both groups increased markedly as early as 3 h and peaked at 6 h (Fig. 2c). Similar to the GOT and GPT profiles, elevations of TNF-α in the proline group preceded those in the control group and the level at 3 h was significantly higher ($P<0.05$). Although differences in plasma TNF-α levels between the two groups were not statistically significant at any time point after 12 h due to the high variability among individual animals for the number of animals (n=4), the mean TNF-α levels in the proline group tended to be lower at 24 and 48 h.($P=0.10$ at 48 h)

These results suggest that proline pre-administration suppresses the predominant elevation of the plasma GOT, GPT at 48 h and TNF-α levels at 24 h and later, despite the preceding elevation seen in the earlier phase.

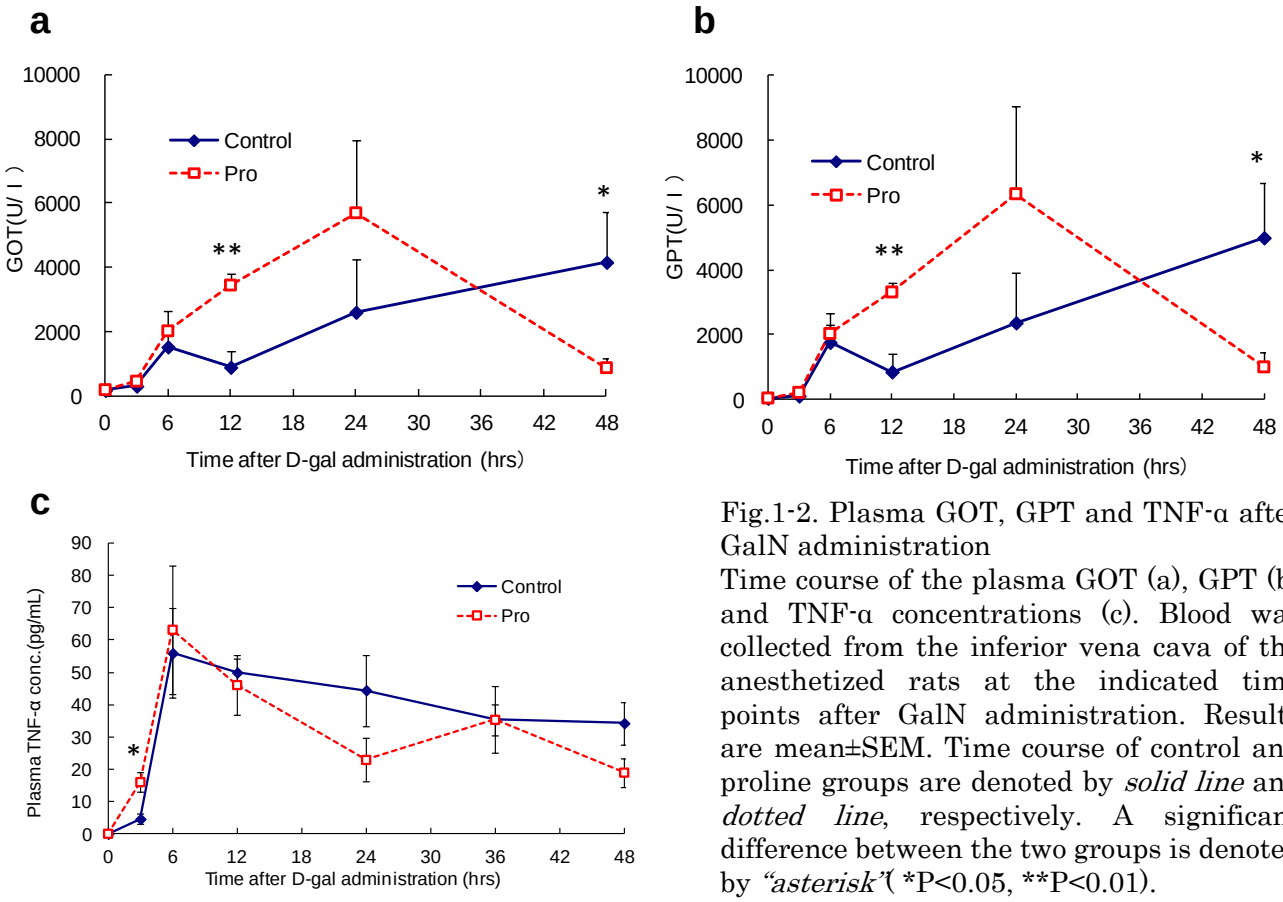

Fig.1-2. Plasma GOT, GPT and TNF-α after GalN administration
Time course of the plasma GOT (a), GPT (b) and TNF-α concentrations (c). Blood was collected from the inferior vena cava of the anesthetized rats at the indicated time points after GalN administration. Results are mean±SEM. Time course of control and proline groups are denoted by *solid line* and *dotted line*, respectively. A significant difference between the two groups is denoted by *"asterisk"*(*P<0.05, **P<0.01).

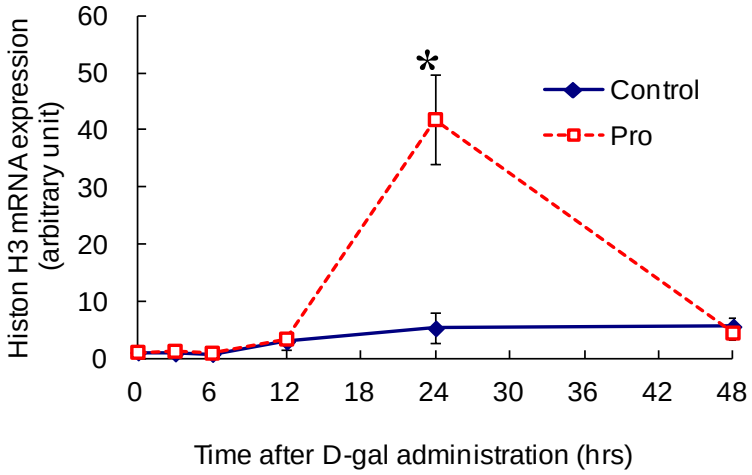

Fig.1-3. Hepatic expression of histone H3 mRNA after GalN administration.
The level of mRNA is expressed as the expression level relative to the average for the control group at 0 h. Results are mean±SEM. Time course of control and proline groups are denoted by solid line and dotted line, respectively. A significant difference between the two groups is denoted by "asterisk"(**P<0.01).

Proline-enhanced proliferation in the liver

To investigate the effect of proline on the regenerative response in the liver, I examined the expression of histone H3, a marker of cell proliferation, in the liver [17]. Histone H3 mRNA is expressed during DNA replication, and this expression is tightly coupled with DNA synthesis. Histone H3 expression was significantly upregulated by approximately 8-fold at 24 h in the proline group relative to the control group (5.23±2.63 vs. 41.79±7.86 (P<0.01), control vs. proline group)(Fig.1-3). In contrast, only a marginal increase in histone H3 expression was observed in the control group prior to the 48-h time point.

Proline-mediated activation of the IL-6/STAT3 pathway

The protective signaling of the IL-6/STAT3 pathway, downstream of TNF-α/NF-κB, has been reported to play a crucial role in the anti-inflammatory response [12,13] and proliferation [4,8,9,11,14,18]. Therefore, I examined the elevation of IL-6 mRNA levels and STAT3 activation in the liver.

Interleukin-6 mRNA expression in the liver from both groups dramatically increased between 3 and 6 h after GalN treatment (Fig.1-4a), and further increased in the proline group at 12 h, while that in the control group dramatically declined. The levels of IL-6 expression at 12 h in the control and proline groups were 208.3±134.6 (an arbitrary unit) and 2998.5±1907.5, respectively, with levels 14 times higher in the proline group (P<0.01) despite substantial individual variations.

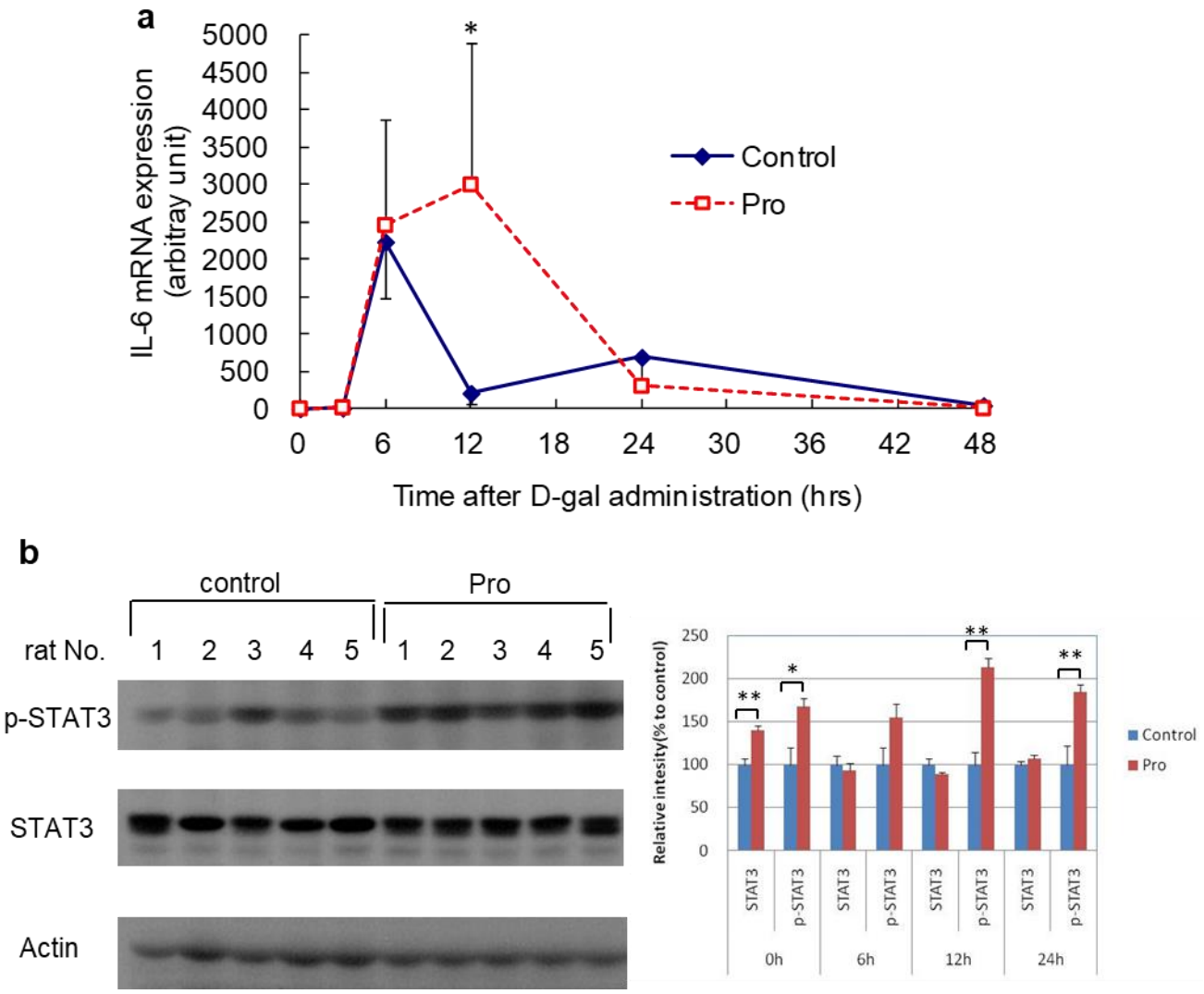

Fig.1-4. Hepatic expression of IL-6 mRNA, STAT3 and p-STAT3 proteins after GalN administration a Time course of hepatic expression of IL-6 mRNA. The level of mRNA is expressed as the expression level relative to the average for the control group at 0 h. Results are mean±SEM. Time course of control and proline groups are denoted by *solid line* and *dotted line*, respectively. A significant difference between the two groups is denoted by *"asterisk"*(**P<0.01). b Western blot of STAT3, p-STAT3(Tyr705), and actin from the livers of 5 rats in each group at 12 h (left panels), and densitometric determination of the protein levels of STAT3 and p-STAT3(Tyr705)(right panel). The protein levels of STAT3 and p-STAT3(Tyr705) was determined by western blot and expressed as the density of blot bands relative to the average of those of control rats at each time point. Results are mean±SEM. A significant difference between the two groups is denoted by *"asterisk"* (*P<0.05, **P<0.01).

I also examined the activation of STAT3, a downstream target of IL-6, in liver tissue. The phosphorylation of Tyr705, which is essential for the activation of STAT3 [19], was detected and quantified by western blot at time points up to 24 h (Fig.1-4b).

The intensity of each band was calculated as the intensity relative to the control group average at each time point and was expressed as a percentage. At 0 h, 1 h after the proline treatment and immediately before GalN injection, the levels of both STAT3 and p-STAT3 protein were significantly higher in the proline group (STAT3: 100.0±7.4% vs. 139.4±5.3% ($P<0.01$); p-STAT3: 100.0±20.0% vs. 167.1±9.8% ($P<0.05$)); control vs. proline group). After 6 h, no difference in STAT3 levels was observed between the two groups. In contrast, p-STAT3 levels remained higher in the proline group, with the maximum difference being a 2 times higther at 12 h (100.0±14.3% vs. 213.3±10.8% ($P<0.01$), control vs. proline group), and 1.8 times higher at 24 h (100.0±22.3 vs. 184.5±8.3 ($P<0.01$), control vs. proline group)

In summary, these results demonstrate that proline pre-administration promotes the activation of the STAT3 transcription factor both directly and indirectly via IL-6 mRNA upregulation.

Proline enhanced the expression of target genes of STAT3 and NF-κB transcription factors

The activation of the transcription factor STAT3, a downstream of TNF-α/NF-κB /IL-6 signaling, is involved in cell protection and proliferation, in combination with other transcription factors, such as NF-κB. In order to confirm the activation of STAT3 and NF-κB, and investigate the hepatoprotective and regenerative effects of these transcription factors, the expression levels of genes regulated by STAT3 and/or NF-κB were assessed by real-time PCR.

The antioxidant protein Ref-1 and the antiapoptotic protein X-linked inhibitor of apoptosis protein (XIAP) are targets of STAT3 and NF-κB, respectively, and mediate anti-apoptotic effects. The expression levels of both Ref-1 and XIAP were significantly upregulated in the proline group at 24 h after GalN administration (Ref-1: 0.88±1.93 vs. 1.81±0.13 ($P<0.01$), 1.10±0.21 vs. 2.74±0.26 ($P<0.01$), control vs. proline group), although there was no difference between control and proline groups at time

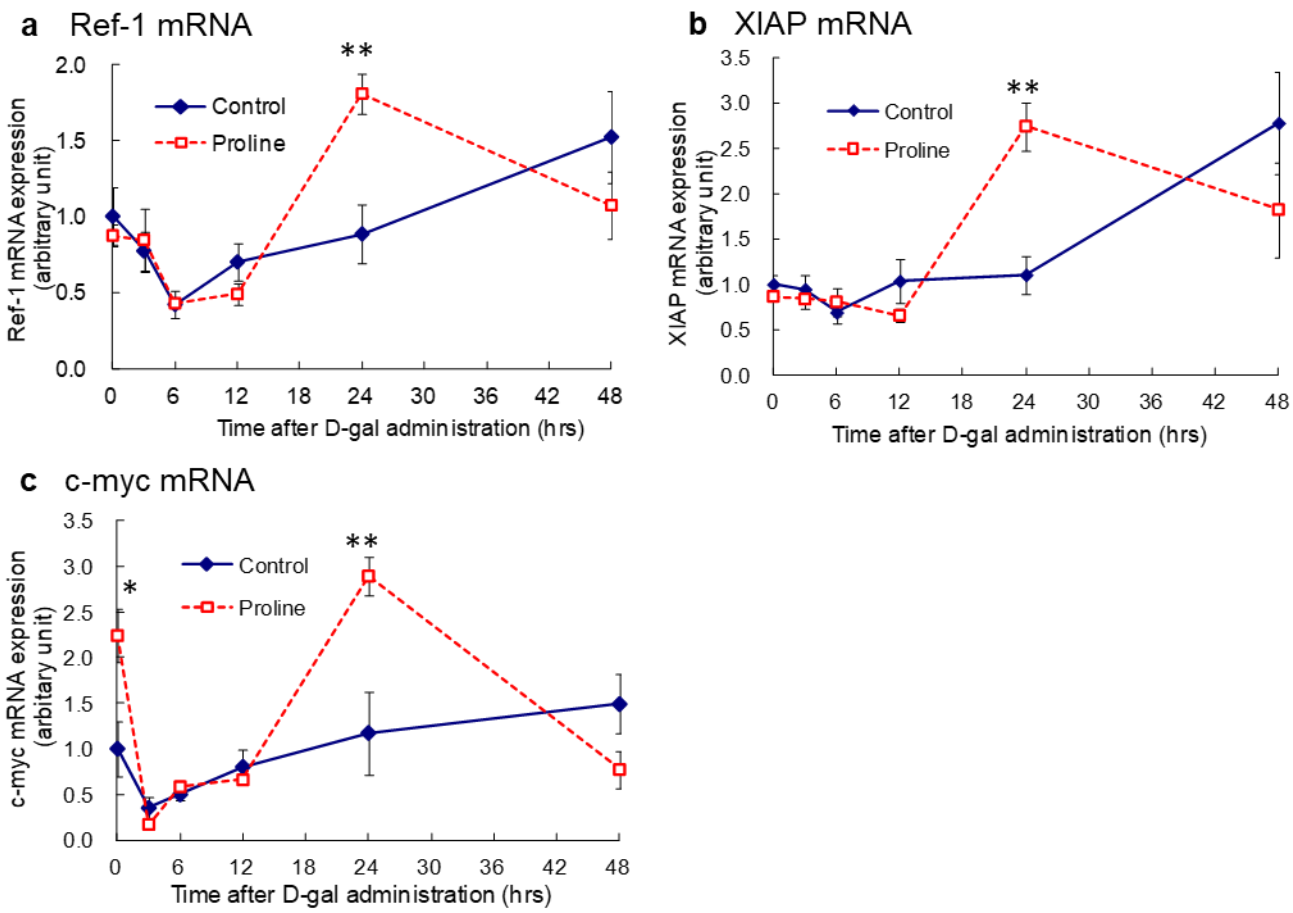

Fig.1-5. Hepatic expression of genes downstream of STAT3 and NF-κB
Hepatic expression of Ref-1 mRNA (a), XIAP mRNA (b), and c-myc mRNA (c). The level of mRNA is expressed as the expression level relative to the average for the control group at 0 h. Results are mean±SEM. Time course of control and proline groups are denoted by *solid line* and *dotted line*, respectively. A significant difference between the two groups is denoted by *"asterisk"* (*P<0.05, **P<0.01).

points up to 12 h (Fig.1-5a,b). After the peak at 24 h, the expression levels of both molecules declined in the proline group, in contrast to the gradual increase up to 48 h observed in the control group.

The proto-oncogene c-myc is involved in cell proliferation and is regulated by various transcription factors, including STAT3 and NF-κB. Higher expression of c-myc mRNA was observed in the proline group at 0 h, one hour after proline administration and immediately before GalN injection (Fig.1-5c). Although the expression in the proline group declined and stayed at the same level as that observed in the control group between 3 to 12 h, it was significantly upregulated at 24 h (1.17±0.45 vs. 2.89±0.21

($P<0.01$), control vs. proline group), in contrast to the marginal increase observed up to 48 h in control animals.

These results suggest that the upregulation of Ref-1 and XIAP expression correlated well with IL-6/STAT3 activation, with a significant difference in IL-6 expression level at 12 h, and in STAT3 activation at 12 h and 24 h. Notably, the upregulation of c-myc mRNA correlated well with STAT3 activation, which was promoted by proline directly at 0 h and indirectly via IL-6 mRNA upregulation between 6 h and 12 h.

Discussion

Proline suppressed inflammatory activation and activated the regenerative response probably via IL-6/STAT3 pathway

Mori et al. reported that the oral administration of proline improved the mortality rate in a GalN-induced model of liver failure by suppressing the plasma GOT and GPT elevation [15]. To investigate the mechanism of the protective effect of proline on this model, I examined the inflammatory response and regenerative activation, which are crucial to hepatic survival. I found that proline administration induced early hepatic upregulation of the histone H3 mRNA (a proliferative marker) at 24 h and decreased the inflammatory infiltration in the liver after 48 h in association with the fewer necrotic area, the significant decrease of plasma GOT, GPT, and the lower trend of plasma TNF-α. These results suggest that the early regenerative activation and the suppression of fulminant inflammation plays important roles in the hepatoprotective effect of proline. I then hypothesized that survival signaling downstream of TNF-α might be upregulated by proline.

It is well known that TNF-α is a mediator of the hepatic acute-phase response to inflammation and induces both cell death and proliferation. D-galactosamine injection induces serum TNF-α elevation, which triggers hepatocyte apoptosis [20]. The activation of NF-κB triggered by TNF-α is essential for cell survival in the acute phase of injury mediated by hepatic toxins, ischemia-reperfusion and partial

hepatectomy. Furthermore, the IL-6/STAT3 pathway, downstream of TNF-α/NF-κB, plays an important role in this protective mechanism.

In this study, I found that proline administration activated the IL-6/STAT3 pathway within 24 h after GalN treatment. Interleukin-6 mRNA upregulation was sustained for a longer time in the livers of proline-treated rats, which exhibited 14-fold higher expression at 12 h, compared with that of control rats. The level of p-STAT3(Tyr705) was 2 times higher at 12 h (maximum difference) and 1.8 times higher at 24 h.

I observed that the inflammatory infiltration was profoundly suppressed in the livers of proline-treated animals at 48 h in contrast to that of control animals, which showed predominant inflammatory infiltration at the same time point with further increase of infiltration up to 72 h. This result is supported by the early decrease of plasma GOT, GPT , and TNF-α in proline group at 48 h, despite the continuous increase of plasma GOT and GPT in control group. These results suggest the importance of STAT3 activation in the suppression of inflammatory activation.

In addition to the early suppression of inflammatory activation, I also found that proline administration markedly induced the mRNA expression of a proliferation marker, histone H3, in the liver at 24 h after GalN treatment. Downstream targets of IL-6, mitogen-activated protein kinase kinase (MAPK) and STAT3 work collaboratively to enhance cell proliferation. Recently, it is also reported that the IL-6/STAT3 pathway regulates hepatocyte proliferation via cyclin D1/p21 [21]. Therefore, the longer period of upregulation of IL-6 mRNA induced by proline from 6 to 12 h should contribute to regenerative activation..

In addition to proliferative and anti-inflammatory effects, STAT3 plays an important role in preventing apoptosis through the induction of antioxidant proteins, such as Ref-1, and antiapoptotic proteins which block caspase activation [22]. Recently, it has also been reported that STAT3 interacts with NF-κB and enhances NF-κB-dependent gene induction [23]. Notably, STAT3 prolongs NF-κB nuclear retention through acetyltransferase p300-mediated RelA proto-oncogene, NF-kB subunit (RelA) acetylation, thereby interfering with NF-κB nuclear export. Reversible acetylation of RelA regulates the

duration of nuclear NF-κB activity [24]. I observed that the antioxidant protein Ref-1 (a known target of STAT3), the antiapoptotic protein XIAP (a known target of NF-κB), and the proto-oncogene c-myc (a known target of both STAT3 and NF-κB) are all significantly increased in the livers of proline-treated animals at 24 h after GalN injection. This timing of mRNA upregulation correlated well with that of IL-6 between 6 and 12 h and p-STAT3 between 12 and 24 h. These results confirm the upregulation of the IL-6/STAT3 pathway in the proline group, and the induction of the expression of these genes may also contribute to the hepatic antiapoptotic response and cell proliferation.

Proline may protect the liver in another way. As shown in Fig. 1-4b, proline administration itself, even without GalN injection, directly upregulated the levels of STAT3 and p-STAT3 protein in the liver. The amount of both proteins was significantly higher at 0 h, that is, 1 h after proline administration and immediately before GalN injection. Based on the report that the administration of proline prior to GalN treatment is more effective than the administration after GalN treatment [15], this result suggests that the direct activation of STAT3 without the upregulation of IL-6 mRNA should also contribute to the tissue-protective effect mediated by proline.

In summary, I found that proline administration enhanced the hepatic regenerative response and suppressed inflammatory activation. These effects are thought to be triggered by prior activation of IL-6/STAT3 pathway, and play crucial roles in the hepatoprotective effect of proline.

Why is the IL-6/STAT3 pathway specifically upregulated by proline administration?

I found that IL-6 mRNA expression downstream of TNF-α signaling was dramatically increased in the liver by proline administration. Although the source of IL-6 within the liver has not been unequivocally established, studies with bone marrow transplantation provide evidence that hepatic Kupffer cells (liver macrophages) are responsible for the production of IL-6 in response to lipopolysaccharide or TNF-α [25]. The transcription factor NF-κB is critical for the induction of IL-6 mRNA expression, and ROS is reported to activate NF-κB in response to TNF-α in immune cells [26]. Furthermore, TNF-α itself is also regulated by NF-κB in immune cells during the inflammatory response.

I found that the elevation of serum TNF-α preceded in the proline group, with the significant difference at 3 h with that of control group. I also found that catalase activity was significantly enhanced in the proline group already at 0 h, which was just before GalN injection (data not shown). Based on this finding, I hypothesized that proline administration increases the production of ROS in the mitochondria before the GalN injection, and that increased ROS worked as a preconditioning before severe inflammation caused by GalN injection.

The first enzyme involved in proline metabolism is proline oxidase (POX), which is tightly bound to the mitochondrial inner membrane and is the rate-limiting enzyme in proline degradation. Proline oxidase converts proline to ⊿1-pyrroline-5-carboxylate, which serves as an obligate carbon bridge between the two major metabolic cycles, the tricarboxylic acid cycle and the urea cycle [27,28]. The catalytic mechanism involves the transfer of electrons from substrate proline to FAD with cytochrome *c* as the subsequent carrier into the electron transport chain. Thus, proline is a direct substrate for the generation of ATP [29,30]. Recently, it was shown that POX can reduce oxygen and generate superoxide [31]. The FAD of POX has direct access to solvent oxygen, and proline-derived electrons can directly reduce oxygen to produce superoxide autogenously.

Regarding ischemia/reperfusion (I/R) injury, it is well known that ROS production and the subsequent secretion of TNF-α significantly contributes to the injury, and short-term ischemia increases resistance to subsequent lethal ischemia/reperfusion with the suppression of massive inflammatory activation. Teoh et al. reported that following the ischemic preconditioning stimulus, there was an early small rise in hepatic and serum TNF-α levels, but during a next prolonged ischemia when TNF-α was secreted more than that during preconditioning, TNF-α release were lower and declined to negligible level earlier compared with naïve mice [32]. This protective effect of preconditioning is mimicked by the pre-administration of single low-dose of TNF-α. These results suggest that the small rise of plasma TNF-α triggered by short ischemia plays an essential role in the protective effect of preconditioning. It is also reported that both preconditioning and pre-administration of TNF-α induced early activation of NF-κB and STAT3 transcription factors and subsequent increase of hepatic cyclin D1 protein expression

and PCNA positive nuclei. Although the exact mechanism of preconditioning has not yet been elucidated, the protective effect of proline is very similar to that observed in preconditioning model of I/R injury, such as small rise of ROS and TNF-α before lethal rise of plasma TNF-α.

Our hypothesis is that the ROS produced by proline administration may accelerates the activation of the NF-κB at very early phase, and subsequent small rise of plasma TNF-α at 3 h after GalN injection may also make a positive effect on the extended activation of NF-κB. Enhanced activation of NF-κB, especially in the immune cells including Kupffer cells, should have contributed to the higher and prolonged activation of IL-6/STAT3 pathway and early regenerative response in the proline group. Although the prior increase of plasma TNF-α enhanced the activities of plasma GOT and GPT at 24 h compared with control animals, the activation of regenerative response at the same time point should counteract the damage in the liver.

In conclusion, this study has demonstrated that the protective mechanism mediated by proline in GalN-induced hepatitis is attributable to the early regenerative response and early reduction of inflammation, which is thought to be triggered by prior activation of the IL-6/STAT3 pathway, downstream of TNF-α/NF-κB signaling in the liver. The generation of ROS through proline metabolism by POX in mitochondria and early small rise of plasma TNF-α may underlie the enhanced activation of the NF-κB transcription factor. These results further emphasize the potential utilization of proline in protecting the liver against drug-induced injury, endotoxin shock, and ischemia-reperfusion injury including liver transplantation, in which TNF-α triggers liver failure.

References

[1] MacDonald JR, Beckstead JH, Smuckler EA: An ultrastructural and histochemical study of the prominent inflammatory response in D(+)-galactosamine hepatotoxicity. Br J Exp Pathol 1987; 68:189-99.

[2] Jirillo E, Caccavo D, Magrone T, Piccigallo E, Amati L, Lembo A, et al: The role of the liver in the response to LPS: experimental and clinical findings. J Endotoxin Res 2002; 8:319-27. doi: 10.1177/09680519020080050501.

[3] Grün M, Liehr H, Rasenack U: Significance of endotoxaemia in experimental "galactosamine-hepatitis" in the rat. Acta Hepatogastroenterol (Stuttg) 1977; 24:64-81.

[4] Xu Y, Bialik S, Jones BE, Iimuro Y, Kitsis RN, Srinivasan A, et al: NF-kappaB inactivation converts a hepatocyte cell line TNF-alpha response from proliferation to apoptosis. Am J Physiol 1998; 275(4 Pt 1):C1058-66.

[5] Kovalovich K, DeAngelis RA, Li W, Furth EE, Ciliberto G, Taub R: Increased toxin-induced liver injury and fibrosis in interleukin-6-deficient mice. Hepatology 2000; 31:149-59. doi: 10.1002/hep.510310123.

[6] Matsumoto T, O'Malley K, Efron PA, Burger C, McAuliffe PF, Scumpia PO, et al: Interleukin-6 and STAT3 protect the liver from hepatic ischemia and reperfusion injury during ischemic preconditioning. Surgery 2006; 140:793-802. doi:10.1016/j.surg.2006.04.010.

[7] Kovalovich K, Li W, DeAngelis R, Greenbaum LE, Ciliberto G, Taub R: Interleukin-6 protects against Fas-mediated death by establishing a critical level of anti-apoptotic hepatic proteins FLIP, Bcl-2, and Bcl-xL. J Biol Chem 2001; 276:26605-13. doi:10.1074/jbc.M100740200.

[8] Cressman DE, Greenbaum LE, DeAngelis RA, Ciliberto G, Furth EE, Poli V, et al: Liver failure and defective hepatocyte regeneration in interleukin-6-deficient mice. Science 1996; 274:1379-83. doi:10.1126/science.274.5291.1379.

[9] Li W, Liang X, Leu JI, Kovalovich K, Ciliberto G, Taub R: Global changes in interleukin-6-dependent gene expression patterns in mouse livers after partial hepatectomy. Hepatology 2001; 33:1377-86. doi:10.1053/jhep.2001.24431.

[10] Singh A, Jayaraman A, Hahn J: Modeling regulatory mechanisms in IL-6 signal transduction in hepatocytes. Biotechnol Bioeng 2006; 95(5):850-62. doi: 10.1002/bit.21026.

[11] Li W, Liang X, Kellendonk C, Poli V, Taub R: STAT3 contributes to the mitogenic response of hepatocytes during liver regeneration. J Biol Chem 2002; 277:28411-7. doi:10.1074/jbc.M202807200.

[12] Moh A, Iwamoto Y, Chai GX, Zhang SS, Kano A, Yang DD, et al: Role of STAT3 in liver regeneration: survival, DNA synthesis, inflammatory reaction and liver mass recovery. Lab Invest 2007; 87:1018-28. doi:10.1038/labinvest.3700630.

[13] Takeda K, Clausen BE, Kaisho T, Tsujimura T, Terada N, Förster I, et al: Enhanced Th1 activity and development of chronic enterocolitis in mice devoid of Stat3 in macrophages and neutrophils. Immunity 1999; 10:39-49. doi:10.1016/S1074-7613(00)80005-9.

[14] Kirillova I, Chaisson M, Fausto N: Tumor necrosis factor induces DNA replication in hepatic cells through nuclear factor kappaB activation. Cell Growth Differ 1999; 10:819-28.

[15] Ajinomoto Co., Inc.: (1996) Japan Patent Kokai 1996-169063.

[16] Hawkins RL, Mori M, Inoue M, Torii K: Proline, ascorbic acid, or thioredoxin affect jaundice and mortality in Long Evans cinnamon rats. Pharmacol Biochem Behav 1995; 52:509-15. doi:10.1016/0091-3057(95)00118-G.

[17] Vemura RP, Aragona E, Gupta S: Analysis of hepatocelluar proliferation: study of archival liver tissue is facilitated by an endogenous marker of DNA replication. Hepatology 1992; 16:968-973.

[18] Taub R: Hepatoprotection via the IL-6/Stat3 pathway. J Clin Invest 2003; 112:978-80. doi:10.1172/JCI200319974.

[19] Schuringa JJ, Dekker LV, Vellenga E, Kruijer W: Sequential activation of Rac-1, SEK-1/MKK-4, and protein kinase Cdelta is required for interleukin-6-induced STAT3 Ser-727 phosphorylation and transactivation. J Biol Chem 2001; 276(29):27709-15. doi:10.1074/jbc.M009821200.

[20] Itokazu Y, Segawa Y, Inoue N, Omata T: D-galactosamine-induced mouse hepatic apoptosis: possible involvement with tumor necrosis factor, but not with caspase-3 activity. Biol Pharm Bull 1999; 22:1127-30.

[21] Fujiyoshi M, Ozaki M: Molecular mechanisms of liver regeneration and protection for treatment of liver dysfunction and diseases. J Hepatobiliary Pancreat Sci 2011; 18(1):13-22.

[22] Haga S, Terui K, Zhang HQ, Enosawa S, Ogawa W, Inoue H, et al: Stat3 protects against Fas-induced liver injury by redox-dependent and -independent mechanisms. J Clin Invest 2003; 112:989-98. doi:10.1172/JCI200317970.

[23] Lee H, Herrmann A, Deng JH, Kujawski M, Niu G, Li Z, et al: Persistently activated Stat3 maintains constitutive NF-kappaB activity in tumors. Cancer Cell 2009; 15:283-93. doi:10.1016/j.ccr.2009.02.015.

[24] Chen Lf, Fischle W, Verdin E, Greene WC: Duration of nuclear NF-kappaB action regulated by reversible acetylation. Science 2001; 293:1653-7. doi:10.1126/science.1062374.

[25] Aldeguer X, Debonera F, Shaked A, Krasinkas AM, Gelman AE, Que X, et al: Interleukin-6 from intrahepatic cells of bone marrow origin is required for normal murine liver regeneration. Hepatology 2002; 35:40-8. doi:10.1053/jhep.2002.30081.

[26] Gloire G, Legrand-Poels S, Piette J: NF-kappaB activation by reactive oxygen species: fifteen years later. Biochem Pharmacol 2006; 72:1493-505. doi:10.1016/j.bcp.2006.04.011.

[27] Phang JM: The regulatory functions of proline and pyrroline-5-carboxylic acid. Curr Top Cell Regul 1985; 25:91-132.

[28] Wu G, Bazer FW, Burghardt RC, Johnson GA, Kim SW, Knabe DA, Li P, Li X, McKnight JR, Satterfield MC, Spencer TE: Proline and hydroxyproline metabolism: implications for animal and human nutrition. Amino Acids 2011; 40(4):1053-63. doi:10.1007/s00726-010-0715-z.

[29] Hagedorn CH, Phang JM: Transfer of reducing equivalents into mitochondria by the interconversions of proline and delta 1-pyrroline-5-carboxylate. Arch Biochem Biophys 1983; 225:95-101. doi:10.1016/0003-9861(83)90010-3.

[30] Adams E, Frank L: Metabolism of proline and the hydroxyprolines. Annu Rev Biochem 1980; 49:1005-61. doi:10.1146/annurev.bi.49.070180.005041.

[31] Donald SP, Sun XY, Hu CA, Yu J, Mei JM, Valle D, et al: Proline oxidase, encoded by p53-induced gene-6, catalyzes the generation of proline-dependent reactive oxygen species. Cancer Res 2001; 61:1810-5.

[32] Teoh N, Leclercq I, Pena AD, Farrell G: Low-dose TNF-alpha protects against hepatic ischemia-reperfusion injury in mice: implications for preconditioning., Hepatology 2003; 37(1):118-28. doi:10.1053/jhep.2003.50009.

Chapter II

The protection mechanism of proline from D-galactosamine hepatitis involves the early activation of ROS-eliminating pathway in the liver

Summary

The oral pre-administration of proline, one on the non-essential amino acids, has been shown to effectively protect the liver from D-galactosamine (GalN)-induced liver injury and dramatically improve the survival rate. In chapter I, I described that protective effect of proline involves the early activation of IL-6/STAT-3 pathway, an anti-inflammatory and regenerative signaling in the liver. Reactive oxygen species (ROS) are mediator of cellular injury and play an important role in hepatic damage during GalN-induced hepatitis. The aim of this study is to investigate the effect of proline on ROS-eliminating system. The activities of major ROS-detoxifying enzymes, i.e., glutathione peroxidase (GP), glutathione reductase (GR), catalase, and the level of glutathione in the liver were determined. Catalase activity was significantly upregulated in proline group from 0 to 3 h after GalN-injection, although GP and GR were downregulated during this period, compared with control group. From 6 to 12 h, the level of reduced glutathione (GSH) was significantly higher and the ratio of GSH/oxidized glutathione (GSSG) tended to be higher in proline group. Consistently with this, at 6 h, the GR activity in the proline group was significantly higher, followed with the higher tendency of GP activity at 12 h. Catalase activity was also significantly higher at 12 h. Taken together, catalase was activated at the beginning, followed with the significant activation of glutathione redox system around 6 to 12 h in proline group. These results suggest that the elimination of ROS in the liver was accelerated in proline group compared with control group at the very early stage of GalN-induced hepatitis.

Introduction

It is reported that endotoxemia significantly contributes to the pathogenesis of GalN hepatitis [1], by activating inflammatory cells followed with the secretion of inflammatory mediators such as TNF-α [2]. Activated macrophages infiltrate into the hepatic stroma and cause extensive hepatocellular necrosis [3]. Activated inflammatory cells, e.g. hepatic macrophages, Kupffer cells, hepatic neutrophils, produce and release large quantities of ROS such as superoxide anion, hydrogen peroxide, nitric oxide, and their derivatives, which target the surrounding tissue and cause oxidative stress intra- or extracelluarly [4-6]. The intracellular components result in dysfunction of mitochondria or mitochondrial enzyme systems [7].

On the other hand, in ischemia/reperfusion (I/R) model, it is well-known that ROS production and the subsequent secretion of TNF-α by inflammatory cells significantly contributes to the injury, and preconditioning by short-term ischemia increases resistance to subsequent lethal ischemia/reperfusion with the suppression of massive inflammatory activation. The protective mechanism of preconditioning involves the enhanced ROS-scavenging activity caused by the production of small amount of ROS by short-term ischemia [8,9].

In chapter I, I described that protective mechanisms mediated by proline supplementation in GalN-induced liver injury is attributable to the early regenerative response thorough the activation of NF-κB/IL-6/STAT3 pathway and early reduction of inflammation [10]. I hypothesized that production of small amount of ROS in the mitochondria through the proline metabolism [11] may activate NF-κB and be attributable to these protective mechanisms, mimicking the protective mechanism of preconditioning model by short-term ischemia.

To further investigate the mechanism of the protective effect of proline on GalN-induced hepatitis, I investigated the effect of proline on the anti-oxidative system in the liver.

Materials and Methods

Animals and experimental design

Nine-week-old male Fischer 344 rats (Charles River Laboratory, Japan), weighing from 180-200 g, were maintained at 23ºC, given standard laboratory chow and water ad libitum, and kept under a 12 h light (7:00-19:00)/12 h dark schedule. Inbred rat, Fischer 344, was chosen because of the large individual difference of liver damage induced by GalN in case of outbred rats. All animals received humane care in accordance with the Japanese guidelines for animal experimentation (Japanese Association for Laboratory Animal Science). All procedures used in animal experiments were approved by the Animal Ethics Committee of the institution. Before the start of the experiment, food was withdrawn for 15 h, but the rats had free access to a 10% glucose solution. The animals were divided to 2 groups, each of which consisted of 5 animals. The control group received a single intraperitoneal injection of 30% GalN saline solution between 9:00 and 10:00 am at a dose of 1.4 g/kg body weight, and the proline group received a 10% proline solution orally at a dose of 2 g/kg body weight 1 h before GalN administration. Pre-administration of proline was determined based on the report that it's more effective than administration after GalN treatment. [12]

After animals were killed by exsanguination at each time point, the livers were harvested and rinsed in ice-cold saline. A part of the liver was immediately frozen in liquid nitrogen for mRNA quantification.

Preparation of the liver sample

For the measurement of glutathione, about 0.1g of the rat liver was precisely weighed and homogenized with Polytron homogenizer in 1ml of extraction buffer (5 % sulfosalicylic acid, 5mM EDTA) on ice. The homogenate was centrifuged at 15000 rpm at 0 ℃ for 10 min, and 100 µl of the supernatant was diluted by 700 µl of MES buffer for sample solution.

For the measurement of catalase, about 0.1g of the rat liver was homogenized with Polytron homogenizer in 0.8 ml phosphate buffer (50 mM potassium phosphate buffer, pH 7.5, 1 mM EDTA). The

homogenate was centrifuged at 10000 rpm at 4 ℃ for 15 min, and the protein concentration of the supernatant was quantified using BCA protein assay (Pierce, IL, USA).

For the measurement of glutathione reductase and peroxidase, glutathione was removed from the supernatant. Briefly describing, 450µl phosphate buffer was added to 50µl supernatant and was subject to ultrafiltration (ULTRAFREE-0.5 Centrifugal Filter Device(UFV5BGC100), Millipore, MA, USA) at 12000 x g at 4 ℃ for 60 min. The retained fluid in the inner tube was filled up to about 100 µl by the phosphate buffer. The inner tube was rinsed with 100 µl phosphate buffer to combine with the retained fluid. The protein concentration of the sample was quantified using BCA protein assay.

Enzyme assays

The activity of GP was assayed by Glutahione Peroxidase Assay Kit (Cayman Chemical, MI, USA) as described in manufacturer's instructions. The supernatant of the liver homogenate was diluted to 0.3 mg/ml of protein concentration for the assay.

The activity of GR was assayed by Glutahione Reductase Assay Kit (Cayman Chemical, MI, USA) as described in manufacturer's instructions. The supernatant of the liver homogenate was diluted to 2.0 mg/ml of protein concentration for the assay.

Catalase activity was assayed by Amplex® Red Catalase Assay Kit (Life Technologies, USA) as described in manufacturer's instructions. The supernatant of the liver homogenate was diluted to 0.375 µg/ml of protein concentration for the assay.

Standard curve of GSH and GSSG

The standards of GSH and GSSG were prepared and diluted in extraction buffer (5 % sulfosalicylic acid, 5 mM EDTA): MES buffer (0.4 M 2-(N-morpholino) ethanesulphoric acid, 0.1 M sodium phosphate, 2mM EDTA, pH 6.5)=1:15 or 1:7 respectively to provide 10 concentrations in the rage of 0.5 – 32 µM.

Fifty microliters of standard solutions were mixed with assay cocktail (12.5μl of 4 mM NADPH in 5 % $NaHCO_3$, 25 μl of GSH reductase solution (Roche, No.105678, 5mg/ml), 12.5 μl of 10 mM 5,5'-dithiobis-2-nitrobenzoic acid in 0.1M phosphate buffer, 75 μl MES buffer, 25 μl distilled water) on 96-well plate. The absorbance at 405 nm was monitored at every 30 sec for 10 min at 37 ℃ to provide calibration curve. From the changes in absorbance over time for standards, the concentration of unknown samples were calculated.

Analysis of total glutathione and GSSG

For total glutathione determination, 100 μl of sample solution was diluted by 150 μl of MES buffer for further analysis. For GSSG determination, 500 μl of sample solution was added 5μl of 1 M 2-vinylpyridine in ethanol, mixed and incubated at room temperature for 60 min to mask the GSH.
Fifty microliters of the above diluted or 2- vinylpyridine -treated sample solution was mixed with assay cocktail on 96-well plate. The absorbance at 405 nm was monitored at every 30 sec for 10 min at 37 ℃.

The amount of GSH was calculated as the difference between total glutathione and GSSG.

Isolation of total RNA and cDNA synthesis

Total RNA was isolated from liver tissue with ISOGEN (Nippon Gene Co., Ltd., Tokyo, Japan) according to the manufacturer's instructions. Total RNA was used as the template for cDNA synthesis with Superscript II reverse transcriptase (Invitrogen, CA, USA).

Real-Time PCR

The specificity of the PCR amplification with each primer pair was electrophoretically confirmed with a 4% NuSieve 3:1 agarose gel (Cambrex Corporation, USA). The PCR reactions were carried out in 20-μl reaction volumes using the SYBR Green PCR Master Mix (Applied Biosystems, USA) with 600 nM oligonucleotide primers and cDNA reverse-transcribed from 10 ng or 40 ng total RNA. For signal

detection, the ABI Prism 7700 sequence detector (Life Technologies, CA, USA) was programmed to execute an initial step of 2 min at 50ºC and 10 min at 95ºC, followed by 40 thermal cycles of 15 sec at 95ºC and 1 min at 60ºC. The amount of the target gene was determined using a calibration curve that was constructed using serial dilutions of the target gene. The level of mRNA was expressed as the expression level relative to the average for the control group at 0 h, which was set to 1.0.

Expression of data and statistical analysis

The results are expressed as the mean ± SEM. The Student's t test was used for the comparison of data from two groups. The difference between groups was considered significant when P was less than 0.05.

Results

The effect of proline on the activation of glutathione redox cycle

Glutathione redox cycle is one of the major pathways of antioxidant defense. In order to investigate the effect of proline on the activation of glutathione redox cycle in the liver, I examined the activity of GP, GR, the amount of glutathione, and the mRNA expression involved in glutathione synthesis in the liver.

The activity of GP and GR dropped at 3 h after GalN administration in the proline group and the level was significantly lower compared with control group (GP activity: 353.4 ± 12.2 vs 303.8 ± 11.7 nmol/min/mg protein ($P<0.01$), GR activity: 25.9±1.3 vs 21.1±1.8 nmol/min/mg protein ($P=0.06$), control vs proline group) (Fig. 2-2a,b). The activity of both GP and GR elevated afterwards with the significantly higher activity of GR at 6 h in the proline group (25.2±0.6 vs 28.5±0.1 nmol/min/mg protein ($P<0.05$),

control vs proline group) and with the higher activity of GP at 12 h (332.0±25.0 vs 380.0±7.6 nmol/min/mg protein (P=0.10), control vs proline group).

The amount of total glutathione in the liver gradually increased in the proline group after GalN administration with levels two-times higher at 12 h relative to the control group (215.2±60.7 vs 412.4± 32.9 μmol/g tissue (P<0.05), control vs proline group)(Fig. 2-2c). The amount of reduced glutathione (GSH) also gradually increased in the proline group with the significantly higher amount at 6 h (224.7± 14.7 vs 277.0±16.8 μmol/g tissue (P<0.05), control vs proline group) and 12 h (167.0±52.8 vs 331.0±27.4 μmol/g tissue (P<0.05), control vs proline group) (Fig.2-2d).

The rate-limiting enzyme of glutathione synthesis, γ-glutamylcysteine synthetase (GCS), is composed of a catalytic (GCS-HS) and regulatory subunit (GCS-LS). Glutathione synthesis is also catalyzed by the second enzyme, glutathione synthetase (GS). Since glutathione synthesis is regulated by these enzymes, I examined the mRNA expression of these enzymes in the liver. Although the mRNA expression of GCS-HS and GS didn't show significant difference between control and proline group at any time points, that of GCS-LS dramatically increased in the proline group at 6 h with the level three times higher (0.76 ±0.10 vs 2.59±0.36 (P<0.01), control vs proline group) (Fig. 2-3).

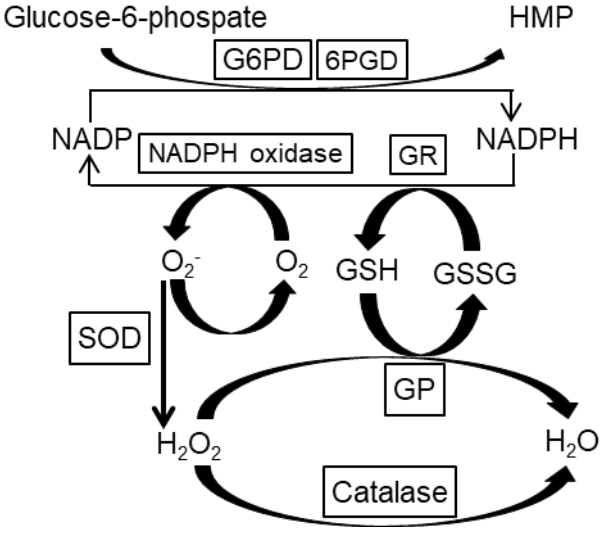

Fig. 2-1 Primary ROS-eliminating system in the liver
NADPH-dependent production and elimination of ROS is shown. The abbreviation stands for as follows:
GP, glutathione peroxidase;
GR, glutathione reductase;
GSH, reduced glutathione;
GSSG, oxidized glutathione;
SOD, superoxide dismutase;
G6PD, glucose-6-phosphate dehydrogenase;
6PGD, 6-phosphogluconate dehyderogenase;
HMP, hexose monophosphate pathway

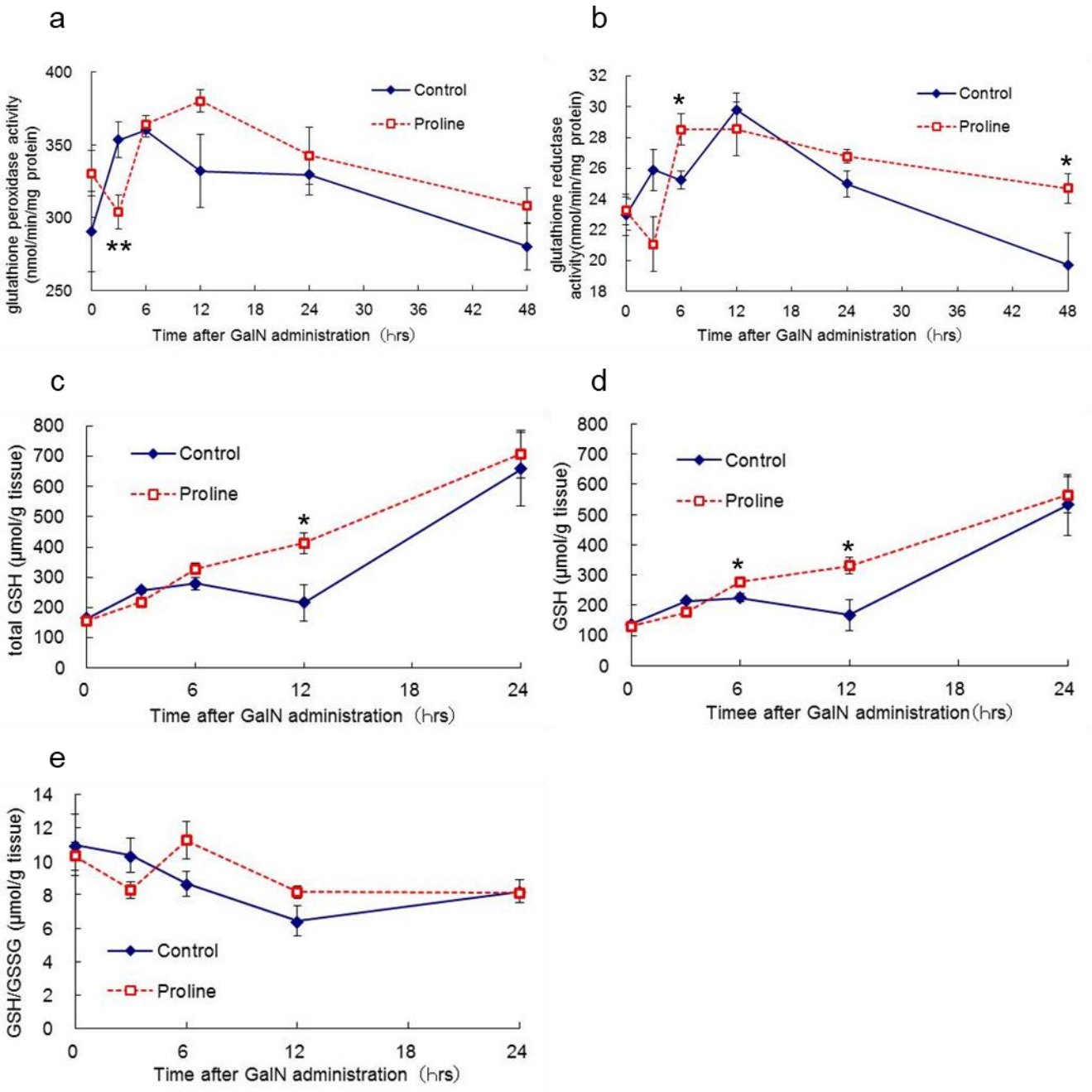

Fig. 2-2 The activity of enzymes involved in glutathione redox cycle and the level of glutathione in the liver

The activity of GP (a), GR (b) and the level of total glutathione (c), GSH (d), GSH/GSSG (e). Enzyme activities and the level of glutathione were determined as described in Materials and Methods. Results are mean±SEM. Time course of control and proline groups are denoted by solid line and dotted line, respectively. A significant difference between the two groups is denoted by "asterisk" (*P<0.05, **P<0.01).

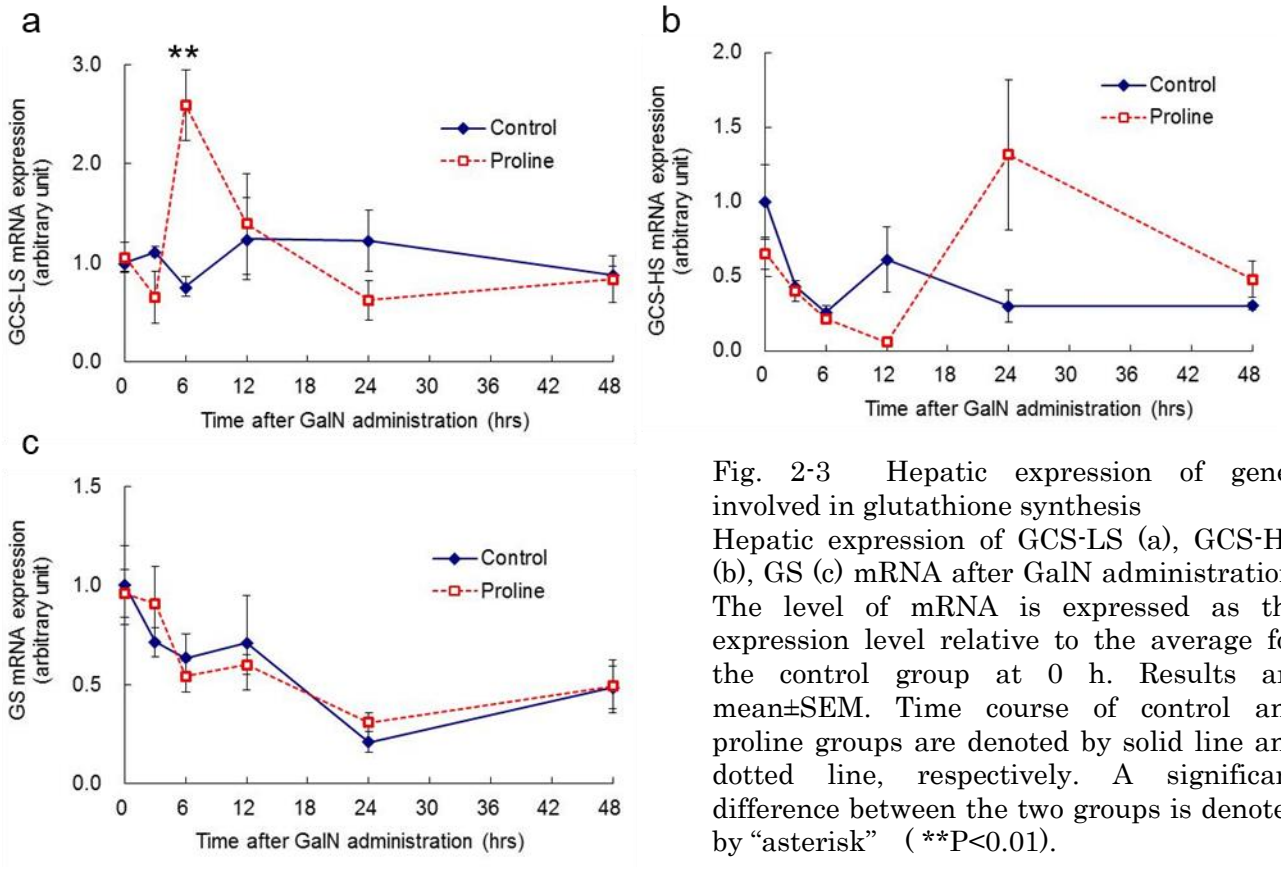

Fig. 2-3 Hepatic expression of genes involved in glutathione synthesis
Hepatic expression of GCS-LS (a), GCS-HS (b), GS (c) mRNA after GalN administration. The level of mRNA is expressed as the expression level relative to the average for the control group at 0 h. Results are mean±SEM. Time course of control and proline groups are denoted by solid line and dotted line, respectively. A significant difference between the two groups is denoted by "asterisk" (**P<0.01).

The effect of proline on catalase activity

In addition to GP, catalase is the other major hydrogen-peroxide-detoxyfying enzyme, which converts hydrogen peroxide to water utilizing NADPH. In order to investigate the effect of proline on the antioxidant defense system in the liver, I examined the catalase activity at each time point before and after GalN administration.

At 0 h, one hour after proline treatment and immediately before GalN injection, the levels of catalase activity was significantly higher in the proline group (1603±63 vs 2042±87 mU/μg protein (P<0.01), control vs proline group)(Fig. 2-4). Until 6 h, the catalase activity in the proline group gradually declined , although it was still significantly higher at 3 h than control group (1670±53 vs 1910±49 mU/μg protein (P<0.05), control vs proline group). At 12 h, the catalase activity in the proline group elevated again with

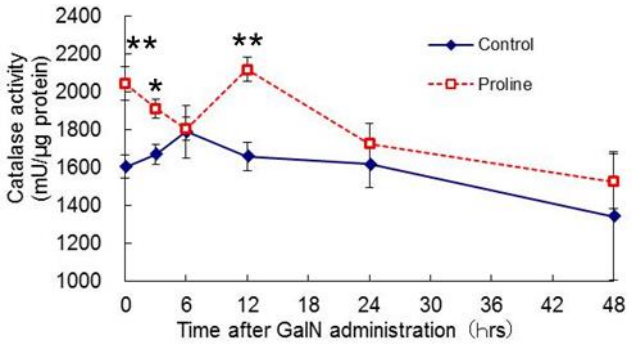

Fig. 2-4 The activity of catalase in the liver after GalN administration
The activity of catalase was determined as described in Materials and Methods. Results are mean±SEM. Time course of control and proline groups are denoted by solid line and dotted line, respectively. A significant difference between the two groups is denoted by "asterisk" (*P<0.05, **P<0.01).

the significantly higher activity in proline group, despite of almost steady level in control group (1657± 75 vs 2116±64 mU/μg protein (P<0.01), control vs proline group).

Discussion

To investigate the effect of proline on the ROS-eliminating system in the liver, I examined the activity of major anti-oxidative enzymes, i.e. catalase, GP, GR, and anti-oxidative substances which relate to the functions of those enzymes, i.e. glutathione. I found that catalase was already activated in proline group before GalN administration, and the activity was sustained at significantly higher level than control group up to 3 h after GalN injection. From this result, it can be assumed that proline administration itself causes oxidative stress in the liver, and it may be probably attributable to the metabolism of proline. There are a couple of possible metabolic reactions of proline which may produce ROS. One of the possibilities is the first enzyme involved in proline metabolism, proline oxidase, as it was already speculated in the previous report [10]. The other possible mechanism is increased reactive oxygen production by the respiratory chain in mitochondria through the enhanced electron flow caused by pyruvate derived from proline [13].

At early phase of GalN hepatitis, i.e. at 3 h after GalN injection, although the total glutathione level began to increase in both groups, the activities of GR and GP in proline group were significantly lower in proline group than those in control group. From these results, it can be assumed that the glutathione redox cycle has not yet been enhanced in proline group relative to control group at 3 h. Taken together, at early phase of GalN hepatitis, enhanced catalase is the major hydrogen peroxide-detoxifying pathway in proline group, and its detoxifying capacity is higher compared with control group.

On the next phase, from 6 to 12 h after GalN ingestion, the GSH level in the liver of the proline group was significantly higher and the GSH/GSSG ratio in the proline group tended to be higher. In addition, GR activity was significantly higher at 6 h, and GP activity tended to be higher at 12 h. These results suggest that the glutathione redox cycle in proline group was significantly activated relative to control group from 6 to 12 h.

At 12 h, catalase activity was also upregulated and significantly higher in proline group and differences of total glutathione and reduced glutathione level between both groups was the most significant with levels two times higher in proline group. These results suggest that from 6 to 12 h after GalN injection, the ROS-eliminating system in the liver of proline group was significantly activated than that of control group, probably with the most significant difference at 12 h. Later than 24 h, catalase, GR and GP activity were still prone to be higher in proline group with the significantly higher activity of GR at 48 h.

Activation of glutathione redox system is very important because GP and GSH S-transferase reduce not only hydrogen peroxide but also organic peroxide. Furthermore, although hydrogen peroxide can also be reduced by catalase which is present only in the peroxisome, glutathione redox cycle is particularly important in the mitochondria, because there is no catalase [14-15]. In the present study, I found that the activity of Mn-SOD, which is known to be expressed only in the mitochondria, tended to be higher in proline group from 6 to 12 h (P=0.13 at 6 h, P=0.19 at 12 h, data not shown). The result strongly suggests the possibility that the ROS production in mitochondria increased at the time. The cooperative

upregulation of glutathione redox system of the proline group should help to more effectively eliminate ROS in the mitochondria, relative to control group.

Glutathione is synthesized in all mammalian cells. Reduced glutathione (GSH) is the predominant form, whereas the GSSG content is less than 1% of GSH [16]. Almost 90% of cellular GSH are in the cytosol , 10% is in the mitochondria and a small percentage is in the endoplasmic reticulum [17].

Glutathione is synthesized in cytosol and the synthetic process involves two ATP-requiring steps. The first step is catalyzed byγ-glutamylcysteine synthetase (GCL) and is considered to be rate limiting step. The second step is catalyzed by glutathione synthetase (GS). γ-Glutamylcysteine synthetase is composed of a heavy or catalytic (GCS-HS) and a light or modifier (GCS-LS) subunit. Modifier subunit is enzymatically inactive but plays an important regulatory function by lowering the Km of GCL for glutamate and raising the Ki for GSH [18-19]. In the present study, I found that regulatory subunit, GCL-LS mRNA was significantly upregulated in proline group at 6 h with the levels three times higher. Since there was no significant difference of the mRNA level of GCS-HS and GS between control and proline group at any time points, it can be assumed that the activity of GCS in proline group might be upregulated by the upregulation of regulatory subunit of GCS, leading to the significant upregluation of total GSH from 6 h to 12 h.

In addition to anti-oxidant function, it is reported that GSH plays an important role in cell proliferation. Lu et al. reported that when rat hepatocytes were plating under low density, which stimulates hepatocyte to shift from Go to G1 phase, increased GSH level with the activation of GCS [20]. It is also reported that after 2/3 partial hepatectomy, hepatic GSH increased due to increased biosynthesis prior to the onset of DNA synthesis [21]. When this increase in GSH was blocked, liver regeneration was impaired [22]. Furthermore, the increase of GSH directly correlates with the growth of liver cancer cells. In our previous study, I reported that the regenerative signaling, IL-6/STAT3 pathway, was strongly activated from 12 to 24 h after GalN injection followed with the significant upregulation of the marker of proliferation, histone H3 mRNA at 24 h in proline group. The significant

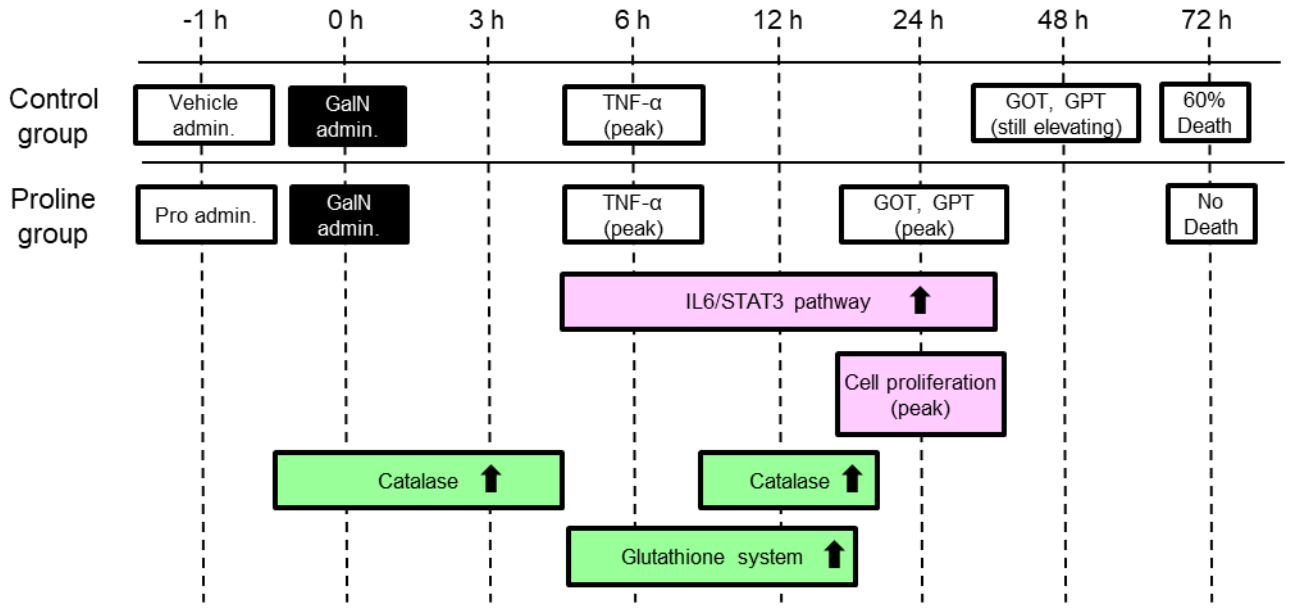

Fig. 2-5 The elevation of the inflammatory indices, the proliferative signaling and the activation of the ROS-eliminating system
Outline of the results obtained so far. The level of inflammatory indices (TNF-α, GOT, GPT), the proliferative signaling (IL-6/STAT3 pathway), and the proliferative marker (histone H3) are investigated in the previous paper (Obayashi, et al, 2012).

activation of proliferative signaling in the liver of the proline group might be partially attributable to the early increase of GSH content.

In the previous study, I also reported that plasma level of TNF-αpeaked at 6 h in both group and gradually decreased later than 12 h [10]. On the other hand, the levels of GOT and GPT began to increase from 3 h in both groups, peaked at 24 h and decreased at 48 h in proline group, although those levels in control group continued to increase up to 48 h (Fig. 2-5). These results suggest that the oxidative stress should be introduced at very early phase in the liver of both groups.

This study has demonstrated that the early introduction of anti-oxidative property in the liver of proline group must significantly contribute to protecting parenchymal and non-parenchymal cells from oxidative stress caused by GalN injection. It should be also noted that early upregulation of GSH in the liver of the proline group should plays an important role in the activation of proliferative signaling within 24 h. The low level production of ROS by metabolic process of proline may work as a

preconditioning to effectively induce anti-oxidative system against the significant oxidative stress induced by GalN injection. As is recently suggested, proline can be considered as a “functional amino acids” [23-25].

This study demonstrated that proline supplementation in GalN-induced liver failure model significantly activated ROS-eliminating system such as catalase and glutathione system in the liver within 24 hours after GalN administration. It is thought that early induction of these antioxidative systems should significantly contribute to the protective mechanism of proline supplementation in this model.

References

[1] Grün M, Liehr H, Rasenack U: Significance of endotoxaemia in experimental "galactosamine-hepatitis" in the rat. Acta Hepatogastroenterol (Stuttg) 1977; 24:64-81.

[2] Jirillo E, Caccavo D, Magrone T, Piccigallo E, Amati L, Lembo A, et al: The role of the liver in the response to LPS: experimental and clinical findings. J Endotoxin Res 2002; 8:319-27. doi: 10.1177/09680519020080050501.

[3] MacDonald JR, Beckstead JH, Smuckler EA: An ultrastructural and histochemical study of the prominent inflammatory response in D(+)-galactosamine hepatotoxicity. Br J Exp Pathol 1987; 68:189-99.

[4] Bautista AP, Mészáros K, Bojta J, Spitzer JJ: Superoxide anion generation in the liver during the early stage of endotoxemia in rats. J Leukoc Biol 1990; 48(2):123-8.

[5] Sakaguchi S: Metabolic aspects of endotoxin as a model of septic shock--approached from oxidative stress. Yakugaku Zasshi 2004; 124(2):69-87.

[6] Sakaguchi S, Furusawa S: Oxidative stress and septic shock: metabolic aspects of oxygen-derived free radicals generated in the liver during endotoxemia. FEMS Immunol Med Microbiol 2006; 47(2):167-77.

[7] Jaeschke H, McGill MR, Ramachandran A: Oxidant stress, mitochondria, and cell death mechanisms in drug-induced liver injury: lessons learned from acetaminophen hepatotoxicity. Drug Metab Rev 2012; 44(1):88-106. doi: 10.3109/03602532.2011.602688.

[8] Morihira M, Hasebe N, Baljinnyam E, Sumitomo K, Matsusaka T, Izawa K, Fujino T, Fukuzawa J, Kikuchi K: Ischemic preconditioning enhances scavenging activity of reactive oxygen species and diminishes transmural difference of infarct size. Am J Physiol Heart Circ Physiol 2006; 290(2):H577-83.

[9] Teoh N, Leclercq I, Pena AD, Farrell G: Low-dose TNF-alpha protects against hepatic ischemia-reperfusion injury in mice: implications for preconditioning., Hepatology 2003; 37(1):118-28. doi:10.1053/jhep.2003.50009.

[10] Obayashi Y, Arisaka H, Yoshida S, Mori M, Takahashi M: Proline protects liver from D-galactosamine hepatitis by activating the IL-6/STAT3 survival signaling pathway. Amino Acids 2012; 43(6):2371-80. doi: 10.1007/s00726-012-1317-8.

[11] Wu G, Bazer FW, Burghardt RC, Johnson GA, Kim SW, Knabe DA, Li P, Li X, McKnight JR, Satterfield MC, Spencer TE: Proline and hydroxyproline metabolism: implications for animal and human nutrition. Amino Acids 2011; 40(4):1053-63. doi: 10.1007/s00726-010-0715-z.

[12] Ajinomoto Co., Inc.: (1996) Japan Patent Kokai 1996-208472.

[13] Marí M, Bai J, Cederbaum AI: Toxicity by pyruvate in HepG2 cells depleted of glutathione: role of mitochondria. Free Radic Biol Med 2002; 32(1):73-83.

[14] Fernández-Checa JC, Kaplowitz N, García-Ruiz C, Colell A, Miranda M, Marí M, Ardite E, Morales A: GSH transport in mitochondria: defense against TNF-induced oxidative stress and alcohol-induced defect. Am J Physiol 1997; 273(1 Pt 1):G7-17.

[15] Garcia-Ruiz C, Fernandez-Checa JC: Mitochondrial glutathione: hepatocellular survival-death switch. J Gastroenterol Hepatol 2006; 21 Suppl 3:S3-6.

[16] Akerboom TP, Bilzer M, Sies H: The relationship of biliary glutathione disulfide efflux and intracellular glutathione disulfide content in perfused rat liver. J Biol Chem 1982; 257(8):4248-52.

[17] Meredith MJ, Reed DJ: Status of the mitochondrial pool of glutathione in the isolated hepatocyte. J Biol Chem 1982; 257(7):3747-53.

[18] Huang CS, Anderson ME, Meister A: Amino acid sequence and function of the light subunit of rat kidney gamma-glutamylcysteine synthetase. J Biol Chem 1993; 268(27):20578-83.

[19] Huang CS, Chang LS, Anderson ME, Meister A: Catalytic and regulatory properties of the heavy subunit of rat kidney gamma-glutamylcysteine synthetase. J Biol Chem 1993; 268(26):19675-80.

[20] Lu SC, Ge JL: Loss of suppression of GSH synthesis at low cell density in primary cultures of rat hepatocytes. Am J Physiol 1992; 263(6 Pt 1):C1181-9.

[21] Huang ZZ, Li H, Cai J, Kuhlenkamp J, Kaplowitz N, Lu SC: Changes in glutathione homeostasis during liver regeneration in the rat. Hepatology 1998; 27(1):147-53.

[22] Huang ZZ, Chen C, Zeng Z, Yang H, Oh J, Chen L, Lu SC: Mechanism and significance of increased glutathione level in human hepatocellular carcinoma and liver regeneration. FASEB J 2001; 15(1):19-21.

[23] Wu G: Functional amino acids in growth, reproduction, and health. Adv Nutr 2010; 1(1):31-7. doi: 10.3945/an.110.1008.

[24] Wu G, Wu Z, Dai Z, Yang Y, Wang W, Liu C, Wang B, Wang J, Yin Y: Dietary requirements of "nutritionally non-essential amino acids" by animals and humans. Amino Acids 2013; 44(4):1107-13. doi: 10.1007/s00726-012-1444-2.

[25] Wu G: Dietary requirements of synthesizable amino acids by animals: a paradigm shift in protein nutrition. J Anim Sci Biotechnol 2014; 5(1):34. doi: 10.1186/2049-1891-5-34.

Chapter III

Anti-atherogenic effect of proline in a rat model of high sucrose diet-induced hyperlipidemia

Summary

Numerous studies have shown that hyperlipidemia triggers inflammatory reaction and endothelial dysfunction, and those are regarded as important risk factors for cardiovascular disease. To investigate the effect of proline on endothelial dysfunction and inflammatory reactions, I used short-term high sucrose diet-fed rat model as hyperlipidemia model. I found that proline supplementation (2 g/kg) not only enhanced endothelium-dependent vasorelaxation but also suppressed the elevated gene expression of adhesion molecules such as ICAM-1, MCP-1 and E-selectin in the thoracic aorta and plasma level of soluble ICAM-1. I also found that the gene expression of cycline dependent kinase inhibitor, p21, whose expression is reported to decrease in disease state and modulate smooth muscle cell proliferation, was significantly increased by proline supplementation. These results suggest that proline supplementation may have anti-atherogenic effect at early phase of cardiovascular events.

Introduction

Reducing the risk of adverse cardiovascular events is important to prevent future fatal outcome by cardiovascular disease. Recently, postprandial hyperlipidemia caused by high-energy diet is recognized as metabolic stress which causes endothelial dysfunction and inflammatory reaction and regarded as an important risk factor for cardiovascular disease [1-3]. Increased inflammatory activity contributes to the development of atherosclerotic plaques, leading to a coronary event. In diabetic patients, circulating levels of proinflammatory cytokines, C-reactive protein and soluble adhesion molecules are elevated, suggesting stimulation of proatherogenic inflammatory activity [4-7].

On the other hand, the oral pre-administration of proline, one of the non-essential amino acids, has been shown to effectively protect the liver from GalN-induced liver injury and dramatically improve the survival rate [8]. In the previous study, I reported that protective effect of proline involves a significant suppression of inflammatory infiltration in the liver after GalN administration, being accompanied by a depletion of the plasma elevation of GOT and GPT [9]. I noticed that in the liver of proline-preadministered rats, the morphology of endothelial cells is relatively well-maintained compared with that of control animals without proline administration during the time when infiltration of inflammatory cells are facilitated (data not shown). In addition, the cell proliferation of perivascular area in the liver of proline-preadministered rats, being detected by proliferating cell nuclear antigen (PCNA)-staining, was significantly enhanced compared with control rats at very early phase.

Based on these observations, I hypothesized that proline may have a protective effect on endothelial cells, and this effect may contribute to anti-inflammatory effect through the suppression of the infiltration of inflammatory cells into parenchyma.

In order to verify our hypothesis, considering the importance of the prevention of cardiovascular events at early phase, I examined the protective effect of proline on endothelial dysfunction and inflammatory reaction, using early atherogenic model, short-term high sucrose diet-fed rat model. This animal model is reported to exhibit a significantly elevated plasma triglyceride and free fatty acid (FFA) levels, and impaired carbamylcholin-induced endothelium-dependent vasorelaxation response [10].

Materials and Methods

Animals and experimental protocol

Male Sprague-Dawley rats aged 8-10 weeks were used. Rats were randomized and assigned to a control group, high sucrose diet-fed group (HS group), and high sucrose diet with proline administration group (Pro-HS group). Rats were housed under controlled environmental conditions (23℃; 30-40% humidity) and a 12 h light/dark cycle (lights on at 8:00). Rats had free access to water and were fed

from 19:00 to 10:00. Controls were fed standard laboratory powder diet (CRF-1,), while the HS group were fed high sucrose diet consisting of 33% (by weight) standard CRF-1 diet, 33% condensed milk (Morinaga, Japan), 7% sucrose and 27% water. Pro-HS group were orally administered proline (2 g/kg, 10% solution) at 18:00 on day 2 and day 3, and fed high sucrose diet. Control and HS groups were orally administered water (20 ml/kg) at 18:00 on day 2 and day 3, instead of proline solution. All animals in the study were maintained on their respective diet for four days before being sacrificed. The rats were anesthetized by ether before dissection between 10:30 and 11:30 on day 4. Blood was collected from the inferior vena cava of anesthetized rats. The rats were sacrificed by exsanguination. The thoracic aorta was carefully harvested and be subject to the assessment of vascular function and mRNA analysis. All animals received humane care in accordance with the Japanese guidelines for animal experimentation (Japanese Association for Laboratory Animal Science). All procedures used in animal experiments were approved by the Animal Ethics Committee of the institution.

Isolation of RNA and cDNA synthesis

Total RNA was extracted using ISOGEN (Nippon Gene, Japan), following the manufacture's instruction. RNA concentration was determined spectrophotometrically. Eight μg of total RNA was reverse-transcribed into first-strand cDNA using Superscript II preamplification system (Invitrogen, California, USA)

Real-time RT-PCR

Based on the published mRNA sequence, gene-specific primers were designed. Specificity of the PCR amplification of each primer pair was confirmed with 4% NuSieve agarose 3:1 gel (Cambrex Corporation, USA). The PCR reaction was carried out using SYBR Green PCR Master Mix (Applied Biosystems, USA). For the signal detection, ABI Prism 7700 Sequence Detector (Life Science Technologies, CA, USA) was programmed to execute an initial step of 2 min at 50℃ and 10 min at 95℃, followed by 40 thermal cycles of 15 sec at 95℃ and 1 min at 60℃. The amount of the target gene was

determined using a calibration curve that was constructed using serial dilutions of the target gene. The level of mRNA was expressed as the expression level relative to the average for the control group, which was set to 100.

Assessment of vascular function

The thoracic aorta were carefully dissected, removed surrounding fat and connective tissue completely, and put in Tyrode buffer [composition(in mM): $NaHCO_3$ 10.0, Glucose 5.0, NaCl 158.3, KCl 4.0, $CaCl_2 \cdot 2H_2O$ 2.0, $MgCl_2 \cdot 2H_2O$ 1.05, NaH_2PO_4 0.42]. Segments (4-5 mm length) of the artery were mounted on two metal holders, one of which was connected to a force displacement transducer (Isometric Transducer TB-981T, Nihon-Denko, Japan) and the other to a movable device that allowed the application of a passive tension of 2.0 g. The vessels were incubated in a 10 ml organ bath containing Tyrode buffer gassed with 95% O_2 and 5% CO_2 at 37℃. After more than 1 h equilibration, arteries were depolarized with high-potassium Tyrode buffer [composition(in mM): $NaHCO_3$ 10.0, Glucose 5.0, NaCl 112.3, KCl 50.0, $CaCl_2 \cdot 2H_2O$ 2.0, $MgCl_2 \cdot 2H_2O$ 1.05, NaH_2PO_4 0.42] To determine endothelial function, the relaxation induced in phenylephrine(10^{-6}M)-preconstricted arteries following exposure to an endothelium-dependent vasodilator, namely acetylcholine(ACh), and an endothelium-independent vasodilator, namely sodium nitroprusside (SNP) was measured. When contraction reached plateau, concentration-response curve were carried out to ACh (10^{-9}～10^{-5}M) and SNP (10^{-9}～10^{-6}M).

Measurement of plasma soluble ICAM-1 level

The collected blood samples were centrifuged to obtain plasma. The plasma soluble ICAM-1 level was measured using a Quantikine® ELISA Rat sICAM-1/CD54 Immunoassay (R&D Systems, Minnesota, USA).

Expression of data and statistical analysis

The results are expressed as the mean ± SEM. The statistical significance of differences was determined by Tukey-Kramer test between 3 groups and Student's t test between 2 groups. The difference between groups was considered significant when P was less than 0.05.

Results

Metabolic data

The effect of high-sucrose diet and simultaneous proline administration on body weight and metabolic index were measured on the 4-day of high-sucrose diet feeding.

There was no significant difference between control, HS, and Pro-HS groups in body weight, blood glucose, and plasma FFAs. Plasma triglyceride was statistically significantly higher in HS and HS-Pro groups than control group (Table 1).

Table 1 Physiological and metabolic characteristics of control diet-fed and high sucrose diet-fed rats

Data are presented as mean ±SEM. Asterisk denotes statistically significant difference compared with control group (* $P<0.05$).

parameters	control	HS	Pro-HS
Body weight (g)			
Initial	309.4±2.9	309.2±3.4	303.3±3.2
Final	336.9±4.8	341.5±5.0	339.9±5.3
Plasma glucose (mg/dl)	161.5±4.0	153.7±4.1	169.8±2.3
Plasma triglyceride (mg/dl)	117.2±13.2	194.0±9.7*	164.0±13.1*
Plasma FFA (mg/dl)	0.156±0.014	0.144±0.006	0.121±0.009

The effect of proline administration on endothelium-dependent and -independent vasorelaxation in vivo

To investigate the effect of high sucrose diet with or without proline administration on endothelium-dependent vasorelaxation, ACh-induced vasorelaxation was evaluated on thoracic aorta harvested after 4-day feeding of high-sucrose diet. There was no significant difference of ACh-induced vasorelaxation between control and HS groups, but that of Pro-HS group was significantly enhanced compared with either of control and HS groups. No significant differences were observed among the 3-groups in SNP-induced endothelium-independent vasorelaxation (Fig.3-1).

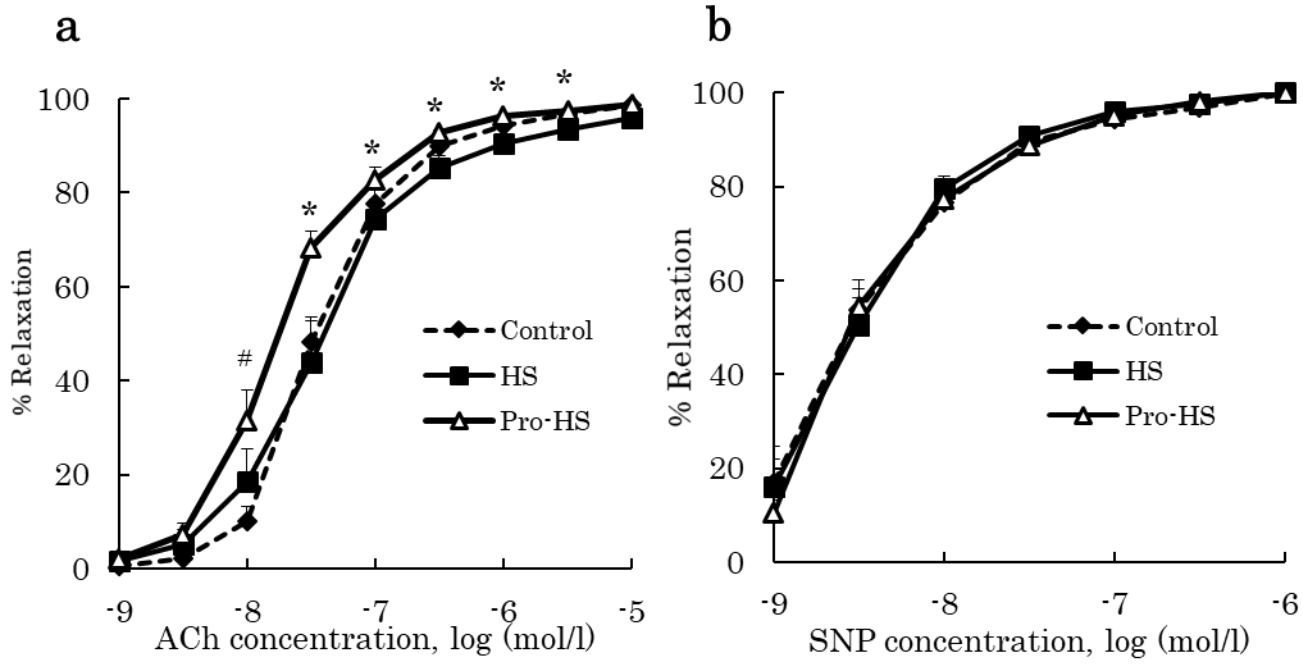

Fig. 3-1 Effect of proline administration on endothelial-dependent (a) and -independent (b) vasorelaxation of areteries of high sucrose diet-fed rats.
Vasorelaxation of control group is denoted by dotted line (◆), and that of HS group (■) and Pro-HS group (△)are denoted by solid line, respectively. Relaxation was induced on phenylephrine-preconstricted arteries by cumulative addition of ACh or SNP. Results are mean±SEM. Asterisk denotes statistically significant differences between HS and Pro-HS group (* $P<0.05$). Pound denotes statistically significant differences between control and Pro-HS group (# $P<0.05$).

The effect of proline administration on the gene expression of NF-κB-induced adhesion molecules in thoracic aorta

Since the transcription factor NF-κB in endothelial cells is reported to be activated during endothelial dysfunction and to play pivotal role on inflammatory response, the gene expression level of NF-κB -inducible adhesion molecules in thoracic aorta, i.e. ICAM-1, MCP-1, E-selection, was quantified to assess indirectly the effect of proline supplementation on NF-κB activation.

After 4-day feeding of high sucrose diet, gene expressions of NF-κB inducible adhesion molecules significantly increased (ICAM-1; 100.0±5.5 vs 119.2±6.3, ($P<0.05$)) or tended to increase (MCP-1; 100.0±12.6 vs 138.5±24.7, E-selectin; 100.0±14.6, 129.5±24.2, control vs HS group) compared with the control group. Proline supplementation significantly ($P<0.05$) decreased expression of 3 genes of NF-κB

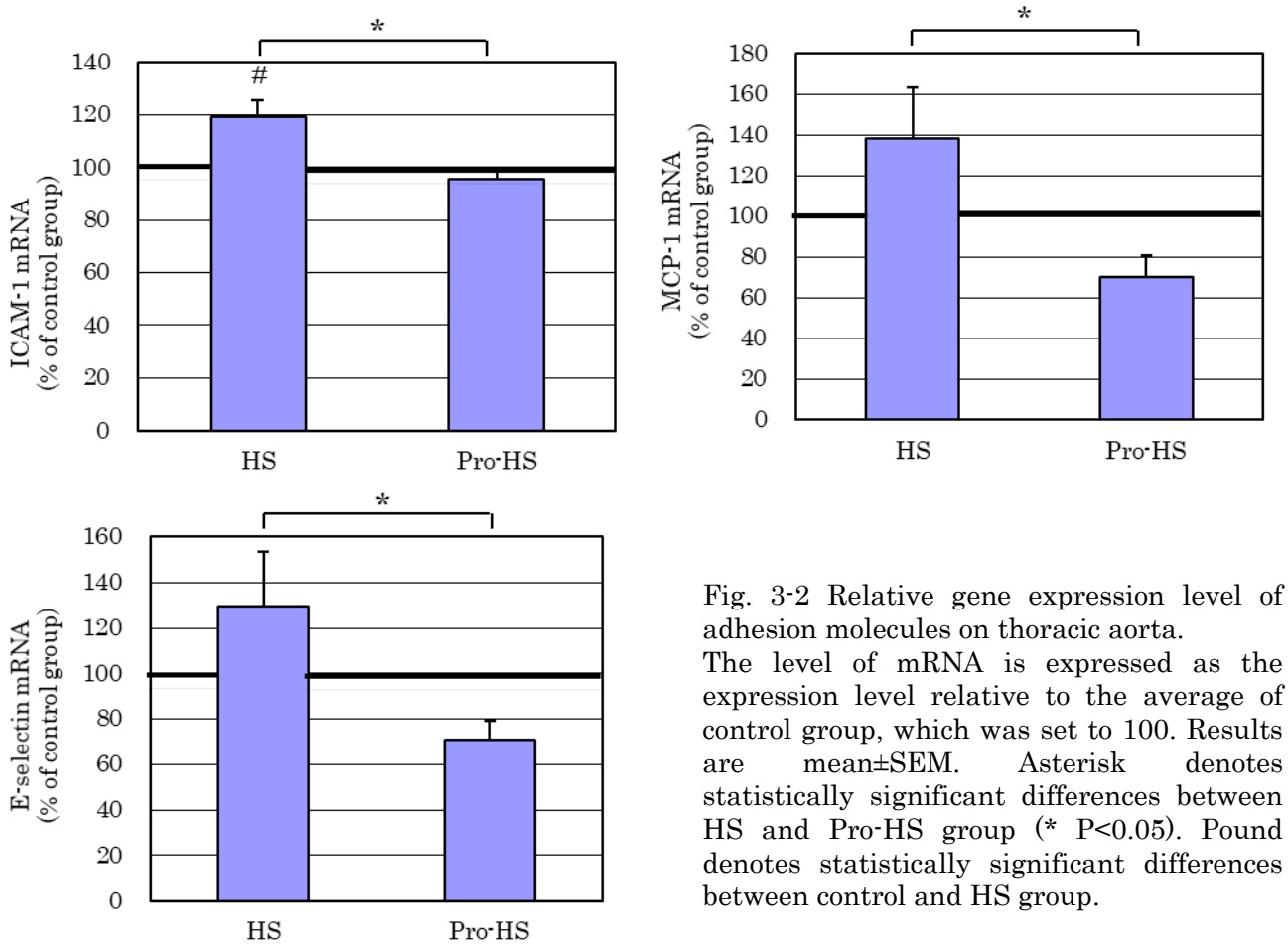

Fig. 3-2 Relative gene expression level of adhesion molecules on thoracic aorta.
The level of mRNA is expressed as the expression level relative to the average of control group, which was set to 100. Results are mean±SEM. Asterisk denotes statistically significant differences between HS and Pro-HS group (* $P<0.05$). Pound denotes statistically significant differences between control and HS group.

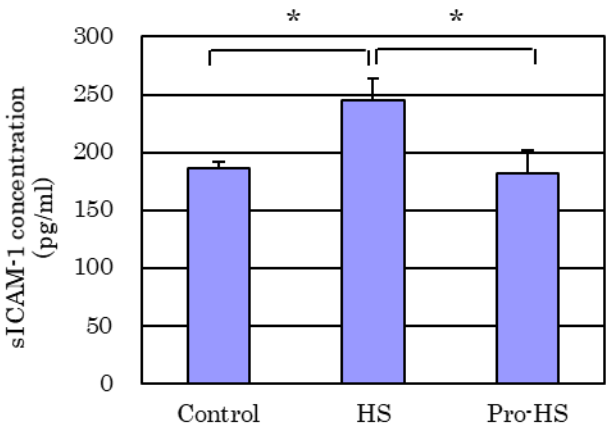

Fig. 3-3 Plasma protein level of soluble ICAM-1.
The protein level is expressed as the expression level relative to the average of control group. Results are mean±SEM. Asterisk denotes statistically significant differences between HS and Pro-HS group (* P<0.05).

inducible adhesion molecules, compared with HS-group (ICAM-1; 119.2±6.3 vs 95.6±3.4, MCP-1; 138.5±24.7 vs 70.0±10.6, E-selectin; 129.5±24.2 vs 70.6±8.8, HS vs Pro-HS group) (Fig. 3-2).

The effect of proline administration on soluble ICAM-1 protein concentration in plasma

As shown in Fig. 3-3, 4-day feeding of high sucrose diet increased soluble ICAM-1 protein concentration in plasma. (186.3±6.0 pg/ml vs 244.6±19.8 pg/ml (P<0.01), control vs HS group) Compared with HS group, proline administration statistically significantly suppressed soluble ICAM-1 in plasma to the equal level of control group. (244.6±19.8 pg/ml vs 181.5±22.6 pg/ml (P<0.05), HS vs Pro-HS group) (Fig.3-3)

The effect of proline administration on the nitric oxide (NO)-inducible gene and endothelial nitric oxide synthase (eNOS) gene expression in thoracic aorta

In order to evaluate the possibility that proline supplementation may increase NO availability derived from eNOS, the expression of eNOS, together with cycline dependent kinase inhibitor, p21, were quantified in thoracic aorta. Cycline dependent kinase inhibitor, p21, is reported to be induced by NO and the decrease of p21 expression plays a pivotal role in disease state.

After 4-day feeding of control or high sucrose diet, the gene expression of p21 in HS group tended to decrease compared with control group, and that in Pro-HS group significantly increased compared with both of control and HS-group (control: 100.0±7.5, HS: 84.49±10.2, Pro-HS: 141.4±14.3 (P<0.05; control vs Pro-HS group, P<0.05; HS vs Pro-HS group, Tukey test)) The gene expression of e-NOS did not altered

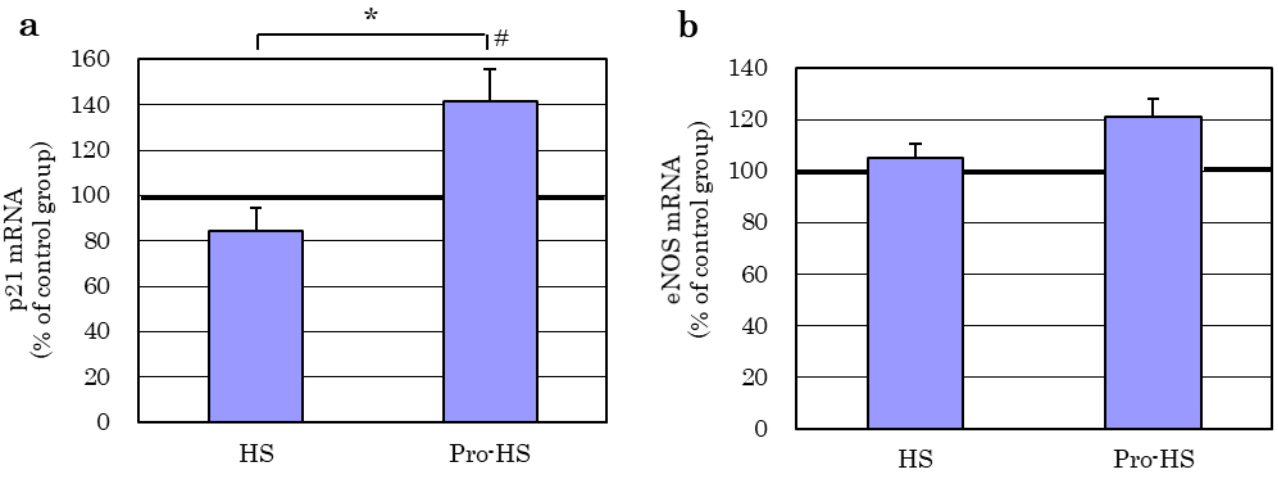

Fig. 3-4 Relative expression level of p21 gene (a) and eNOS gene (b) on thoracic aorta.
The level of mRNA is expressed as the expression level relative to the average of control group, which was set to 100. Results are mean±SEM. Statistical analysis was conducted by Tukey test. Asterisk denotes statistically significant differences between HS and Pro-HS group (* $P<0.05$). Pound denotes statistically significant differences between control and Pro-HS group (# $P<0.05$).

significantly, but that of Pro-HS group tended to be higher than control and HS group (control: 100.0±6.6, HS: 105.4±5.3, Pro-HS: 121.3±6.7) (Fig.3-4).

Discussion

In the present study, I investigated the effect of proline on early atherogenic response of thoracic aorta caused by hyperlipidemia, using short-term high sucrose diet-fed rat model. I found that proline administration enhanced endothelium-dependent vasorelaxation on thoracic aorta compared with both of control and HS group. Proline supplementation did not affect endothelium-independent vasorelaxation induced by NO donor, SNP.

Acetylcholine-induced vasorelaxation is mediated by the release of soluble mediators from vascular endothelium which causes vasorelaxation. The major relaxation factors include NO, prostacyclin, cyclooxygenase (COX) metabolite of arachidonic acid, and the group of compounds called

endothelium-derived hyperpolarizing factor (EDHF) [11-13]. It is reported that in conduit arteries such as thoracic aorta, the relative contribution of NO to endothelium-dependent vasorelaxation is greatest, whereas that of EDHF increases as vessel size decreases [14].

I also found that high sucrose diet significantly increased the expression of inflammatory adhesion molecules such as ICAM-1 gene on thoracic aorta and plasma soluble ICAM-1 protein and tended to increase MCP-1 and E-selection gene expression on the thoracic aorta, and proline administration significantly reduced their enhanced expressions.

It is reported that hyperlipidemia causes endothelial dysfunction and inflammatory response, accompanied with the elevation of plasma inflammatory cytokines. Inflammatory mediators such as TNF-α, IL-1 upregulate the expression of adhesion molecules on neutrophils (β2 integrins) and on endothelial cells (ICAM-1, MCP-1, E-selectin, etc.) through the activation of transcription factor NF- κB to facilitate neutrophil adhesion to vascular endothelium [15,16].

Nitric oxide is known as an important molecule in preventing inflammatory cell-mediated tissue injury. Decreased NO availability on endothelial cells, which is a part of endothelial dysfunction, plays an important role in the development of inflammatory activation during the progress of atherosclerosis. It is reported that NO produced by eNOS has anti-inflammatory and protective effects, partly through the suppression of the activation of the nuclear transcription factor, NF-κB [17]. The activation of NF-κB is controlled by a family of inhibitors, inhibitor of kappa B (IκBs), that binds to NF-κB to retain it under inactivated conditions. Nitric oxide derived from e-NOS suppresses the activation of NF-κB through stabilization and induction of IκB [18]. Thus, reduced NO availability due to endothelial dysfunction is thought to facilitate endothelial inflammatory response through the reduced suppression of NF- κB activation.

One of the possible mechanism for protective effect of proline against endothelium dysfunction and inflammatory reaction may be the increase of NO availability on endothelial cells. This hypothesis was also supported by the finding that the gene expression of cycline dependent kinase inhibitor, p21, on thoracic aorta, which is reported to be induced by NO, was significantly increased by proline

supplementation, compared with both of control and HS group. Cycline dependent kinase inhibitor, p21, inhibits cell proliferation of smooth muscle cells. Reduced NO generation due to decreased eNOS activity attributable to dysfunction of endothelial cells has been proposed to result in increased smooth muscle cell proliferation in disease states, such as atherosclerosis and restenosis [19].

On the other hand, the observation that proline supplementation significantly increased p21 gene expression than control group, which was not subject to intense metabolic stress such as postprandial hyperlipidemia, is consistent with the observation in the experiment for endothelium-dependent vasorelaxation in which the vasorelaxation was significantly enhanced in Pro-HS group compared with control group. These results suggest a possibility that the common mechanism triggered by proline supplementation controls both increase of p21 and endothelium-dependent vasorelaxation. Proline supplementation may increase NO-availability on endothelial cells without the stress such as hyperlipidemia. Unchanged response of vasorelaxation to NO donor, SNP, by proline suggests that proline did not change the vascular response to exogenous NO.

Possible regulatory mechanisms to increase NO availability by proline are assumed to be such as eNOS activation by hydrogen peroxide derived from proline metabolism in mitochondria [20-22], activation of Akt/eNOS signaling [23,24], and so on. In order to elucidate the mechanism of protective effects of proline supplementation on early atherogenic response, further detailed investigation is required.

In conclusion, this study demonstrated that on short-term high sucrose diet-fed rat model, proline supplementation increased endothelium-dependent vasorelaxation, decreased mRNA expression of adhesion molecules such as ICAM-1 MCP-1, E-selectin on thoracic aorta, decreased plasma soluble ICAM-1 level, and increased p21 mRNA expression on thoracic aorta. These results suggest that proline supplementation prevents early atherogenic response on aorta.

Reference

[1] Shimabukuro M, Chinen I, Higa N, et al: Effects of dietary composition on postprandial endothelial function and adiponectin concentrations in healthy humans: a crossover controlled study. Am J Clin Nutr 2007; 86:923-928.

[2] Miglio C, Peluso I, Raguzzini A, et al: Antioxidant and inflammatory response following high-fat meal consumption in overweight subjects. Eur J Nutr 2013; 52:1107-1114.

[3] Nappo F, Esposito K, Cioffi M, et al: Postprandial endothelial activation in healthy subjects and in type 2 diabetic patients: role of fat and carbohydrate meals. J Am Coll Cardiol 2002; 39:1145-1150.

[4] Pickup JC, Mattock MB, Chusney GD, Burt D: NIDDM as a disease of the innate immune system: association of acute-phase reactants and interleukin-6 with metabolic syndrome X. Diabetologia 1997; 40:1286-1292.

[5] Arnalich F, Hernanz A, López-Maderuelo D, et al: Enhanced acute-phase response and oxidative stress in older adults with type II diabetes. Horm Metab Res 2000; 32:407-412.

[6] Ceriello A, Falleti E, Motz E, et al: Hyperglycemia-induced circulating ICAM-1 increase in diabetes mellitus: the possible role of oxidative stress. Horm Metab Res 1998; 30:146-149.

[7] Marfella R, Esposito K, Giunta R, et al: Circulating adhesion molecules in humans: role of hyperglycemia and hyperinsulinemia. Circulation 2000; 101:2247-2251.

[8] Ajinomoto Co., Inc. Japan Patent Kokai, 1996; 1996-208472.

[9] Obayashi Y, Arisaka H, Yoshida S, Mori M, Takahashi M: Proline protects liver from D-galactosamine hepatitis by activating the IL-6/STAT3 survival signaling pathway. Amino Acids 2012; 43:2371-80.

[10] Naderali EK, Williams G: Effects of short-term feeding of a highly palatable diet on vascular reactivity in rats. Eur J Clin Invest 2001; 31:1024-1028.

[11] Ignarro LJ, Buga GM, Wood KS, et al: Endothelium-derived relaxing factor produced and released from artery and vein is nitric oxide. Proc Natl Acad Sci USA 1987; 84:9265-9269.

[12] Moncada S, Vane JR: Pharmacology and endogenous roles of prostaglandin endoperoxides, thromboxane A2, and prostacyclin. Pharmacol Rev 1978; 30:293-331.

[13] Cohen RA, Vanhoutte PM: Endothelium-dependent hyperpolarization. Beyond nitric oxide and cyclic GMP. Circulation 1995; 92:3337-3349.

[14] Matoba T, Shimokawa H, Nakashima M, et al: Hydrogen peroxide is an endothelium-derived hyperpolarizing factor in mice. J Clin Invest 2000; 106:1521-30.

[15] Jaeschke, H: Mechanisms of neutrophil-mediated liver cell injury during ischemia-reperfusion and other acute inflammatory conditions, Am J Physiol Gastrointest Liver Physiol 2006; 290:G1083–1088.

[16] Bevilacqua MP, Pober JS, Mendrick DL, et al: Identification of an inducible endothelial-leukocyte adhesion molecule. Proc Natl Acad Sci USA 1987; 84:9238-9242.

[17] Kubes P, Suzuki M, Granger DN: Nitric oxide: an endogenous modulator of leukocyte adhesion, Proc Natl Acad Sci USA 1991; 88:4651-4655.

[18] Peng HB, Libby P, Liao JK: Induction and stabilization of I kappa B alpha by nitric oxide mediates inhibition of NF-kappa B, J Biol Chem 1995; 270:14214-14219.

[19] Sato J, Nair K, Hiddinga J, et al.: eNOS gene transfer to vascular smooth muscle cells inhibits cell proliferation via upregulation of p27 and p21 and not apoptosis, Cardiovasc Res 2000; 47:697-706.

[20] Goncalves RL, Rothschild DE, Quinlan CL, et al: Sources of superoxide/H2O2 during mitochondrial proline oxidation, Redox Biol 2014; 2:901-909.

[21] Drummond GR, Cai H, Davis ME, et al.: Transcriptional and posttranscriptional regulation of endothelial nitric oxide synthase expression by hydrogen peroxide, Circ Res 2000; 86:347-54.

[22] Thomas SR, Chen K, Keaney JF Jr: Hydrogen peroxide activates endothelial nitric-oxide synthase through coordinated phosphorylation and dephosphorylation via a phosphoinositide 3-kinase-dependent signaling pathway, J Biol Chem 2002; 277:6017-6024.

[23] Kureishi Y, Nakano T: Angiogenesis and Intracelullar Signaling: Role of Akt-eNOS Signaling. J Jpn Coll Angiol 2003; 43: 591-594.

[24] Natarajan SK, Zhu W, Liang X, et al: Proline dehydrogenase is essential for proline protection against hydrogen peroxide-induced cell death. Free Radic Biol Med 2012; 53:1181-1191.

Chapter IV

Impaired lipid accumulation in the liver of Tsc2-heterozygous mice during liver regeneration

Summary

Tuberin is a negative regulator of mTOR pathway. To investigate the function of tuberin during liver regeneration, I performed 70% hepatectomy on wild-type and *Tsc2*+/- mice. I found the tuberin phosphorylation correlated with mTOR activation during early liver regeneration in wild-type mice. However, liver regeneration in the *Tsc2*+/- mice was not enhanced. Instead, the *Tsc2*+/- livers failed to accumulate lipid bodies, and this was accompanied by increased mortality.

These findings suggest that tuberin plays a critical role in liver energy balance by regulating hepatocelluar lipid accumulation during early liver regeneration. These effects may influence the role of mammalian target of rapamycin complex 1 (mTORC1) on cell growth and proliferation.

Introduction

Tuberin and hamartin, which are the products of genes TSC1 and TSC2, form a complex that negatively regulates mammalian target of rapamycin (mTOR). This complex works as a critical nutrient sensor, which regulates cell growth and proliferation via mTOR pathway. Mammalian target of rapamycin is activated by Ras-related small GTPase Rheb, which is a target of tuberin-hamartin complex. Tuberin is a GTPase-activating protein and stimulates the intrinsic GTPase activity of Rheb, thereby converting Rheb from its GTP-bound active state to GDP-bound inactive state. The insulin signaling pathway inactivates tuberin via the protein kinase, Akt. Inoki et al. reported that tuberin is

directly phosphorylated by Akt at Thr1462, followed by an inactivation of tuberin, a disruption of its interaction with hamartin, and the activation of mTOR [1].

Under energy starvation (e.g., increased AMP:ATP ratio), AMPK becomes activated and phosphorylates tuberin to enhance its activity to inhibit mTOR signaling and cell growth/proliferation. Furthermore, phosphorylation of tuberin by 5'AMP-activated protein kinase (AMPK) protects cells from energy deprivation-induced apoptosis [2]. Taken together, these results indicate that tuberin inhibits cell growth/proliferation through the inactivation of mTOR under energy deprivation, and stimulates growth through the activation of mTOR when it receives growth-stimulating signals.

Jiang et al. reported that P70 ribosomal S6 kinase (p70S6K), the downstream targets of mTORC1, was highly activated by phosphorylation at Thr389 in response to partial hepatectomy, and this activation was inhibited by rapamycin administration, leading to the attenuation of liver regeneration [3]. Accordingly, one would predict that enhanced mTORC1 activity could accelerate liver regeneration following partial hepatectomy by promoting cell growth and proliferation.

In the present study, I investigated the role of tuberin in liver regeneration by determining the time-dependent change of p70S6K phosphorylation at Thr389 and tuberin phosphorylation following 70% hepatectomy in C57BL/6 mice. I further performed 70% hepatectomy on *Tsc2*+/- mice, whose livers expressed half of the normal level of tuberin, and examined if liver regeneration is accelerated with hyperactivation of mTOR.

The results of these analyses indicate that tuberin phosphorylation strongly correlated with p70S6K activation during liver regeneration, but the process was not accelerated in the *Tsc2*+/- mice. Instead, I found impaired accumulation of lipid vesicles in the liver of these animals during the initial phase of liver regeneration, which serves as a primary energy source during early regeneration. These findings provide insights into the multiple functions of tuberin during liver regeneration.

Materials and Methods

Antibodies

Anti-tuberin (C-20) antibody (cat# sc-893) was obtained from Santa Cruz Biotechnology, Inc. (Santa Cruz, CA). Anti-β-actin antibody (cat# A5441) was obtained from Sigma (St.Louis, MO). Anti-p70S6 kinase (cat# 9202), anti-p-p70S6 kinase (Thr389, 1A5)(cat# 9206), anti-phospho-Protein Kinase B (PKB)/Akt-substrate (RXRXXS*/T*, 110B7)(cat# 9614) were obtained from Cell Signaling (Beverly, MA). Anti-adipophilin antibody (cat# GP40) was obtained from Progen Biotechnik (Germany).

Partial hepatectomy

Eight to nine-week old C57 black 6 (C57BL/6) or *Tsc2*+/- (gift of D. Kwaitkowski, Harvard) male mice were fasted overnight. The next morning between 8:00 and 10:00, the mice were anesthetized with isoflurane (Abbott, cat# 05260-05) and the median and left lateral lobes of the liver were ligated at their stem and excised. Control mice were subjected to sham operation, which consisted of laparotomy and a brief manipulation of the liver with a cotton swab prior to wound closure. Food was re-introduced 6 to 8 hrs after surgery. The animals were sacrificed by cervical dislocation at the indicated time points following surgery. All experiments were approved by the Institutional Animal Care and Use Committee of the University of Washington, which is certified by the Association for Assessment and Accreditation of Laboratory Animal Care International.

Adipophilin immunostaining

Liver sections were fixed in 10% formalin, paraffin embedded, and stained with anti-adipophilin antibody using Vectastain Elite ABC Kit (Vector Laboratories, cat# PK-6101). Sections were reacted with 3,3'-diaminobenzizine (DAB) hydrochloride (Sigma, cat# D4293), followed by conterstaining with Harris hematoxylin.

Oil Red O staining

Liver sections were fixed in 10% formalin for 2 to 3 hours, equilibrated in 30% sucrose, and embedded in OCT. Frozen liver sections were stained with Oil Red O and counterstained with Harris hematoxylin.

Detection of phospho-tuberin recognized with anti-Phospho-Akt Substrate (RXRXXS*/T*) antibody

Liver tissue was homogenized in NP-40 lysis buffer (50mM Tris(hydroxymethyl)aminomethane hydrochloride (Tris-HCl) (pH 7.4), 150mM NaCl, 2.5mM ethylenediaminetetraacetate・$2H_2O$, 1% Nonidet P-40, 50 mM sodium fluoride, 0.5 mM 4-(2-Aminoethyl)benzenesulfonyl fluoride hydrochloride (AEBSF), 1 mM benzamidine, 10 μg/ml aprotinin, 10 μg/ml pepstatin, 1 mM sodium Orthovanadate, 1 mM dithiothreitol, 10 μg/ml leupeptin, 50 μg/ml Trypsin inhibitor from Glycine max (SBTI), 200 nM Microcystin). Four micrograms anti-tuberin antibody was added to 5 mg protein and was rocked at 4ºC overnight for immunoprecipitation. Tuberin-antibody complex was absorbed with 40μl Protein A sepharose (1g/4ml, Sigma, cat# P3391, MO, USA), followed with washing by 1 ml NP-40 lysis buffer three times. The Protein A Sepharose was boiled with 25μl of protein loading buffer at 1.5 time higher concentration for 5 min., and was subject to western blot analysis with anti-Phospho-Akt Substrate (RXRXXS*/T*) antibody as a primary antibody.

Western blot analysis

Liver tissue was homogenized in lysis buffer (50mM Tris-HCl (pH7.4), 1% Triton X100, 150mM NaCl, 50mM β-glycerohosphate, 10% glycerol, 2mM 2.5mM ethylenediaminetetraacetate・$2H_2O$, 0.48mM AEBSF, 1mM benzamidine, 10μg/ml aprotinin, 10μg/ml pepstatin, 1mM sodium orthovanadate, 1mM dithiothreitol, 10μg/ml leupeptin, 50μg/ml SBIT, 0.2μM microcystin) and then centrifuged for 15min at 4ºC. Protein concentration of the supernatant was quantified with BCA Protein Assay Kit (Pierce, cat#2161297A). An aliquot of protein was boiled with protein loading buffer for 5min, and was loaded on Sodium dodecyl sulfate (SDS) polyacrylamide gel (7% for tuberin, 10% for p70S6K). After

electrophoresis at constant voltage of 100V, proteins were transferred onto Polyvinylidene difluoride (PVDF) membranes and blotted against primary antibodies. Membranes were washed with Tris-buffered saline with 0.1% Tween-20 and incubated with a 1:5000 dilution of hourseradish peroxidase-conjugated secondary antibodies for 1 hour. Protein bands were visualized by chemiluminescence using SuperSignal West Pico Chemiluminescent Substrate (Pierce, cat#34080)

Expression of data and statistical analysis

The results are expressed as the mean ± SEM. The Student's t test was used for the comparison of data from two groups. The difference between groups was considered significant when P was less than 0.05.

Results and Discussion

Hepatectomy induces P70S6K activation, downstream of mTOR signaling, during early liver regeneration.

In order to investigate the time-dependent change of the mTOR activation after 70 % partial hepatectomy (PH) in C57BL/6 mice, I quantified the level of p-P70S6K (Thr389), using western blot analysis after PH.

I found that P70S6K was specifically phosphorylated in PH mice in contrast to sham-operated mice (Fig.4-1a). The PH-specific phosphorylation already began at 0.5 hrs, peaked around 4-8 hrs, and gradually decreased by 24 hrs (Fig.4-1a, b). These results indicate that mTOR signaling is activated at very early phase of liver regeneration.

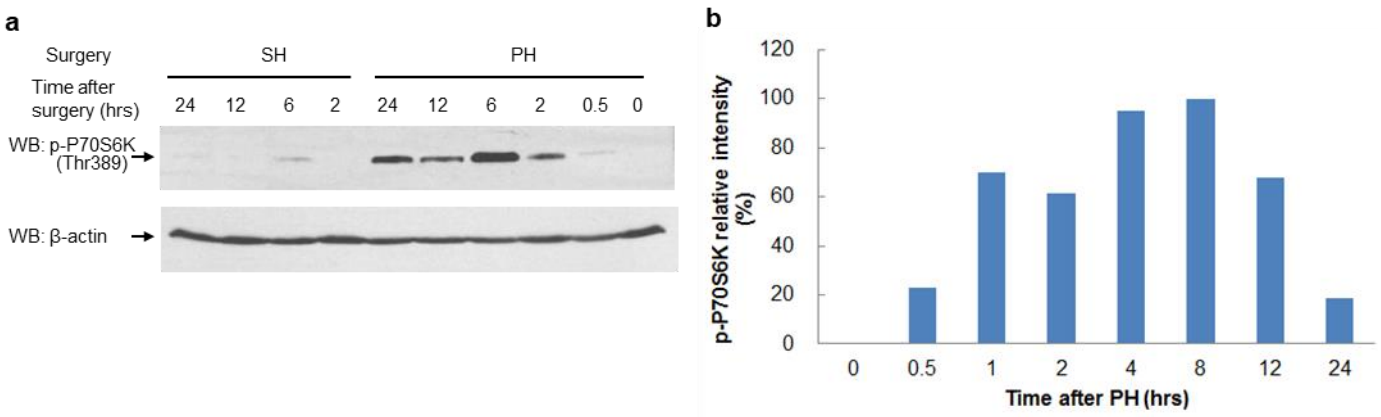

Fig. 4-1 Time course of phosphorylation of p70S6K during early liver regeneration.
(a) Representative western blot of p-P70S6K (Thr389) from the liver of sham-operated and partially-hepatectomized mice at each time point. (b) Densitometric determination of the protein level of p-P70S6K. The protein level was determined by western blot from 2 mice at each time point. The average of density from 2 mice is expressed as the relative density to the highest one at 8 hrs after surgery.

Hepatectomy induces tuberin phosphorylation, which strongly correlates with P70S6K activation.

Given that tuberin regulates mTORC1 and hence, p70S6K activity, I next investigated tuberin activity based on its phosphorylation state. Following partial hepatectomy, Hong et al. reported rapid activation of Akt, which in turn, can phosphorylates tuberin at multiple sites to suppress its function [4]. Based on the consensus sequence, RXRXX(S/T), Akt phosphorylation can be detected using a well-characterized anti-phospho PKB/Akt-substrate antibody. To determine such sites in tuberin following partial hepatectomy, I performed western blotting with this antibody following immunoprecipitation of tuberin from liver lysates. The western blot analysis at 2 hrs after surgery showed specific phosphorylation of tuberin in the PH group in contrast to minimally detectable phosphorylation in the sham group. (Fig.4-2a) In addition, there was strong correlation between the levels of phosphorylation of tuberin and that of P70S6K (Thr389) in the liver from multiple mice at 2 hrs. The temporal pattern of tuberin phosphorylation as detected by the Akt-substrate antibody paralled that of p70S6K phosphorylation beginning at 0.5 hrs, peaked around 2 to 6 hrs, and continued up to 12 hours. (Fig.4-2c)

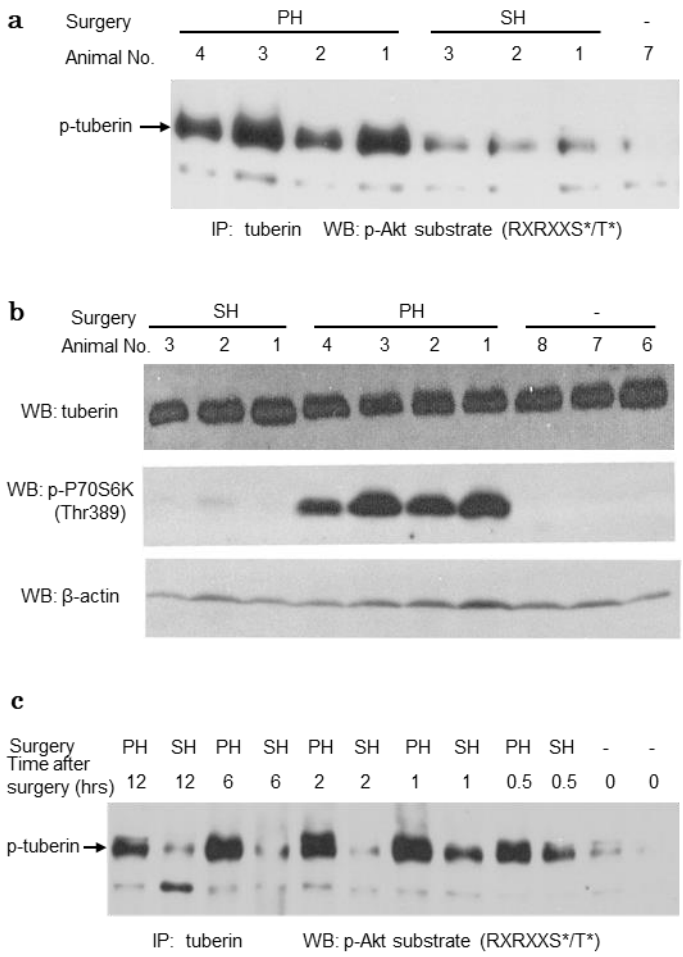

Fig. 4-2 Specific phosphorylation of tuberin, which correlates with the activation of mTORC1 pathway after PH.
(a) Specific phophosrylation of tuberin in the liver after PH. Total protein extracts from the remnant livers of three sham-operated and four partially-hepatectomized animals at 2 hrs after surgery were subjected to immunoprecipitation with anti-tuberin antibody followed by western blot analysis with anti-p-Akt substrate (RXRXXS*/T*) antibody. (b) Western blot of tuberin and p-P70S6K in the liver after PH. The same protein extracts with (a) was subject to western blot analysis. (c) Time course of phosphorylation of tuberin during early liver regeneration. Total protein extracts from the remnant livers of sham-operated and partially-hepatectomized animals at each time point were subject to immunoprecipitation with anti-tuberin antibody followed by western blot analysis with anti-p-Akt substrate (RXRXXS*/T*) antibody. Representative results from each time points are shown.

To further determine which Akt sites were phosphorylated in tuberin, I used a phospho-specific antibody to detect phosphorylation of TSC2(Thr1462). However, the antibody failed to detect significant expression of tuberin throughout the first 24 hrs after PH (data not shown) suggesting that Thr1462 was not significantly phosphorylated in this setting. Others have also reported that the anti-Akt substrate antibody did not detect the TSC2(Thr1462) site [5]. Besides Akt, phosphorylation of the RXRXX(S/T) motif is catalyzed by other AGC-family kinases such as cAMP-dependent protein kinase (PKA), cGMP-dependent protein kinase (PKG), protein kinase C and $p90^{RSK}$. Therefore, I predict that the phosphorylation of tuberin during early liver regeneration may be triggered by AGC-family kinase besides Akt/PKB.

Collectively, I found that tuberin in wild-type liver is specifically phosphorylated immediately following PH at a site independent of Thr1462. This phosphorylation is recognized by the anti-phospho PKB/Akt-substrate antibody and strongly correlates with P70S6K phosphorylation (Thr389), which is induced by mTOR signaling.

The effect of tuberin deficiency on liver regeneration

It is known that tuberin deficiency induces constitutive hyperactivation of mTOR signaling [6,7]. I postulate that liver may regenerate faster under condition of mTORC1 hyperactivity. To test this hypothesis, we performed 70% hepatectomy in *Tsc2*+/- mice; these animals have been bred in the C57BL/6J background.

First, I determined the expression level of tuberin in the livers of *Tsc2*+/- mice before and after partial hepatechtomy. Figure 4-3a, b shows that tuberin expression in the heterozygous liver was approximately 50% of the wild-type controls, and the amount did not significantly change following partial hepatectomy (Fig. 4-3b). However, this did not translate to significantly higher levels of p70S6K phosphorylation in the Tsc2+/- compared to Tsc2+/+ livers (data not shown).

Nonetheless, I observed several deaths among the *Tsc2*+/- mice between 48 and 72 hours in contrast to no mortality in the *Tsc2*+/+ mice. Liver:body weight ratios were not significantly different between the two groups (Figure 4-3c). Therefore, despite lower expression levels of tuberin in the *Tsc2*+/- livers, hepatic mTORC1 activity was not enhanced, and liver regeneration was not accelerated in the mutant mice. Hence, it was surprising to find a higher mortality rate occurring between 48 and 72 hrs after PH in the *Tsc2*+/- mice. These results indicate that tuberin may have other functions during liver regeneration, in addition to negative regulation of mTORC1 .

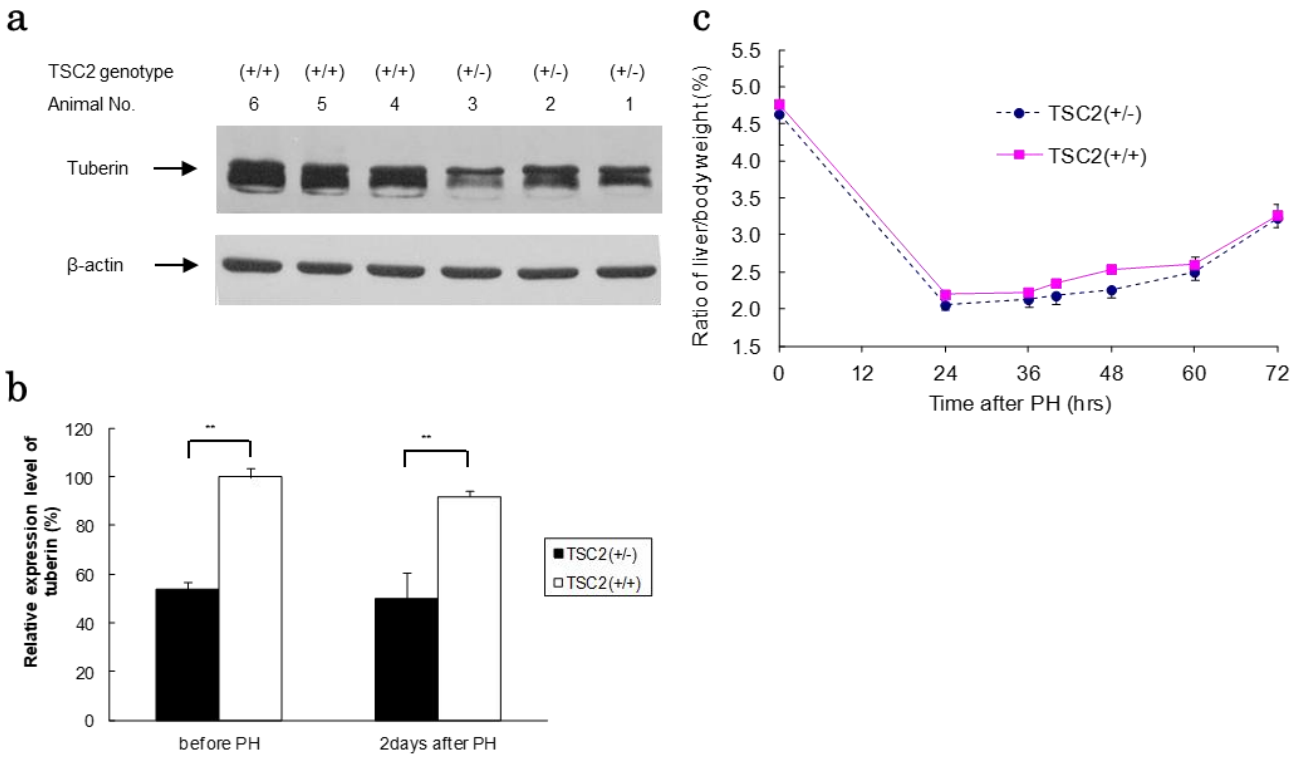

Fig. 4-3 The protein expression level of tuberin in the liver and liver:body weight ratio of TSC2(+/-) and TSC2(+/+) mice before and after PH.
(A) Western blot of tuberin in the liver of TSC2(+/+) and TSC2(+/-) mice before surgery. Protein extracts from the liver was subject to western blot analysis with anti-tuberin antibody.
(B) Densitometric determination of the hepatic protein level of tuberin in TSC2(+/+) and TSC2(+/-) mice before and 2 days after PH. The average of density from 6-7mice is expressed as the relative density to that of the TSC2(+/+) mice before PH. Results are mean±SEM. ** $P<0.01$ vs. TSC2(+/+) mice. (C) Liver:body weight ratio of TSC2(+/-) (solid line) and TSC2(+/+) (dotted line) mice after PH. The average of 4-6 mice at each time point was shown. Results are mean±SEM.

Heaptocellular Lipid Body Formation after PH was severely Impaired in TSC2(+/-) mice.

It has been reported that lipid accumulation during early (first 24 hrs) liver regeneration plays a critical role on liver regeneration [8]. Shtyer et al. showed the suppression of lipid accumulation in the liver by leptin administration impaired liver regeneration [9]. These results suggest the importance of lipid as a primary energy source for hepatocyte proliferation during early liver regeneration.

I examined hepatic lipid accumulation after hepatectomy in the *Tsc2*+/- mice using oil red O staining. At 24 hrs following surgery, I found a striking difference in the amount of hepatocyte lipid accumulation between the wild-type and mutant livers (Figure 4-4a, b). As expected, there was considerable oil red O

staining in the wild-type livers, but very little was found in the *Tsc2*+/- livers. To confirm this finding, I performed immunohistochemical analyses using formalin-fixed paraffin-embedded liver sections with anti-adipophilin antibody, which recognizes a surface marker of lipid droplets. I found that the average size of the adipophilin-stained hepatocellular lipid bodies of *Tsc2*+/- mice at 24 hrs was markedly smaller than that of the *Tsc2*+/+ mice. Furthermore, the shape of the lipid bodies was severely distorted (Fig. 4-4c). In contrast, wild-type mice exhibited considerable accumulation of adipophilin+ lipid droplets with large, round vesicles at the same time point (Fig. 4-4d). These results suggest that even a 50% reduction in tuberin expression may cause a disruption in hepatocellular lipid body formation during early liver regeneration.

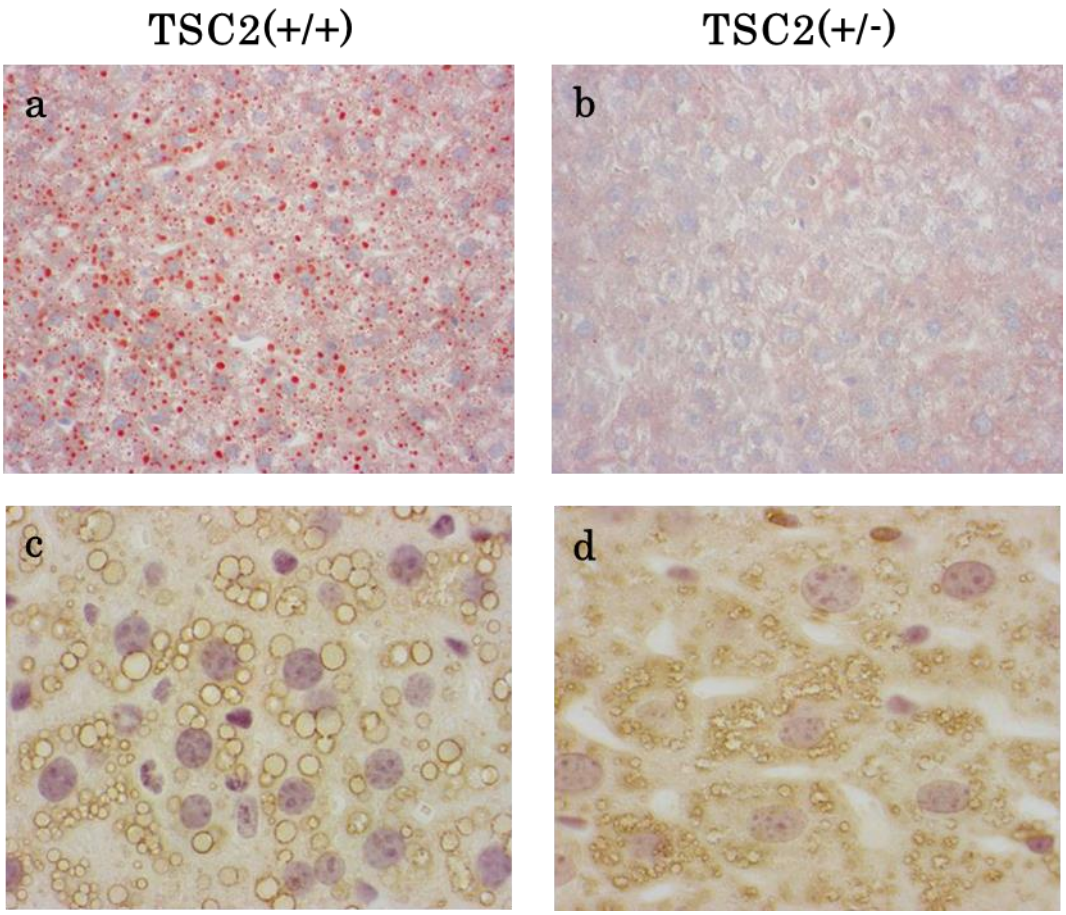

Fig. 4-4 Hepatic lipid accumulation at 24 h after PH.
(a)(b) Oil red O staining of Frozen liver sections of TSC2(+/+) (a) and TSC2(+/-) mice (b). (c)(d) Hepatic lipid body formation in TSC2(+/+) (c) and TSC2(+/-) mice (d). Immunohistochemical staining of adipophilin (marker of lipid body) was performed on paraffin-embedded liver sections, followed by Harris hematoxylin staining.

Surgical injury induces the release of a variety of stress hormones such as catecholamines, glucocorticoid, glucagon, which trigger a cascade of metabolic adjustments to promote catabolism and substrate mobilization in the postoperative period. It is reported that catabolism of systemic adipose stores is essential for hepatic lipid accumulation after PH and normal liver regeneration [10]. Walldorf et al. reported that beta-adrenergic blocker, propranolol, impaired liver regeneration, accompanied by a lower hepatic triglyceride content after PH [11]. These studies suggest that hepatic lipid accumulation after PH is triggered by catecholamins to mobilize peripheral adipose tissue and provides lipid substrates to the liver. The observation that glucose supplementation after PH exhibits inhibitory effect on the regeneration [12] and that systemic lipolysis followed by hypoglycemia is essential for normal liver regeneration [10] support the notion that lipid accumulation in the liver after PH provides the necessary energy substrates during the initial phase of liver regeneration. The higher mortality rate in the hepatectomized *Tsc2*+/- mice may be associated with a relative deficiency of lipid-based energy source.

.

What is the mechanism of impaired hepatocelluar lipid body formation during early liver regeneration in *Tsc2*+/- mice?

Tuberin was reported to reside in multiple subcelluar compartments, serving multiple functions. Jones et al. reported that tuberin was cofractionated with caveolin-1 in lipid raft fraction and regulated its localization. In cells lacking tuberin, most of the endogenous caveolin-1 was displaced from plasma membrane to a Berefeldin-A-sensitive post-Golgi compartment, resulting in a disruption in caveolae formation. These results suggest that tuberin plays a role in the subcellular localization of caveolin-1 and consequently caveolae formation during post-Golgi transport[13]. I further showed that the trafficking of caveolin-1 was under the influence of microtubule-associated protein, CLIP-170, which acts as a substrate for mTORC1 [14]. Interestingly, caveolin-1 deficient mice exhibit impaired liver regeneration and low survival rate after PH. [15] Livers of these mice show dramatically reduced lipid droplet accumulation, and their survival was rescued by glucose supplementation. While this work

supports our findings, the role of caveolin-1 in liver regeneration remains controversial [16]. In a recent study comparing multiple strains of Cav1(-/-) mice, Fernandez-Rojo et al. reported that mice of certain genetic background can compensate for caveolin-1 deficiency through the activation of anabolic metabolism, thus explaining the discrepant findings [17]. They concluded that caveolin-1 is required for efficient hepatic lipid storage during liver regeneration. Taken together, these results suggest that the impaired lipid droplet accumulation in the *Tsc2*+/- livers may be secondary to dysregulated caveolin-1 trafficking.

In summary, I found that tuberin phosphoryration is induced by partial hepatectomy, and this correlated with P70S6K activation during the early phase of regeneration. However, contrary to my expectation, liver regeneration of *Tsc2*+/- mice was not enhanced, and I attribute this to the reduction in lipid body formation following hepatectomy, which serves as an important energy source. This is consistent with the effects of tuberin on caveolin-1 trafficking and the role of caveolin-1 on regulating lipid-dependent energy metabolism in the liver. It remains to be determined whether the complete absence of Tsc2 in the liver accelerates or retards hepatic regeneration. It is known that mice with liver-specific deletion of Tsc1 are resistant to steatosis even when challenged with high-fat diet [18]. But whether hyperactivation of mTORC1 can compensate for the diminished lipid pool to promote hepatocyte proliferation and regeneration remains to be investigated.

References

[1] Inoki K, Li Y, Zhu T, Wu J, Guan KL: TSC2 is phosphorylated and inhibited by Akt and suppresses mTOR signaling. Nat Cell Biol. 2002; 4(9):648-57.

[2] Inoki K, Zhu T, Guan KL, TSC2 mediates cellular energy response to control cell growth and survival. Cell 2003; 115(5):577-90.

[3] Jiang YP, Ballou LM, Lin RZ, Rapamycin-insensitive regulation of 4e-BP1 in regenerating rat liver. J Biol Chem 2001; 276(14):10943-51.

[4] Hong F, Nguyen VA, Shen X, Kunos G, Gao B, Rapid activation of protein kinase B/Akt has a key role in antiapoptotic signaling during liver regeneration. Biochem Biophys Res Commun 2000; 279(3):974-9.

[5] Rolfe M, McLeod LE, Pratt PF, Proud CG: Activation of protein synthesis in cardiomyocytes by the hypertrophic agent phenylephrine requires the activation of ERK and involves phosphorylation of tuberous sclerosis complex 2 (TSC2). Biochem J 2005; 388(Pt 3): 973-84.

[6] Kenerson HL, Aicher LD, True LD, Yeung RS: Activated mammalian target of rapamycin pathway in the pathogenesis of tuberous sclerosis complex renal tumors, Cancer Res 2002; 62(20):5645-50.

[7] Gao X, Zhang Y, Arrazola P, Hino O, Kobayashi T, Yeung RS, Ru B, Pan D: Tsc tumour suppressor proteins antagonize amino-acid-TOR signaling. Nat Cell Biol 2002; 4(9):699-704.

[8] Glende EA Jr, Morgan WS, Alteration in liver lipid and lipid fatty acid composition after partial hepatectomy in the rat. Exp Mol Pathol. 1968; 8(2):190-200.

[9] Shteyer E, Liao Y, Muglia LJ, Hruz PW, Rudnick DA: Disruption of hepatic adipogenesis is associated with impaired liver regeneration in mice, Hepatology 2004; 40(6):1322-32.

[10] Gazit V, Weymann A, Hartman E, Finck BN, Hruz PW, Tzekov A, Rudnick DA, Liver regeneration is impaired in lipodystrophic fatty liver dystrophy mice. Hepatology 2010; 52(6):2109-17.

[11] Walldorf J, Hillebrand C, Aurich H, Stock P, Hempel M, Ebensing S, Fleig WE, Seufferlein T, Dollinger MM, Christ B: Propranolol impairs liver regeneration after partial hepatectomy in C57Bl/6-mice by transient attenuation of hepatic lipid accumulation and increased apoptosis. Scand J Gastroenterol 2010; 45(4):468-76.

[12] Weymann A, Hartman E, Gazit V, Wang C, Glauber M, Turmelle Y, Rudnick DA: p21 is required for dextrose-mediated inhibition of mouse liver regeneration. Hepatology 2009; 50(1):207-15.

[13] Jones KA, Jiang X, Yamamoto Y, Yeung RS: Tuberin is a component of lipid rafts and mediates caveolin-1 localization: role of TSC2 in post-Golgi transport. Exp Cell Res 2004; 295(2):512-24.

[14] Jiang X, Yeung RS: Regulation of microtubule-dependent protein transport by the

TSC2/mammalian target of rapamycin pathway. Cancer Res 2006; 66(10):5258-69.

[15] Fernández MA, Albor C, Ingelmo-Torres M, Nixon SJ, Ferguson C, Kurzchalia T, Tebar F, Enrich C, Parton RG, Pol A: Caveolin-1 is essential for liver regeneration. Science 2006; 313(5793):1628-32.

[16] Mayoral R, Fernández-Martínez A, Roy R, Boscá L, Martín-Sanz P: Dispensability and dynamics of caveolin-1 during liver regeneration and in isolated hepatic cells. Hepatology 2007; 46(3): 813-22.

[17] Fernández-Rojo MA, Restall C, Ferguson C, Martel N, Martin S, Bosch M, Kassan A, Leong GM, Martin SD, McGee SL, Muscat GE, Anderson RL, Enrich C, Pol A, Parton RG: Caveolin-1 orchestrates the balance between glucose and lipid-dependent energy metabolism: implications for liver regeneration. Hepatology 2012; 55(5): 1574-84.

[18] Kenerson HL, Yeh MM, Yeung RS: Tuberous sclerosis complex-1 deficiency attenuates diet-induced hepatic lipid accumulation. PLoS One 2011; 29;6(3):e18075.

Chapter V

The effect of cisplatin on blood ammonia elevation by alanyl-glutamine supplementation

Summary

Although there are many clinical studies in which the beneficial effect of glutamine formulation on mucositis induced by chemo/radiotherapy was evaluated, the results are sometimes conflicting with the report of clinical deterioration. Then, we hypothesized that chemotherapy may increase the incidence of hyperammonemia without comparable change of major parameters of hepatic/renal disorder.

To verify our hypothesis, we examined the increase in blood ammonia level with one-hour intravenous infusion of alanyl-glutamine on day 1-4 after cisplatin (CDDP) administration in rats and assessed the correlation with hepatic/renal parameters.

Hepatic parameters (glutamate-oxaloacetic transaminase : GOT, glutamic-pyruvic transaminase : GPT) with CDDP did not change until day 3 and only GOT increased on day 4. Renal parameters (plasma creatinine, blood urea nitrogen : BUN) with CDDP continuously increased up to day 4. Alanyl-glutamine infusion significantly elevated blood ammonia level of CDDP rats with the peak on day 3, although the same dose did not change that of control rats.

These results indicates that CDDP enhances the increase in blood ammonia level by glutamine supplementation without correlating with primary parameters for hepatic/renal dysfunction.

Introduction

During chemo/radiotherapy in cancer patients, mucositis in digestive organs, one of primary adverse effects, would be an important dose limiting factors and affects the duration of the therapy and clinical outcomes. Since glutamine is a primary metabolic fuel of enterocytes, many clinical studies to evaluate the beneficial effect of oral/parenteral glutamine supplementation on mucositis associated with chemo/radiotherapy were reported. However, the results were sometimes conflicting [1-8]. Especially in case of high-dose chemotherapy, deterioration of overall conditions by alany-glutamine supplementation is also reported [9]. Since two ammonia molecules are generated from glutamine metabolism, primary ammonia detoxification system such as metabolism through urea cycle in the liver and excretion by kidney are very important for the safe use of glutamine formulation [10,11].

Although Ward et al. reported the dose finding study of glutamine on pediatric oncology patients with chemotherapy, focusing on the elevation of blood ammonia and glutamine level after single oral dose of glutamine[12], there are very few reports on hyperammonemia relating to chemotherapy.

We hypothesized that a variety of antitumor agents, especially cytotoxic agents, may impair hepatic and renal function even without manifest or correlated changes to major indexes of hepatic and renal dysfunction, leading to a decreased ammonia detoxification capacity which results in an increased incidence of hyperammonemia by glutamine supplementation. Hyperammonemia causes various systemic disorders especially on nervous system.

The primary adverse effects of platinum-based anti-tumor agents are reported to be nephrotoxicity, peripheral neuropathy, and digestive symptoms, whereas hepatotoxicity induced by platinum-based chemotherapy does not draw much attention.

In the present study, we examined the increase in blood ammonia level with intravenous alanyl-glutamine infusion, using CDDP-administered rat model. We also analyzed the correlation of this parameter with the primary hepatic and renal indices which are often used in clinical practice.

Materials and Methods

Animals

Seven-week-old male Wistar Imamichi rats (Sankyo Labo Service Corporation,INC, Tokyo, Japan), weighing from 190-210 g, were maintained at 23ºC, given standard laboratory chow and water ad libitum, and kept under a 12-hr light (7:00-19:00)/12-hr dark schedule. All animals received humane care in accordance with the Japanese guidelines for animal experimentation (Japanese Association for Laboratory Animal Science). All procedures used in animal experiments were approved by the Animal Ethics Committee of the institution.

Surgical procedures and experimental design

After 6 day-acclimation period, the rats were anesthetized with isoflurane (Eskine, Merck, Germany). The neck and interscapular region were shaved and prepared in a sterile manner for catherterization. A silastic catheter was inserted through the right juggler vein and was tunneled subcutaneously to being brought out through the interscapular region. Rats were maintained in individual cage for 6 days to recover. After a post-surgical recovery period, on the starting day of experiment (day 0), the food was withdrawn from 9:45 to 18:00. At 14:00, 4 mg/8ml /kg CDDP (10 mg/20 ml, Nichi-Iko Pharmaceutical Co., Ltd., Toyama, Japan) (CDDP group) or 8 ml/kg saline was administered through the catheter (Control group).

Measurement of plasma GOT, GPT, creatinine, BUN and blood ammonia

Blood collected from catheter was centrifuged to obtain plasma. The plasma GOT, GPT, and creatinine levels were measured using FUJIDRI-CHEM analyzer (Fuji Film Corporation, Japan). Blood ammonia and BUN were measured by FUJIDRI-CHEM analyzer, using whole blood.

Alanyl-glutamine load test

On the designated day after the administration of CDDP or saline, the food was withdrawn at 9:45. Between 14:00-15:00, 10 ml/kg alanyl-glutamine solution was intravenously administered through the catheter for 1 h at the total dose of 1.0 g/kg or 0.7 g/kg. Blood was collected from catheter at the indicated time point and the blood ammonia was measured using FUJIDRI-CHEM analyzer (Fuji Film Corporation, Japan).

Measurement of plasma glutamine and glutamate

Blood collected from catheter was centrifuged to obtain plasma. One hundred microliters of 10% trichloroacetic acid solution was added to 200 µl plasma and mixed thoroughly for deproteinization. After the plasma sample was kept on ice for 10 min, the sample was centrifuged. The supernatant was filtered using a ultrafiltration filter (Ultracel YM-10 regenerated cellulose 10000 MWCO Cat. No. 42407, Merk Millipore, Darmstadt, Germany). The glutamine and glutamate concetration in ultrafiltered sample were measured by an automatic amino acid analyzer (L-8800; Hitachi,Tokyo, Japan). Briefly, amino acids, separated by cation-exchange chromatography, were detected spectrophotometrically after postcolumn reaction with ninhydrin reagent.

Expression of data and statistical analysis

The results are expressed as the mean ± SEM. The statistical significance of differences was determined by Dunnet test between more than 2 groups and Student's t test between 2 groups. The difference between groups was considered significant when P was less than 0.05.

Results

The effect of CDDP administration on parameters of hepatic and renal function

The plasma GOT and GPT are most frequently used parameters whose elevation reflects liver cellular injury caused by hepatotoxicity, hepatitis, and so on. In order to examine hepatotoxicity of CDDP, we first measured those parameters on day 1-4 after CDDP administration in CDDP group and compared with control group. The experimental protocol was summarized in Fig. 5-1.

As shown in Fig.5-2a, b, both plasma GOT and GPT levels did not significantly change up to day 3, whereas only GOT increased on day 4 without a change of GPT. (GOT ; 74.7±6.4 vs 101.0±4.5 U/l ($P<0.05$), control vs CDDP-day4)

In order to examine renal function, plasma creatinine and BUN were monitored. As shown in Fig. 5-2c, d, both parameters continuously increased up to day 4 with the significant difference with the control group on day 3 and 4.

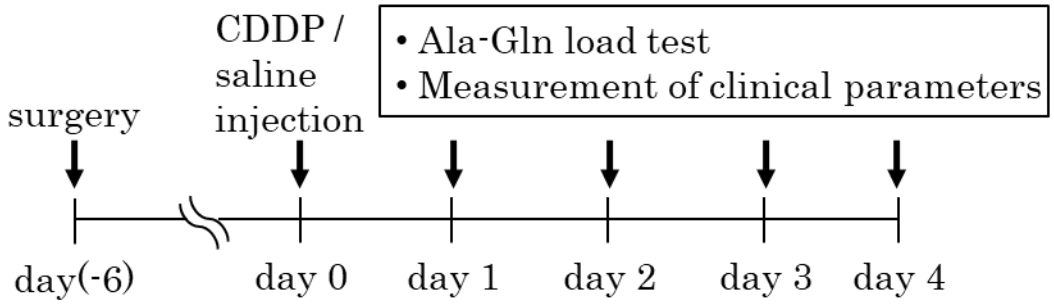

Fig. 5-1 The schedule of animal experiment
Six days after the surgery, the rats were administered CDDP (CDDP group) or saline (control group). The day when CDDP or saline was injected was defined as day 0.

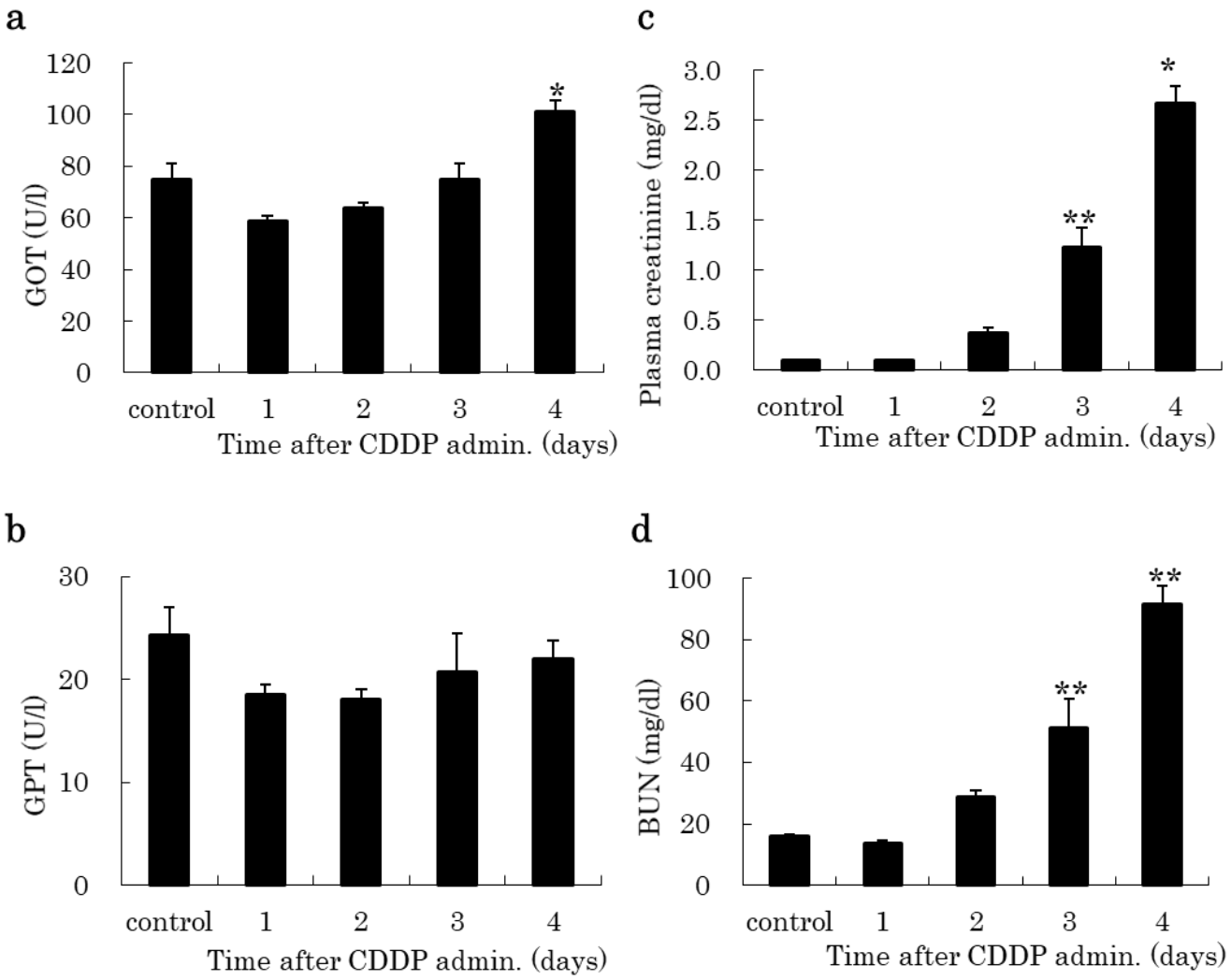

Fig. 5-2 The effect of CDDP on hepatic and renal parameters.
The level of GOT(a), GPT(b), plasma creatinine(c) and BUN(d) of control group on day3 and those of CDDP group on day 1-4. Results are mean ± SEM (n=5).

The effect of CDDP on the increase in blood ammonia level with intravenous alanyl-glutamine infusion

The increase of plasma GOT, creatinine and BUN after CDDP administration suggested the possibility of hepatic and renal toxicity. Although GOT did not significantly increased until day 3, in the previous study, we found that plasma prealbumin, an rapid turnover protein synthesized in the liver and reflect the hepatic function, decreased on day 2 [13]. From these results, we hypothesized that hepatic detoxification capacity for ammonia might already be deteriorated around day 2, when GOT and

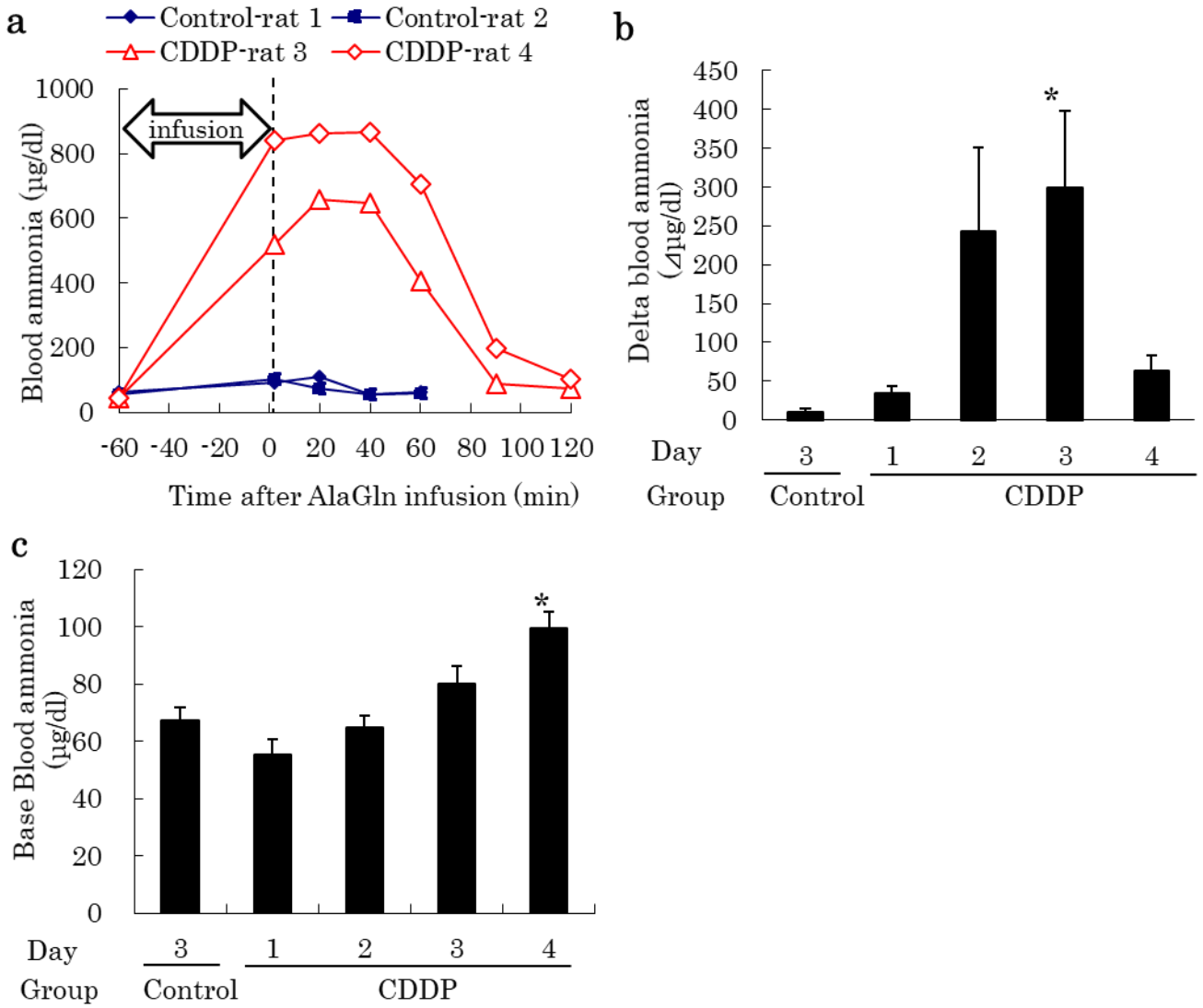

Fig. 5-3 The effect of CDDP on the increase in blood ammonia with alanyl-glutamine load test and the base blood ammonia level.
(a)The time course of blood ammonia level of an individual animal before and after alanyl-glutamine infusion on day 3 of control and CDDP group, (b)the increase in blood ammonia from base level with alanyl-glutamine load test and (c)the base blood ammonia level of control group on day 3 and CDDP group on day 1-4. Intravenous alanyl-glutamine infusion was carried out for 1 h between -60 min to 0 min ((a)1.0 g/kg, (b)0.7 g/kg). The increase in blood ammonia level (b) was calculated by the deduction of the ammonia level before infusion from that 1min after the completion of the infusion. The ammonia level before the infusion is regarded as a base ammonia level (c). In (b) and (c), a significant difference from control group is denoted by "asterisk" (*P<0.05, n=4).

GPT has not yet increased. Then, we performed alanyl-glutamine load test to monitor the blood ammonia level triggered by intravenous alanyl-glutamine infusion for 1 h (1.0 g/kg) on day 3 in control

and CDDP rats. The blood ammonia level was measured just before the start of infusion (-60 min) and 2, 20, 40, 60, 90, 120 min after the completion of infusion. Since this was a preliminary experiment with monitoring at many time points to verify if CDDP makes a significant effect on the increase in blood ammonia level, we examined only two animals of each group and showed the result of individual animal in Fig.5-3a.

In control group, the blood ammonia level did not evidently change on both two rats by alanyl-glutamine infusion. In contrast, in CDDP group, the blood ammonia level on both two rats increased and the peak level was sustained by 40 min after the completion of the infusion (500-900 μg/dl).

The daily change of the increase in blood ammonia with intravenous alanyl-glutamine infusion and the base blood ammonia level

In order to examine the daily change in the increase of blood ammonia with intravenous alanyl-glutamine infusion, CDDP rats were subject to alanyl-glutamine load test from day 1 to day 4 and compared with control rats.

Since we found that the peak blood ammonia level was sustained by 40 min after the completion of the alanyl-glutamine infusion by the same test on day 3, the increase of blood ammonia was calculated as a difference of the levels of before and 1 min after the infusion.

As shown in Fig.5-3b, the increase in blood ammonia level by alanyl-glutamine infusion gradually became higher by day 3, and finally dropped on day 4. In contrast, in control group, alanyl-glutamine infusion did not raise blood ammonia level (10.7±4.4 ⊿μg/dl vs 299.5±99.0 ⊿μg/dl ($P<0.05$), conrol vs CDDP-day3).

The blood ammonia level just before alanyl-glutamine infusion was shown in Fig.5-3c as a base blood ammonia level. We found that base blood ammonia level did not change by day 3, but increased on day 4 (67.3±4.3 vs 99.3±5.8 μg/dl ($P<0.05$), control vs CDDP-day4).

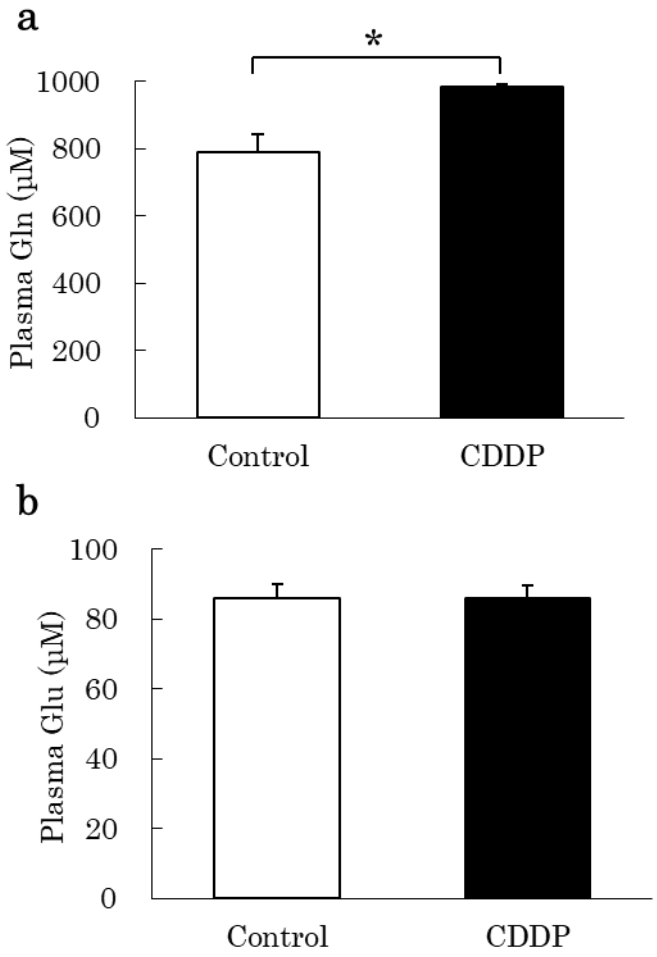

Fig. 5-4 The effect of CDDP administration on plasma glutamine and glutamate level.
Plasma concentration of glutamine (a) and glutamate (b) on day 3 with (CDDP group) or without (control group) CDDP administration. Results are mean ± SEM (n=5).

The effect of CDDP administration on plasma glutamine and glutamate level

Large part of ammonia in the systemic circulation is detoxified to urea through urea cycle in the liver. However, when blood ammonia level increases, such as by urea cycle disorders, blood glutamine level is elevated due to the activation of glutamine synthesis from ammonia and glutamate in extrahepatic tissues, mainly in muscle, to remove toxic ammonia from the circulation[13,14,15]. In order to assess the sensitivity of this parameter, we measured plasma glutamine and glutamate level on day 3, when the elevation of blood ammonia by alanyl-glutamine infusion was the highest but the hepatic parameters (e.g., GOT, GPT) and the base blood ammonia level did not change.

As shown in Fig.5-4a, b, on day 3, plasma glutamine in CDDP group showed significantly higher level than control, whereas plasma glutamate was not different (plasma glutamine; 789.9±52.8 vs 983.1±8.4 μM ($P<0.05$), plasma glutamate; 86.0±3.9 vs 85.9±3.7 μM, control vs CDDP group).

Discussion

The aim of this study was to verify our hypothesis that chemotherapy may increase the incidence of hyperammonemia without comparable change of major parameters of hepatic and renal dysfunctions. We examined the increase in blood ammonia level with intravenous alanyl-glutamine infusion on CDDP-administered rats and assessed the correlation with major parameters of hepatic and renal toxicity.

In the present study, we chose the dose of CDDP at 4 mg/kg. This dose caused atrophy of mucosa in the intestine which peaked on day 3 and then recovered. (data not shown). Renal toxicity is reported to be one of primary side effects of CDDP but hepatotoxicity does not draw much attention. Consistently, our present result showed that CDDP significantly elevated plasma creatinine and BUN on day 3-4. Since both creatinine and BUN continuously increased up to day 4 and the increase was quite significant, it is highly possible that CDDP caused renal dysfunction. On the other hand, regarding hepatic parameters, although GOT increased on day 4, it is not clear if this increase is attributable to hepatotoxicity because the elevated level of GOT on day 4 was just about 100 U/I and GPT did not increase, at least, by day 4. Glutamate-oxaloacetic transaminase (GOT) are found not only in the liver but also found in kidney, heart, muscle, and elevated values up to 300 U/L are considered nonspecific [14].

On the other hand, in the previous study, we found a significant decrease of plasma prealbumin on day 2 [13]. Prealbumin is a rapid turnover protein synthesized in the liver and reflects a hepatic function.[15] However, since plasma prealbumin is excreted by kidney, its plasma level is also affected by renal function. Consistent with this, our previous study showed that plasma prealbumin significantly dropped on day 2 and gradually increased after day 3 in parallel with the increase of creatinine and BUN. These results suggest that plasma prealbumin cannot be used as an index of hepatic function when renal dysfunction occurs, but there is a possibility that hepatic function declined on day 2. In the present study, intravenous alanyl-glutamine infusion significantly raised blood ammonia level of CDDP

rats without affecting that of control rats, and the increase in blood ammonia of CDDP rats peaked on day 3. This result suggests that CDDP deteriorates ammonia detoxification/excretion capacity, but the change of the increase in blood ammonia by alanyl-glutamine infusion did not correlate with that of typical hepatic and renal parameters, such as GOT, GPT, creatinine and BUN. More specifically, there was no significant increase in GOT and GPT on day 3 when the increase in blood ammonia by alany-glutamine infusion peaked, and creatinine and BUN continuously increased up to day 4.

Alanyl-glutamine infused to the circulation is rapidly degraded into glutamine and alanine [16]. Two and one ammonia are generated through the metabolism of glutamine and alanine, respectively. Ammonia in the circulation is mainly detoxified by periportal hepatocytes through urea cycle.[17] Extra ammonia not used by urea cycle is taken up by perivenous hepatocyte and is detoxified to glutamine by glutamine synthetase (GS) [18]. The significance of the contribution of hepatic ammonia-detoxifying capacity to control blood ammonia level is evident from the fact that 90% of hyperammonemia cases in adults relates to liver disease [19]. When the ammonia detoxification capacity in the liver is not sufficient due to liver dysfunction and leads to the increase of the circulating ammonia, the extra ammonia is eliminated in kidney, brain and skeletal muscle by being converted to glutamine by GS reaction [20-22]. The main glutamine producer in the body is skeletal muscle because of its large mass relative to the other GS-containing organs [23]. In kidney, ammonia and urea are excreted through urine.

Considering the results that : (1) plasma prealbumin significantly decreased on day 2 in the previous study, (2)the increase in blood ammonia was significantly alleviated on day 4 when renal failure continues to deteriorate, (3)the increase in blood ammonia occurred within a short time in response to an intravenous infusion of alanyl-glutamine for one hour, as well as that the contribution of hepatic ammonia detoxification capacity to control blood ammonia level is significant[19], we assume that liver dysfunction, rather than renal dysfunction, mainly contributes to this short-term hyperammonemia. The primary toxicity criteria for drug-induced liver injury which are widely used in clinical practice are plasma GOT, GPT, alkaline phosphatase (ALP), γ-glutamyltransferase and bilirubin. However, our

results suggest that even if plasma GOT and GPT are within the normal range, the hepatic capacity to detoxify ammonia in the circulation may be significantly deteriorated, leading to hyperammonemia when glutamine formulation is administered. Since significant atrophy of intestinal mucosa is induced in this CDDP-model around day 2-3 (data not shown), it is possible that bacterial translocation followed by endotoxaemia and elevation of blood pro-inflammatory cytokines may contribute to liver dysfunction.

In addition to a lack of correlation between the increase in blood ammonia with intravenous alanyl-glutamine infusion and the major parameters of hepatic and renal disorder, it should be noted that base blood ammonia level also did not correlate with the increase in blood ammonia with alanyl-glutamine infusion. The base blood ammonia level of CDDP group did not change up to day 3 and significantly increased only on day 4. On the other hand, plasma glutamine level in CDDP group significantly increased on day 3, when the increase in blood ammonia with alanyl-glutamine infusion peaked. Since the increase of plasma glutamine is attributable to the increase in the conversion of glutamate to glutamine, mainly in muscle, to eliminate extra ammonia from circulation when circulating ammonia level increases, it is reasonable that the elevation of plasma glutamine precedes that of base blood ammonia. From these results, it is speculated that compared with base blood ammonia level, plasma glutamine may be more sensitive parameter which reflects deterioration of ammonia detoxification/excretion capacity at earlier timing than base ammonia. The reason why base blood ammonia continued to increase up to day 4 when the increase in blood ammonia by alanyl-glutamine infusion began to decline may be that base blood ammonia is affected not only by hepatic ammonia detoxification capacity but also by renal excretion capacity for ammonia.

Taken together, the present study demonstrates that CDDP enhances the increase in blood ammonia level with intravenous alanyl-glutamine infusion without a significant change of major hepatic parameters such as GOT, GPT and base blood ammonia level. Major renal parameters such as creatinine and BUN also does not correlate with the increase in blood ammonia with alanyl-glutamine infusion. These results indicate that when amino acid is administered under pathological conditions for

beneficial effect, tolerance to amino acids, that is, systemic ammonia detoxification capacity, should be properly examined even when primary hepatic parameters are within the normal range.

References

[1] Fox AD, Kripke SA, Depaula J et al: Effect of a glutamine supplemented enteral diet on methotrexate-induced entorecolitis. J Parent Enteral Nutr 1988; 12: 325-331.

[2] Anderson PM, Schroeder G, Skubitz MD: Oral glutamine reduces the duration and severity of stomatitis after cytotoxic cancer chemotherapy. Cancer 1998; 83: 1433-1439.

[3] Jebb SA, Osborne RJ, Maughn TS: 5-Fluorouracil and folinic acid-linduced mucositis: no effect of glutamine supplementation. Br J Cancer 1994; 70: 732-735.

[4] van Zannen HCT, van der Leilie H, Timmer JG et al: Parenteral glutamine dipeptide supplementation does not ameliorate chemotherapy-induced toxicity. Cancer 1994; 74: 2879-2884.

[5] Ziegler TR, Young L, Benfell K et al: Clinical and metabolic efficacy of glutamine supplemented parenteral nutrition after bone marrow transplantation. Ann Intern Med 1992; 116: 821-828.

[6] Ziegler TR, Bye RL, Persinger RL et al: Effects of glutamine supplementation on circulating lymphocytes after bone marrow transplantation. Am J Med Sci 1998; 315: 4-10.

[7] Schloerb P, Amare M: Total parenteral nutrition with glutamine in bone marrow transplantation and other clinical application. J Parent Ent Nutr 1993; 17: 407-413.

[8] Anderson PM, Ramsay NKC, Shu XO et al: Effect of lowdose oral glutamine on painful stomatitis during bone marrow transplantation. Bone Marrow Transplant 1998; 22: 339-344.

[9] Pytlík R, Benes P, Patorková M, et al: Standardized parenteral alanyl-glutamine dipeptide supplementation is not beneficial in autologous transplant patients: a randomized, double-blind, placebo controlled study. Bone Marrow Transplant 2002; 30(12):953-961.

[10] Walker V: Ammonia toxicity and its prevention in inherited defects of the urea cycle. Diabetes Obes Metab 2009; 11(9):823-35.

[11] Owen EE, Johnson JH, Tyor MP: The effect of induced hyperammonemia on renal ammonia metabolism. J Clin Invest 1961; 40:215-221.

[12] Ward E, Picton S, Reid U, et al: Oral glutamine in paediatric oncology patients: a dose finding study. Eur J Clin Nutr 2003; 57(1):31-36.

[13] Ajinomoto Co., Inc.: Japan Patent Kokai 2012-41324.

[14] Shivaraj Gowda, Prakash B. Desai, Vinayak V. Hull, Avinash A K. Math, Sonal N. Vernekar, Shruthi S. Kulkarni: A review on laboratory liver function tests, Pan Afr Med J 2009; 3: 17-27.

[15] Mizuguchi T, Kawamoto M, Meguro M, Hui TT, Hirata K: Preoperative liver function assessments to estimate the prognosis and safety of liver resections. Surg Today 2014; 44(1):1-10.

[16] Fürst P, Albers S, Stehle P: Glutamine-containing dipeptides in parenteral nutrition. JPEN J Parenter Enteral Nutr 1990; 14(4 Suppl):118S-124S.

[17] Walker V: Ammonia toxicity and its prevention in inherited defects of the urea cycle. Diabetes Obes Metab 2009; 11(9):823-35.

[18] Hakvoort TB, He Y, Kulik W, Vermeulen JL, Duijst S, Ruijter JM, Runge JH, Deutz NE, Koehler SE, Lamers WH: Pivotal role of glutamine synthetase in ammonia detoxification. Hepatology 2017; 65(1):281-293.

[19] Cichoż-Lach H, Michalak A: Current pathogenetic aspects of hepatic encephalopathy and noncirrhotic hyperammonemic encephalopathy. World J Gastroenterol 2013; 19(1):26-34.

[20] Girard G, Butterworth RF: Effect of portacaval anastomosis on glutamine synthetase activities in liver, brain, and skeletal muscle. Dig Dis Sci 1992; 37(7):1121-1126.

[21] Maestri NE, McGowan KD, Brusilow SW: Plasma glutamine concentration: a guide in the management of urea cycle disorders. J Pediatr 1992; 121(2):259-261.

[22] Clemmesen JO, Kondrup J, Ott P: Splanchnic and leg exchange of amino acids and ammonia in acute liver failure. Gastroenterology 2000; 118(6):1131-1139.

[23] Huizenga JR, Gips CH, Tangerman A: The contribution of various organs to ammonia formation: a review of factors determining the arterial ammonia concentration. Ann Clin Biochem 1996; 33 (Pt 1):23-30.

Conclusion

In this thesis, I studied the mechanism of the protective effect of proline on GalN-induced hepatitis and the role of tuberin, the negative regulator of mTOR pathway, in liver regeneration. I also investigated the effect of cisplatin (CDDP), widely used anti-tumor agent, on systemic ammonia detoxification capacity.

In chapter I, using GalN-induced hepatitis rat model, I demonstrate that proline pre-administration strongly activates IL-6/STAT3 pathway, which is a regenerative, anti-inflammatory signaling pathway and is downstream of TNF-α/NFκB, with subsequent activation of regenerative response and suppression of massive inflammatory infiltration in the liver. In proline-treated rats, IL-6/STAT3 signaling was activated within 24 h after GalN treatment, followed by upregulation of the mRNA expression of histone H3, a marker of proliferation, in the liver at 24 h. Proline administration significantly suppressed inflammatory infiltration in the liver after 48 h, which was accompanied by depletion of plasma TNF-α, glutamic oxaloacetic transaminase (GOT) and glutamic pyruvic transaminase (GPT).

In chapter II, I demonstrate that proline pre-administration on GalN-induced hepatitis rat activates haptic major ROS-eliminating system, such as catalase and glutathione redox system at very early phase after GalN treatment. In proline-treated rats, catalase was significantly activated from 0 to 3 h after GalN treatment as well as that the level of reduced glutathione (GSH) was significantly higher from 6 to 12 h. The activity of glutathione reductase (GR) and glutathione peroxidase (GP), the regulators of glutathione redox system, was also upregulated in the liver at 6 and 12 h, respectively.

This is the first study to demonstrate that protective effect of proline on GalN-induced hepatitis rat involves the early activation of regenerative, anti-inflammatory signaling as well as that of hepatic major ROS-eliminating system.

In chapter III, I describe the protective effect of proline on endothelial dysfunction and inflammatory reaction, using early atherogenic model, i.e., short-term high sucrose diet-fed rat model. I demonstrate

that proline-treated rats showed increased endothelium-dependent vasorelaxation, decreased mRNA expression of adhesion molecules such as ICAM-1 MCP-1, E-selectin on thoracic aorta, decreased plasma soluble ICAM-1 level, and increased cycline dependent kinase inhibitor (p21) mRNA expression on thoracic aorta. Cycline dependent kinase inhibitor inhibits cell proliferation of smooth muscle cells and its downregulation in disease states, such as atherosclerosis and restenosis, plays pivotal role in increased proliferation of smooth muscle cells that contributes to the progress of disease state. This is the first study to demonstrate that proline supplementation could prevent early atherogenic response on aorta.

In chapter IV, to further understand liver regeneration, I examined a role of tuberin, a negative regulator of mTOR pathway, in liver regeneration, using 70% hepatectomy model of wild-type and Tsc2+/- mice. I found the tuberin phosphorylation which correlated with mTOR activation during early liver regeneration in wild-type mice. However, liver regeneration in the Tsc2+/- mice was not enhanced. Instead, the Tsc2+/- livers failed to accumulate lipid bodies which serves as an important energy source during liver regeneration. This is the first study to demonstrate that tuberin plays a critical role in liver energy balance by regulating hepatocelluar lipid accumulation during early liver regeneration.

In chapter V, I demonstrate that cisplatin (CDDP) treatment deteriorates systemic ammonia detoxification capacity without correlating with primary parameters for hepatic/renal dysfunction. Cisplatin treatment enhances the increase in blood ammonia level with intravenous alanyl-glutamine infusion without a significant change of major hepatic parameters such as GOT, GPT and base blood ammonia level. Major renal parameters such as creatinine and BUN also does not correlate with the increase in blood ammonia with alanyl-glutamine infusion. These results indicate that when amino acid is administered under pathological conditions for beneficial effect, tolerance to amino acids, i.e., systemic ammonia detoxification capacity, should be properly examined even when primary hepatic parameters are within the normal range.

Acknowledgements

I would like to express my very great appreciation to Professor Yasuyoshi Sakai, Division of Applied Life Sciences, Graduate School of Agriculture, Kyoto University, for his valuable suggestions and warm encouragement to construct and write this thesis. His willingness to give his time so generously is very much appreciated.

I would like to express my deep gratitude to my research supervisor, Dr. Michio Takahashi, Research Institute for Health Fundamentals in Ajinomoto Co., Inc., for his patient guidance and useful critiques of a part of this research work.

I would also like to thank Professor Raymond S. Yeung, Department of Surgery in University of Washington (Seattle, WA, USA), for his valuable and constructive guidance during the planning and development of a part of this research work.

My grateful thanks are extended to Dr. Masato Mori, Dr. Shintaro Yoshida, Ms. Harumi Arisaka, Dr. Eiji Nakamura (Ajinomoto Co., Inc.) and Dr. Jean S. Campbell (UW Medicine Pathology, University of Washington, USA) for their valuable support during the course of this work.

I would also like to extend my thanks to the technicians of the laboratories of Ajinomoto Co., Inc. and UW Medicine Pathology department in University of Washington (USA) for their help in offering me the resources in running the program.

Finally, I wish to thank my parents for their support and encouragement throughout my study.

Publications

1) Obayashi Y, Arisaka H, Yoshida S, Mori M, Takahashi M: Proline protects liver from D-galactosamine hepatitis by activating the IL-6/STAT3 survival signaling pathway. Amino Acids 2012; 43 (6): 2371-2380. doi: 10.1007/s00726-012-1317-8.

2) Obayashi Y, Arisaka H, Yoshida S, Mori M, Takahashi M: The protection mechanism of proline from D-galactosamine hepatitis involves the early activation of ROS-eliminating pathway in the liver. Springerplus 2015; 4:199. doi: 10.1186/s40064-015-0969-8.

3) Obayashi Y., Arisaka H., Takahashi M: Anti-atherogenic effect of proline in a rat model of high sucrose diet-induced hyperlipidemia (in preparation).

4) Obayashi Y, Campbell JS, Fausto N, Yeung RS: Impaired lipid accumulation in the liver of Tsc2-heterozygous mice during liver regeneration. Biochem Biophys Res Commun 2013; 437 (1):146-150. doi: 10.1016/j.bbrc.2013.06.056.

5) Obayashi Y, Kajiwara K, Nakamura E: The effect of cisplatin on blood ammonia elevation by alanyl-glutamine supplementation. Pharmacology 2018; 101:156–162. doi: 10.1159/000485919.

Related patent

1) Obayashi Y, Kajiwara K, Inui K (Ajinomoto Co., Inc.): Suppressant for deterioration in hepatic function induced by platinum-containing drug. Japan Patent Kokai JP2012-41324A (Mar. 1, 2012).

Other publications

1) Obayashi Y, Nagamura Y: Does monosodium glutamate really cause headache? : a systematic review of human studies. J Headache Pain 2016; 17:54. doi: 10.1186/s10194-016-0639-4.

2) Ohtsuki T, Nakamura R, Kubo S, Otabe A, Oobayashi Y, Suzuki S, Yoshida M, Yoshida M, Tatebe C, Sato K, Akiyama H: Development of an HPLC Method with an ODS Column to Determine Low Levels

of Aspartame Diastereomers in Aspartame. PLoS One. 2016; 11(3): e0152174. doi: 10.1371/journal.pone.0152174.

3) Ito E, Yamauchi K, Obayashi Y, Yamashita J, Umeda A, Dohmoto H, Kajiwara K: Effects of amino acids-enriched TPN in postoperative malnourished rats. Jpn J Surg Metab Nutr 2013; 47(1):15-24 (In Japanese). doi: 10.11638/jssmn.47.1_15.

4) Sakai Y, Abe T, Isaka K, Ohbayashi Y, Yamamoto K, Tani Y, Kato N: Bioconversion of 7-Aminocephalosporanic acid (7-ACA) by Intact Cells of *Rhodotorula glutinis*. Appl Environ Microbiol 1996; 62:2669-2672.